

NATIONAL BUREAU OF STANDARDS REPORT

8663

MATHEMATICAL ANALYSIS OF TEMPERATURE RISE
IN THE
HEAT CONDUCTION REGION OF AN UNDERGROUND SHELTER

by
F. J. Jerome Drapeau and Neil V. Baggette

Prepared for
Office of Civil Defense
Department of the Army

under
Contract No. OCD-OS-62-44,
Subtask 1211A



U. S. DEPARTMENT OF COMMERCE
NATIONAL BUREAU OF STANDARDS

THE NATIONAL BUREAU OF STANDARDS

The National Bureau of Standards is a principal focal point in the Federal Government for assuring maximum application of the physical and engineering sciences to the advancement of technology in industry and commerce. Its responsibilities include development and maintenance of the national standards of measurement, and the provisions of means for making measurements consistent with those standards; determination of physical constants and properties of materials; development of methods for testing materials, mechanisms, and structures, and making such tests as may be necessary, particularly for government agencies; cooperation in the establishment of standard practices for incorporation in codes and specifications; advisory service to government agencies on scientific and technical problems; invention and development of devices to serve special needs of the Government; assistance to industry, business, and consumers in the development and acceptance of commercial standards and simplified trade practice recommendations; administration of programs in cooperation with United States business groups and standards organizations for the development of international standards of practice; and maintenance of a clearinghouse for the collection and dissemination of scientific, technical, and engineering information. The scope of the Bureau's activities is suggested in the following listing of its four Institutes and their organizational units.

Institute for Basic Standards. Applied Mathematics. Electricity. Metrology. Mechanics. Heat. Atomic Physics. Physical Chemistry. Laboratory Astrophysics.* Radiation Physics. Radio Standards Laboratory.* Radio Standards Physics; Radio Standards Engineering. Office of Standard Reference Data.

Institute for Materials Research. Analytical Chemistry. Polymers. Metallurgy. Inorganic Materials. Reactor Radiations. Cryogenics.* Materials Evaluation Laboratory. Office of Standard Reference Materials.

Institute for Applied Technology. Building Research. Information Technology. Performance Test Development. Electronic Instrumentation. Textile and Apparel Technology Center. Technical Analysis. Office of Weights and Measures. Office of Engineering Standards. Office of Invention and Innovation. Office of Technical Resources. Clearinghouse for Federal Scientific and Technical Information.**

Central Radio Propagation Laboratory.* Ionospheric Telecommunications. Tropospheric Telecommunications. Space Environment Forecasting. Aeronomy.

* Located at Boulder, Colorado 80301.

** Located at 5285 Port Royal Road, Springfield, Virginia 22171.

DDC AVAILABILITY

Qualified requestors may obtain copies of this report from
Defense Documentation Center, Cameron Station, Alexandria, Va.

DDC release to the Federal Clearinghouse is not authorized.

NATIONAL BUREAU OF STANDARDS REPORT

NBS PROJECT

42103-12-4210436

April 1965

NBS REPORT

8663

MATHEMATICAL ANALYSIS OF TEMPERATURE RISE IN THE HEAT CONDUCTION REGION OF AN UNDERGROUND SHELTER

by

F. J. Jerome Drapeau and Neil V. Baggette
Mechanical Systems Section
Building Research Division

Prepared for
Office of Civil Defense
Department of the Army

under

Contract No. OCD-OS-62-44
Subtask 1211A

This report has been reviewed in the Office of Civil Defense and approved for issuance. Approval does not signify that the contents necessarily reflect the views and policies of the Office of Civil Defense.

IMPORTANT NOTICE

NATIONAL BUREAU OF STANDARDS
for use within the Government. This report
and review. For this reason, the
whole or in part, is not authorized for
Bureau of Standards, Washington, D.C.
the Report has been specifically prepared

Approved for public release by the
Director of the National Institute of
Standards and Technology (NIST)
on October 9, 2015.

accounting documents intended
subjected to additional evaluation
isting of this Report, either in
Office of the Director, National
he Government agency for which
ies for its own use.



U. S. DEPARTMENT OF COMMERCE
NATIONAL BUREAU OF STANDARDS

NATIONAL BUREAU OF STANDARDS REPORT

NBS PROJECT

42103-12-4210436

April 1965

NBS REPORT

8663

MATHEMATICAL ANALYSIS OF TEMPERATURE RISE IN THE HEAT CONDUCTION REGION OF AN UNDERGROUND SHELTER

by

F. J. Jerome Drapeau and Neil V. Baggette
Mechanical Systems Section
Building Research Division

Prepared for
Office of Civil Defense
Department of the Army

under

Contract No. OCD-OS-62-44
Subtask 1211A

This report has been reviewed in the Office of Civil Defense and approved for publication. Approval does not signify that the contents necessarily reflect the views and policies of the Office of Civil Defense.

IMPORTANT NOTICE

NATIONAL BUREAU OF STANDARDS REPORTS are usually preliminary or progress accounting documents intended for use within the Government. Before material in the reports is formally published it is subjected to additional evaluation and review. For this reason, the publication, reprinting, reproduction, or open-literature listing of this Report, either in whole or in part, is not authorized unless permission is obtained in writing from the Office of the Director, National Bureau of Standards, Washington 25, D.C. Such permission is not needed, however, by the Government agency for which the Report has been specifically prepared if that agency wishes to reproduce additional copies for its own use.



U. S. DEPARTMENT OF COMMERCE
NATIONAL BUREAU OF STANDARDS

TABLE OF CONTENTS

	PAGE
ABSTRACT	1
1. Introduction	2
1.1 Objectives	2
1.2 Scope	3
1.3 Types of Solutions	5
2. Summary of Problems	6
3. Evaluation of Experimental Parameter Data	9
3.1 Average Initial Temperature	10
3.2 Properties of Concrete	11
3.3 Properties of Earth	12
3.4 Heat Flux	14
4. Solution I	15
One-dimensional, homogeneous, semi-infinite region, uniform initial temperature, constant heat flux.	
4.1 Statement of Problem	15
4.2 Mathematical Summary	15
4.3 Assumptions	16
4.4 Results	17
4.5 Discussion	17
5. Solution II	26
Spherical cavity, homogeneous, infinite region, uniform initial temperature, constant heat flux.	
5.1 Statement of Problem	26
5.2 Mathematical Summary	26
5.3 Assumptions	27
5.4 Results	29
5.5 Discussion	29

TABLE OF CONTENTS (Cont.)

	PAGE
6. Solution III	32
Infinite cylindrical cavity, homogeneous, infinite region, uniform initial temperature, constant heat flux.	
6.1 Statement of Problem	32
6.2 Mathematical Summary	32
6.3 Convergence	33
6.4 Assumptions	34
6.5 Results	35
6.6 Discussion	35
7. Solution IV	38
One-dimensional, composite, semi-infinite region, uniform initial temperature, constant heat flux.	
7.1 Statement of Problem	38
7.2 Mathematical Summary	38
7.3 Convergence	40
7.4 Assumptions	40
7.5 Results	41
7.6 Discussion	48
8. Solution V	49
One-dimensional, composite, semi-infinite region, prescribed initial temperature, constant heat flux.	
8.1 Statement of Problem	49
8.2 Mathematical Summary	49
8.3 Convergence	53
8.4 Assumptions	55
8.5 Results	58
8.6 Discussion	62

TABLE OF CONTENTS (Cont.)

	PAGE
9. Solution VI	63
One-dimensional, composite, semi-infinite region, prescribed initial temperature, constant heat flux.	
9.1 Statement of Problem	63
9.2 Mathematical Summary	63
9.3 Convergence	69
9.4 Assumptions	69
9.5 Results	72
9.6 Discussion	72
10. General Discussion	75
10.1 Geometry	75
10.2 Composition of Region	79
10.3 Initial Temperature	82
10.4 Thermal Properties	85
10.5 Shelter Irregularities	87
10.6 Shelter Environment	88
11. Conclusions	90
APPENDIX A Initial Temperature Distribution	92
APPENDIX B Heat Flux	96
APPENDIX C Numerical Example	102
APPENDIX D References	105

LIST OF FIGURES

FIGURE	TITLE	PAGE
4.4.1	Solution I - NBS Test 3 Predicted Surface Temperatures for North Wall Region	18
4.4.2	Solution I - NBS Test 3 Predicted Surface Temperatures for West Wall Region	19
4.4.3	Solution I - NBS Test 4 Predicted Surface Temperatures for North Wall Region	20
4.4.4	Solution I - NBS Test 4 Predicted Surface Temperatures for West Wall Region	21
4.4.5	Solution I - NBS Test 5 Predicted Surface Temperatures for North Wall Region	22
4.4.6	Solution I - NBS Test 5 Predicted Surface Temperatures for West Wall Region	23
5.4.1	Solution II - NBS Test 3 Predicted Surface Temperatures for Equivalent Spherical Radius a	30
5.4.2	Solution II - NBS Test 5 Predicted Surface Temperatures for Equivalent Spherical Radius a	31
6.5.1	Solution III - NBS Test 3 Predicted Surface Temperatures for Equivalent Cylindrical Radius a	36
6.5.2	Solution III - NBS Test 5 Predicted Surface Temperatures for Equivalent Cylindrical Radius a	37
7.5.1	Solution IV - NBS Test 3 Predicted Surface Temperatures for North Wall Region	42

LIST OF FIGURES (Cont.)

FIGURE	TITLE	PAGE
7.5.2	Solution IV - NBS Test 3 Predicted Surface Temperatures for West Wall Region	43
7.5.3	Solution IV - NBS Test 5 Predicted Surface Temperatures for North Wall Region	44
7.5.4	Solution IV - NBS Test 5 Predicted Surface Temperatures for West Wall Region	45
8.4.1	Solution V - NBS Test 3 Initial Temperature Distribution in Heat Conduction Region	56
8.5.1	Solution V - NBS Test 3 Predicted Surface Temperatures for North Wall Region, Various Concrete and Earth Thermal Properties	59
8.5.2	Solution V - NBS Test 3 Predicted Surface Temperatures for West Wall Region, Various Concrete and Earth Thermal Properties	60
8.5.3	Solution V - NBS Test 5 Predicted Surface Temperatures for West Wall Region	61
9.4.1	Solution VI - NBS Test 3 Initial Temperature Distribution in Heat Conduction Region	70
9.5.1	Solution VI - NBS Test 3 Predicted Surface Temperatures for North Wall Region, Various Concrete and Earth Thermal Properties	73
9.5.2	Solution VI - NBS Test 3 Predicted Surface Temperatures for West Wall Region, Various Concrete and Earth Thermal Properties	74

LIST OF FIGURES (Cont.)

FIGURE	TITLE	PAGE
10.1.1	Comparison of Solutions I, II, & III NBS Test 3 - Predicted Surface Temperatures, Earth Thermal Properties	76
10.1.2	Comparison of Solutions I, II, & III NBS Test 4 - Predicted Surface Temperatures, Earth Thermal Properties	77
10.1.3	Comparison of Solutions I, II, & III NBS Test 5 - Predicted Surface Temperatures, Earth Thermal Properties	78
10.2.1	Solution I vs. Solution IV NBS Test 3 - Predicted Surface Temperatures for West Wall Region	80
10.3.1	Comparison of Solutions IV, V, & VI NBS Test 3 - Predicted Surface Temperatures for North Wall Region	83
10.3.2	Comparison of Solutions IV, V, & VI NBS Test 3 - Predicted Surface Temperatures for West Wall Region	84
A.1	NBS Test 3. Initial Temperature Distribution in Heat-Conduction Region on Sept. 13, 1959	93
A.2	NBS Test 4. Initial Temperature Distribution in Heat Conduction Region on Oct. 6, 1959	94
A.3	NBS Test 5. Initial Temperature Distribution in Heat Conduction Region on March 25, 1960	95
B.1	Solution IA. NBS Test 3 - Predicted Surface Temperatures for North Wall Region $K = 0.75$ $= 0.026$	100
B.2	Solution IA. NBS Test 3 - Predicted Surface Temperatures for West Wall Region $K = 0.75$ $= 0.026$	101

LIST OF TABLES

TABLE	TITLE	PAGE
1.1.1	Schedule of NBS Test Conditions for OCDM-NBS-60-1	2
3.1.1	Initial Temperatures	11
4.4.1	Interior Surface Temperatures Predicted by Solution I, $K = 1.15$	24
7.5.1	Interior Surface Temperatures Predicted by Solution IV $K_1 = 1.15$, $K_2 = 0.75$	46
7.5.2	Interior Surface Temperatures Predicted by Solution IV $K_1 = 1.40$, $K_2 = 1.04$	47
8.4.0	Values of Curve-Fitting Constants for Solution V	57
9.4.0	Values of Curve-Fitting Constants for Solution VI	71
B.1	Cumulative Average Values of Heat Flux, F_0	99

LIST OF SYMBOLS

a	curve-fitting constant; also equivalent radius, feet
b, m	curve-fitting constants
c	curve-fitting constant; also specific heat, Btu/lb-°F
F_o	heat flux, Btu/hr-ft ²
k	$\sqrt{\frac{\alpha_1}{\alpha_2}}$
K	thermal conductivity, Btu/hr-ft-°F
$K_o(qr), K_1(qa)$	modified Bessel functions of the second kind
l	thickness of concrete, feet
n	summation index
p	Laplace transform variable
q	$\sqrt{\frac{p}{\alpha}}$
r	radial distance, feet
t	time, hours
T	Fourier time, dimensionless
u	temperature in the medium, °F
\bar{u}	transformed temperature
u_o	average initial temperature in concrete and earth, °F
x	linear distance, feet

LIST OF SYMBOLS (Cont.)

α	thermal diffusivity, ft ² /hr
β	$\frac{\sigma - 1}{\sigma + 1}$
θ	temperature rise in the medium, °F
$\bar{\theta}$	transformed temperature rise
ρ	density, lb/ft ³
σ	$\frac{K_2}{K_1}k$
$\text{erfc}(x)$	complementary error function
$i^n \text{erfc}(x)$	integral error function of order n
$\exp(x)$	e^x
$D(x)$	$e^{-x^2} \int_0^x e^{\lambda^2} d\lambda$, Dawson's integral
	the subscripts 1 and 2 denote concrete and earth, respectively.

MATHEMATICAL ANALYSIS OF TEMPERATURE RISE
IN THE HEAT CONDUCTION REGION
OF AN UNDERGROUND SHELTER

by

F. J. Jerome Drapeau and Neil V. Baggette

ABSTRACT

Six analytic solutions of the heat conduction equation to predict interior surface temperatures in an underground concrete shelter are presented in this report. Four solutions employ one-dimensional, semi-infinite geometry and are applied to the wall and floor heat conduction regions of the small NBS test shelter. These solutions are not applicable to the roof region. Two solutions use spherical and cylindrical geometry, respectively, and are applied to the entire shelter. These solutions are not applicable to individual surfaces. The one-dimensional solutions were used primarily to examine the importance of the initial temperature distribution, the composite nature of the heat conduction regions, and in conjunction with the other two solutions, the geometry of the model. Surface temperature predictions for selected surfaces, together with the observed performance, are presented for the one-dimensional solutions in tabular and/or graphical form, covering a range of assumed thermal properties. Similar results are presented for the spherical and cylindrical solutions in graphical form, for two sets of thermal properties and two values of equivalent shelter radius. The results show that the one-dimensional solutions give high predictions, the spherical solution low predictions, and the cylindrical solution generally good agreement with observed performance of the NBS test shelter.

1. INTRODUCTION

1.1 Objectives

In February 1959, a study was begun to determine the thermal characteristics of a family-size underground concrete shelter with simulated occupancy.

The first phase of this study was experimental, with the objective of obtaining performance data on the environmental factors of temperature, humidity, ventilation, and heat exchange in an underground installation of this type during fourteen-day periods of occupancy in summer and winter. This objective was accomplished and the results [1]¹ reported in March 1961.

The schedule of test conditions from which the NBS performance data were obtained is presented in the following table. This report will compare analytical predictions of shelter surface temperatures with experimental data from NBS Tests 3, 4, and 5 only.

TABLE 1.1.1

SCHEDULE OF NBS TEST CONDITIONS [1]

NBS Test Number	Date at Start mo-da-yr	Duration of Test days	Internal Heat Input Btu/hr	Ventilation Air		
				Flow Rate CFM	Avg. Dry Bulb Temp. °F	Dew Point Temp. °F
1	8-13-59	7	110	42	85	69
2	8-28-59	7	2500	0	--	--
3	9-13-59	14	2500	42	85	69
4	10-6-59	14	2500	18	85	69
5	3-25-60	14	2500	18	35	33

¹ Figures in brackets indicate literature references at the end of this report.

The experimental phase indicated that theoretical approaches were desirable in order to provide methods for predicting environmental conditions in a shelter of any size or shape under various ambient conditions, and thus to reduce the need for exhaustive testing under an empirical approach. Tests in a few representative shelters could then be used to verify the applicability of those methods. One such approach was to develop mathematical equations which would predict air temperature and relative humidity inside shelters characterized by the following known parameters:

- a) initial earth temperatures
- b) thermal properties of earth and wall materials
- c) construction detail
- d) shape and size
- e) weather conditions
- f) ventilation rate
- g) internal heat sources

This objective would also include a comparison of the theoretically predicted results with the performance data obtained in the experimental phase, and with any other data on shelters, when available.

When these equations were adequately substantiated by experiment for sufficient ranges of the above-listed parameters, they would be used to develop a design manual, including extrapolated ranges.

1.2 Scope

The scope of this report was confined to the presentation of mathematical solutions to the problem of transient heat conduction in a certain class of shelter models, and a comparison of predicted shelter temperatures with observed temperatures in the NBS test series [1]. The class

of models considered were those characterized by a single space variable (linear distance, spherical radius, or cylindrical radius), and a constant heat flux applied at the interior boundary of the heat conduction region.

This report, then, deals with only part of the whole problem--the heat conduction region, and all solutions begin at the interior boundary. They do not include the parameters of heat generation and ventilating air inside the shelter, the mechanisms of transfer from these sources to the surfaces by convection, radiation, condensation, and evaporation, or weather conditions above the shelter. However, experience with prototype shelters has shown that wall surface temperature is a good index of effective air temperature, especially in small shelters, where they are about equal.

This division of the problem was possible because the rate of heat flow to all of the interior surfaces as a function of time ^{was} determined experimentally during each test on the shelter studied at the National Bureau of Standards. This method had the obvious and important advantage of isolating existing sources of error to those lying in the heat conduction region. Poor agreement between observed and predicted results could not be attributed to poor assumptions associated with the parameters of heat generation or the coefficients of heat transfer from air to surface.

In summary, therefore, this first attempt at obtaining mathematical solutions to an inherently complicated problem was simplified by dealing with available data measured at the boundary, instead of undetermined heat exchange processes inside the shelter. It provided a means of studying some of the heat conduction aspects of this problem, such as the importance of a prescribed initial temperature distribution in the region and the effects of the thermal and physical properties of the materials comprising the region. It also provided a means of determining the applicability of the linear heat flow theory (i.e. temperature and position independent coefficients), to a problem of this kind.

1.3 Types of Solutions

Four solutions contained in this report were based on the one-dimensional model. In this model, the heat conduction region exterior to the wall and floor boundaries of the rectangular parallelepiped cavity was represented by a layer of infinite thickness and infinite surface area. Each region was considered to be either a single homogeneous layer of earth or a composite of concrete and earth. The heat flux was presumed to be applied uniformly over the entire surface so that heat flowed in only one direction, normal to each plane surface. The finite (roof) region is not treated in this report.

An infinitely thick layer, such as described above, is called a semi-infinite region. This denotes a region bounded on one side only, $0 \leq x < \infty$ in the homogeneous case, or $-\ell \leq x < 0$ and $0 \leq x < \infty$ in the composite case.

One solution was based on the spherical model in which the heat conduction region was represented by an infinite, homogeneous mass of earth bounded internally by a spherical cavity of radius a . The heat flux was presumed to be applied uniformly over the entire surface so that heat flowed radially in all directions.

In the cylindrical solution, the heat conduction region was also represented by an infinite, homogeneous earth medium, bounded internally by an infinitely long cylindrical cavity of radius a . The heat flux was presumed to be applied uniformly over the entire surface so that heat flowed only radially to the cylinder.

The assumption of uniform heat flux application over the entire surface of each model permitted the mathematical treatment of the Cartesian (x, y, z) model, the spherical (r, θ, ϕ) model, and the cylindrical (r, θ, z) model as simple models of only one $(x$ or $r)$ space variable.

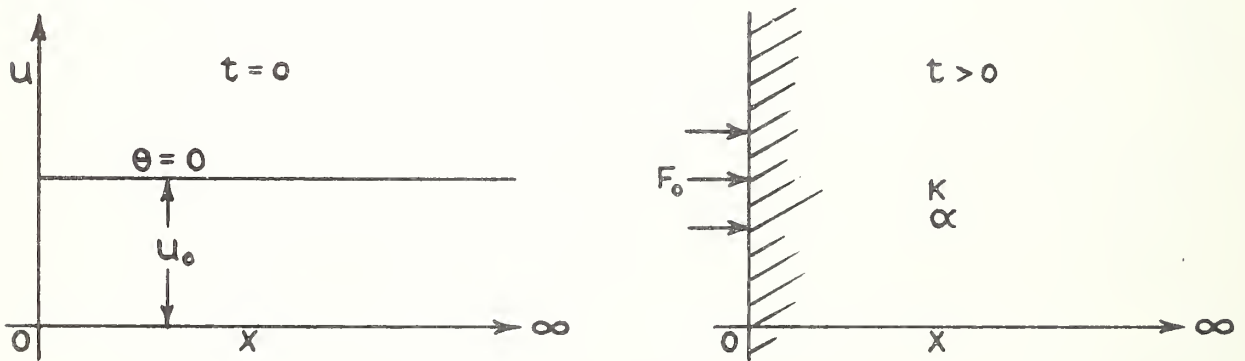
Each mathematical model represents a simplification of the actual physical shelter, and the effects of this simplification will be discussed later in the report.

2. SUMMARY OF PROBLEMS

Six mathematical solutions to study temperature predictions in an underground shelter, as determined by heat conduction into the surrounding wall and floor regions, are presented in this report. The boundary conditions and assumptions for each of the heat transfer models are summarized for each solution. The initial temperature distribution and the heat conduction model are shown diagrammatically for each summary.

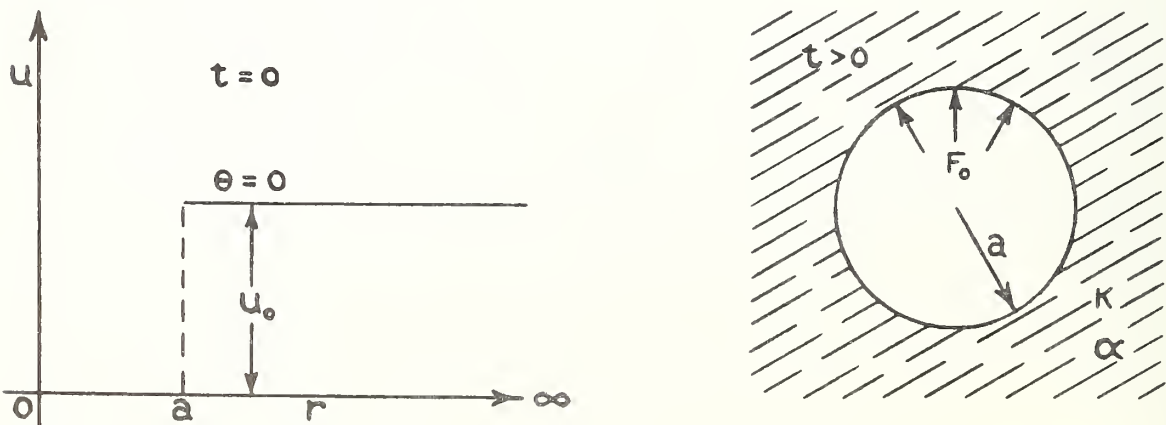
SOLUTION I — One-dimensional, homogeneous, semi-infinite heat conduction region; uniform initial temperature; constant heat flux across the surface.

This solution was used as a first approximation to predict NBS shelter performance.



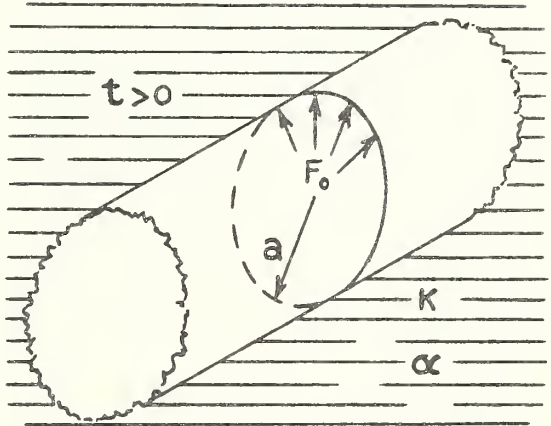
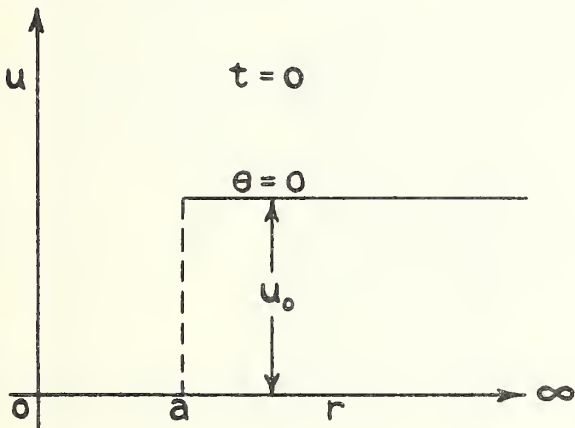
SOLUTION II — Spherical cavity bounded by an infinite, homogeneous heat conduction region; uniform initial temperature; constant heat flux across the surface.

This solution was used as a second approximation to predict performance.



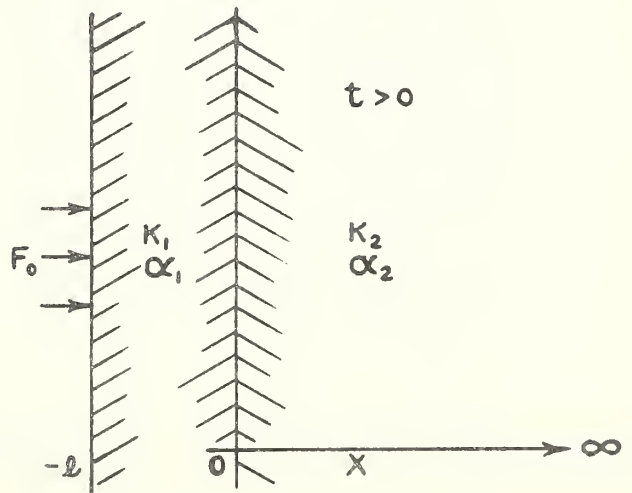
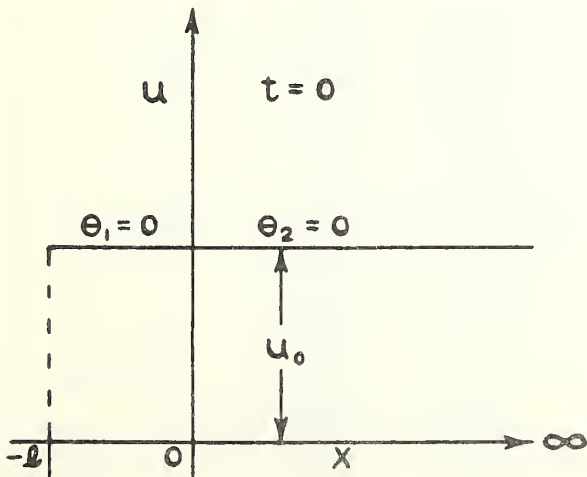
SOLUTION III - Infinitely long cylindrical cavity bounded by an infinite, homogeneous heat conduction region; uniform initial temperature; constant heat flux across the surface.

This solution was used as a third approximation to predict performance.



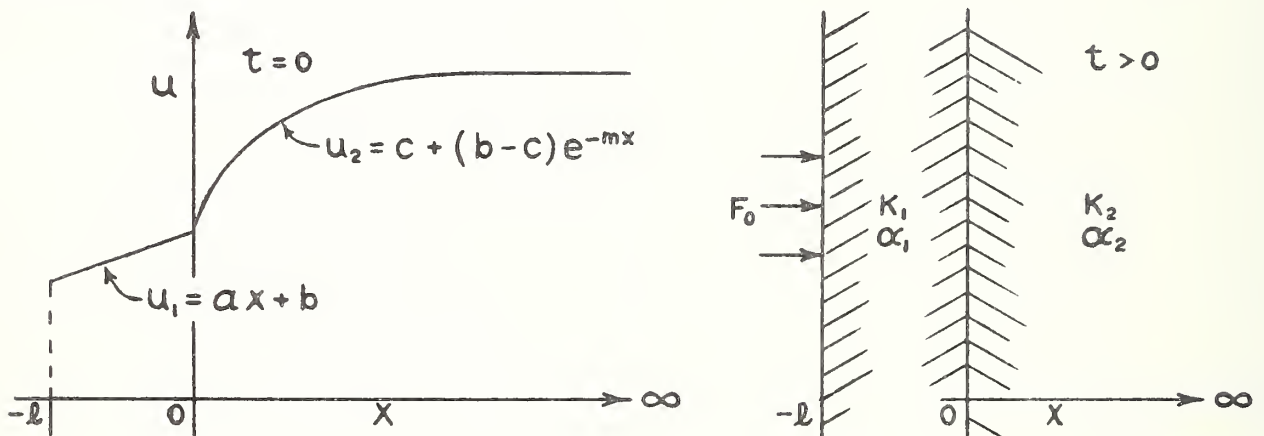
SOLUTION IV - One-dimensional, composite, semi-infinite heat conduction region; uniform initial temperature; constant heat flux across the surface.

This solution was used to observe the effect of the composite region assumption.



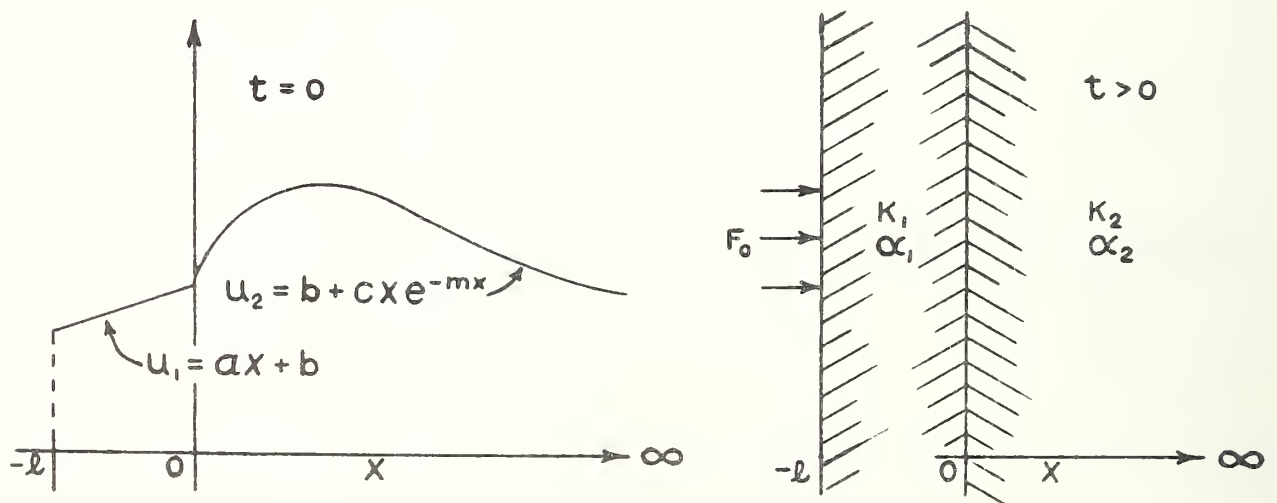
SOLUTION V - One-dimensional, composite, semi-infinite heat conduction region; prescribed initial temperature; constant heat flux across the surface.

This solution was derived on the basis of a prescribed initial temperature distribution, and used to observe the effect of such a distribution.



SOLUTION VI - One-dimensional, composite, semi-infinite heat conduction region; prescribed initial temperature; constant heat flux across the surface.

This solution is similar to the preceding solution, differing only in the mathematical expression for initial temperature distribution in the earth conduction region.



3. EVALUATION OF EXPERIMENTAL PARAMETER DATA

The purpose of this analysis was not only to develop mathematical solutions, but also to extract results from those solutions for comparison with experimental observations. For this reason, it was necessary to establish numerical values for the several parameters appearing in each solution. This section deals with the selection of these values for each of the following parameters, namely

- 1) average initial temperature
- 2) properties of concrete
- 3) properties of earth
- 4) heat flux.

3.1 Average Initial Temperature

Solutions I through IV were based on the assumption that the initial temperature distribution throughout each region was constant (or zero for mathematical convenience). Therefore, a single value of temperature had to be used for computing numerical results.

Since the initial temperature distribution for all regions deviated to some extent from a constant value over the domain in question (see Appendix A), the average initial temperature u_o was calculated for each composite region on the basis of the following heat balance:

$$x_1 \rho_1 c_1 (u_o - u_{o1}) = x_2 \rho_2 c_2 (u_{o2} - u_o) \quad (1)$$

where the subscripts 1 and 2 denote concrete and earth.

u_o , and u_{o2} were calculated by graphically evaluating the integrals

$$u_{o1} = \frac{1}{x_1} \int_{-x_1}^0 u(x) dx \quad (2)$$

and

$$u_{o2} = \frac{1}{x_2} \int_0^{x_2} u(x) dx \quad (3)$$

using the interface as the reference point. The functions $u(x)$ are the initial temperature profiles shown in Appendix A.

The values of average initial temperature obtained by this method are listed in Table 3.1.1.

It will be noted in the graphs for Solutions I and IV that the origins of the observed temperature curves shown in Sections 4 through 7 are not necessarily the same as those of the predicted curves. This is because the initial temperature of the observed curve is the actual value at the interior surface (see Appendix A), whereas the initial temperature of any predicted curve is the average value shown in Table 3.1.1.

TABLE 3.1.1
COMPUTED INITIAL TEMPERATURES

NBS Test Number	Average Region Temperature u_0 , °F					
	Heat Conduction Region					
	North	West	South	East	Roof	Floor
1	70.8	68.7	69.6	70.1	72.2	64.2
2	71.2	69.3	69.5	71.0	72.7	64.5
3	71.7	69.7	68.3	71.0	67.5	64.8
4	68.7	67.7	67.9	68.0	66.8	64.7
5	43.9	45.4	45.0	44.0	42.8	50.5

3.2 Properties of Concrete

The density of the shelter concrete was taken to be 145 lb/ft³. This value was based on the total weight of cement and aggregates, approximately 63,200 pounds, an estimated water of hydration content of 2,400 pounds, and the purchased volume of 16.75 cubic yards.

The specific heat of mass concrete varies but little with the type of aggregate and richness of mix, and for practical purposes is usually taken as a constant for a given concrete at about 0.22 Btu/lb-°F [2, p.585].

A mean value of thermal conductivity was selected from among several references [3,4,5,6] as 1.15 Btu/hr-ft-°F, based on an estimated moisture content and a physical composition fitting that of the shelter concrete described above.

The thermal diffusivity was determined from the relation $\alpha_1 = \frac{K_1}{\rho_1 c_1}$, the subscript (1) denoting concrete,

and the computed value was $0.036 \text{ ft}^2/\text{hr}$. These values of thermal properties were thought to be representative of those in the NBS test shelter, and will henceforth be referred to as the "preferred" concrete values.

The references consulted on this subject listed widely divergent thermal property values for concrete in the $140\text{-}155 \text{ lb/ft}^3$ density range. The values of specific heat ranged from 0.156 to 0.230 , thermal conductivities from 0.50 to 1.35 , and calculated thermal diffusivities from 0.016 to 0.046 . As a result, minimum and maximum values were also used for analytical predictions.

3.3 Properties of Earth

During the excavation process, representative samples of earth were removed for density and moisture content determinations. Three distinct earth strata were found and the average values of density and moisture content were determined to be approximately 100 lb/ft^3 and 17 percent.

A value of $0.17 \text{ Btu/lb-}^\circ\text{F}$ was selected as a representative average specific heat for the three earth strata in the dry state [7, p.33]. Since specific heat is known to vary with moisture content, the selected value was corrected for 17 percent moisture, giving a value of $0.29 \text{ Btu/lb-}^\circ\text{F}$ for specific heat of the moist earth [7, p.89].

A determination of the thermal diffusivity was made from experimental data obtained during the NBS test series. The solution of the heat conduction equation for a one-dimensional, homogeneous, semi-infinite region with a simple periodic boundary condition at the surface yields a convenient expression for determining the thermal diffusivity, based on the time lag between the maxima of the ground surface temperature wave and the corresponding wave at any depth below the surface. (This phase-lag method is more accurate than the temperature-amplitude method because the values of amplitude are difficult to measure accurately [8]).

The expression is

$$\alpha = \frac{P^2 x^2}{4\pi t^2},$$

where P = period, hours

x = depth of temperature measurement, feet

t = time lag between maxima, hours

Although temperatures were measured at several depths in undisturbed earth near the shelter, only two were useful for this determination - those made at the six-inch and one-foot depths. Measurements made at the two-foot depth exhibited no clearly defined wave form, if any at all. The amplitude of the daily cycle decreases rapidly with depth and is almost completely damped out at the two-foot depth [9]. For this reason, thermal diffusivity determinations in deeper ground are extremely difficult on a diurnal cycle basis, and must be made on averages of annual cycles.

Ambient temperatures were used because ground surface temperatures were not recorded. However, ambient and ground surface temperature maxima occur in phase, for practical purposes. It was observed that the temperature maxima at the six-inch and one-foot depths, during three early consecutive days of NBS Test 3, lagged the ambient maxima by about 4 1/4 and 8 1/2 hours, respectively. These phase-lags each indicate a thermal diffusivity of 0.026 ft²/hr.

A similar determination was based on data obtained during three late consecutive days of NBS Test 5, with exactly the same phase-lags and results. No precipitation had occurred for at least six weeks prior to the start of or during NBS Test 3, whereas two feet of snow had completely melted a few days before the start of NBS Test 5.

The thermal conductivity was determined from the same relation $K_2 = \rho_2 c_2 \alpha_2$, the subscript (2) denoting earth, and the computed value was 0.75 Btu/hr-ft-°F.

These values of thermal properties are likely to be representative of at least the upper two-foot layer of earth surrounding the NBS experimental shelter, and possibly deeper. They will henceforth be referred to as the preferred earth values. However, in order to account for the likelihood of other values at greater depths, and changes occurring in the upper layer during the intervening times, minimum and maximum values were again selected to form a range which would account for reasonable variations.

3.4 Heat Flux

Although the term "constant heat flux" is used throughout the discussion of Solutions I to VI, inclusive, the actual value of the heat flux F_0 was used for each plotted value of time. The heat flux used for time t was a cumulative average of heat flow meter readings, averaged over the interval from 0 to t . This procedure was intended to approximate, to some extent, the effect of the observed exponential decay of the heat flux. This is discussed more fully in Appendix B which also contains a table listing the cumulative average values used in each solution.

The west and north wall regions were selected for analysis and graphical presentation of the results because they were considered to be most and least closely approximated by the one-dimensional model. The reasons for these selections will be discussed in greater detail in Section 10.5.

4. SOLUTION I

4.1 Statement of Problem

Semi-infinite homogeneous region. The heat flux F_0 is constant across the surface $x = 0$. The initial temperature is uniform.

4.2 Mathematical Summary

The differential equation to be satisfied by the temperature rise θ is

$$\frac{\partial \theta}{\partial t} = \alpha \frac{\partial^2 \theta}{\partial x^2}, \quad x > 0, \quad t > 0 \quad (1)$$

with the following initial and boundary conditions:

$$x > 0 \quad t = 0 \quad \theta = 0 \quad (2)$$

$$x = 0 \quad t > 0 \quad -K \frac{\partial \theta}{\partial x} = F_0 \quad (3)$$

$$x \rightarrow \infty \quad t > 0 \quad \theta \rightarrow 0 \quad (4)$$

The solution of the Laplace transformed equation is

$$\bar{\theta} = \frac{F_0}{qKp} \exp(-qx) \quad (5)$$

and the inverse transformation yields the solution for temperature rise

$$\theta = \frac{2F_0}{K} \left\{ \left[\frac{\alpha t}{\pi} \right]^{\frac{1}{2}} \exp \left[-\frac{x^2}{4\alpha t} \right] - \frac{x}{2} \operatorname{erfc} \frac{x}{2\sqrt{\alpha t}} \right\} \quad (6)$$

For an initial temperature u_0 , the temperature at any distance x in the region is given by

$$u = u_0 + \theta \quad (7)$$

At the interior surface $x = 0$, Eq. 4.2(6) reduces to

$$\theta = \frac{2F_0}{K} \left[\frac{\alpha t}{\pi} \right]^{\frac{1}{2}} \quad (8)$$

4.3 Assumptions

This solution [10, p. 75] was used as a first approximation for predicting shelter performance for all heat conduction regions except the roof region.

The assumptions used in this approximation are listed and discussed below.

1) geometry - one-dimensional model

The NBS shelter deviated from the one-dimensional model discussed in Section 1.3 in that the shelter surfaces were finite in area with the result that the solution, being one-dimensional, could not account for heat lost to the corner regions. Except for the floor, deviation from the one-dimensional model was also caused by the additional boundary at the ground surface.

2) homogeneous heat conduction region

Since the region was considered to be homogeneous, only one thermal conductivity and one thermal diffusivity appear in the solution, i.e. both the concrete and earth media are assumed to have identical thermal properties. These properties are assumed to be invariant with position and changes in temperature and moisture content. For more detail, see Section 10.4.

3) uniform initial temperature

Figures 1 through 5 of Appendix A show that the initial temperature distribution in each region was not uniform for all tests. The assumed initial condition 4.2(2) most nearly fitted the wall regions of NBS Tests 1 and 5, but did not fit, for example, the wall regions of NBS Test 3. In order to obtain numerical results, the temperature u was computed on the basis of the average initial temperatures u_0 listed in Table 3.1.1.

4.4 Results

Figures 4.4.1 and .2 show interior surface temperatures versus time, predicted by Solution I, for the north and west wall conduction regions of NBS Test 3, together with the observed performance. Figures 4.4.3 through .6 show similar temperature-time curves for NBS Tests 4 and 5.

Curves 1, 2, and 3 show predicted performance based on an estimated range of earth thermal properties, including the preferred values. Curve 4 is based on the preferred concrete properties, values which would be reasonable if the concrete predominated in the heat storage.

Table 4.4.1 shows predicted surface temperatures for the five semi-infinite regions of NBS Tests 3, 4, and 5, evaluated at elapsed times of one and two weeks, together with the observed temperatures and the resulting deviations. The predicted temperatures were computed using the preferred concrete properties, the values producing the best general agreement with the observed performance.

4.5 Discussion

Inspection of Figures 4.4.1 through 4.4.6 shows that the lower thermal properties gave better agreement for the north wall region, and that the higher properties were better for the west wall region. The behavior of the other three surfaces, in most cases, was similar to that of the west wall region in this respect. This can be seen from Table 4.4.1 which shows that in 11 out of 15 cases, use of the preferred concrete thermal properties produced agreement to within 1.5°F at the end of a two-week period.

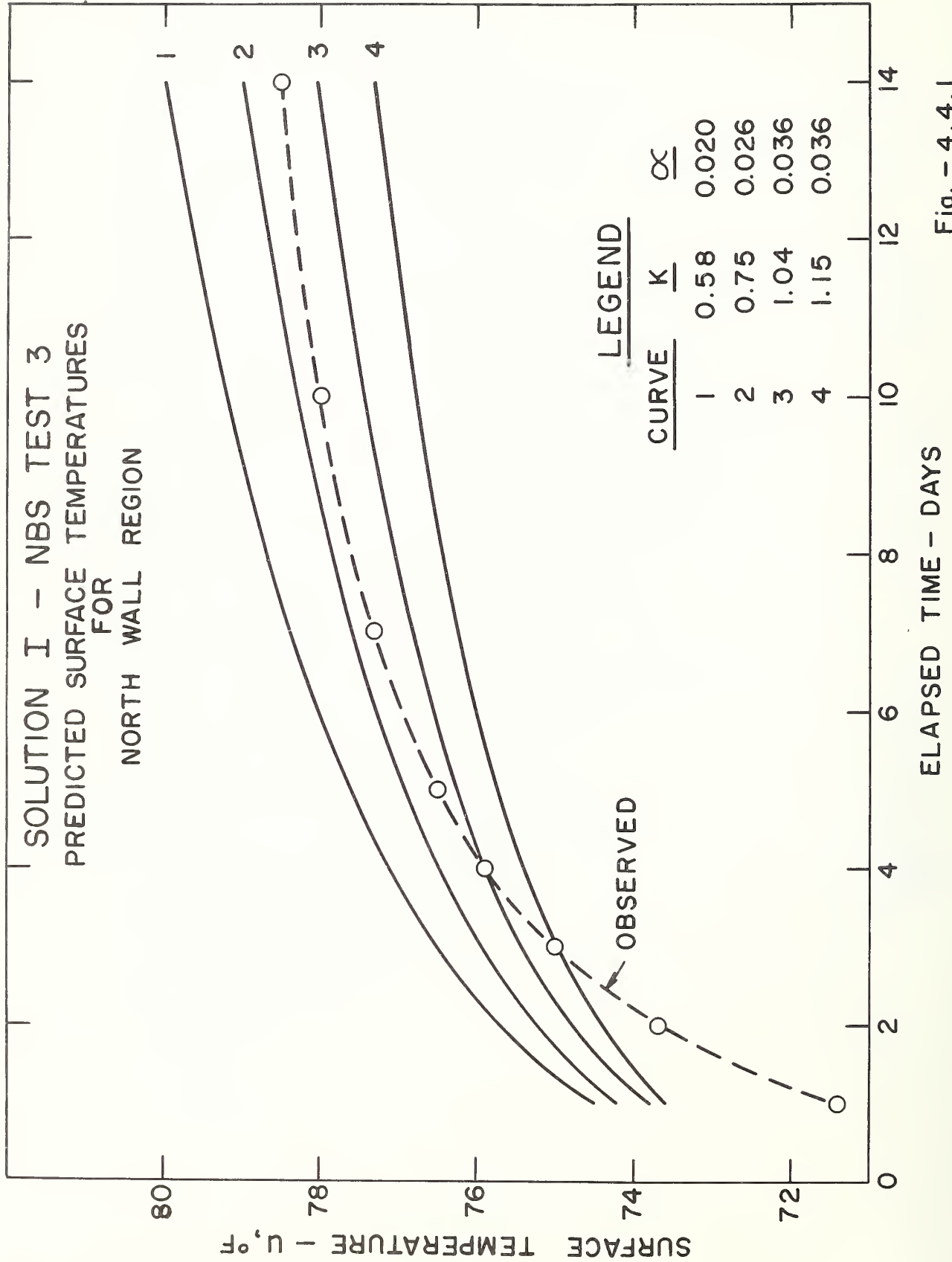


Fig. - 4.4.1

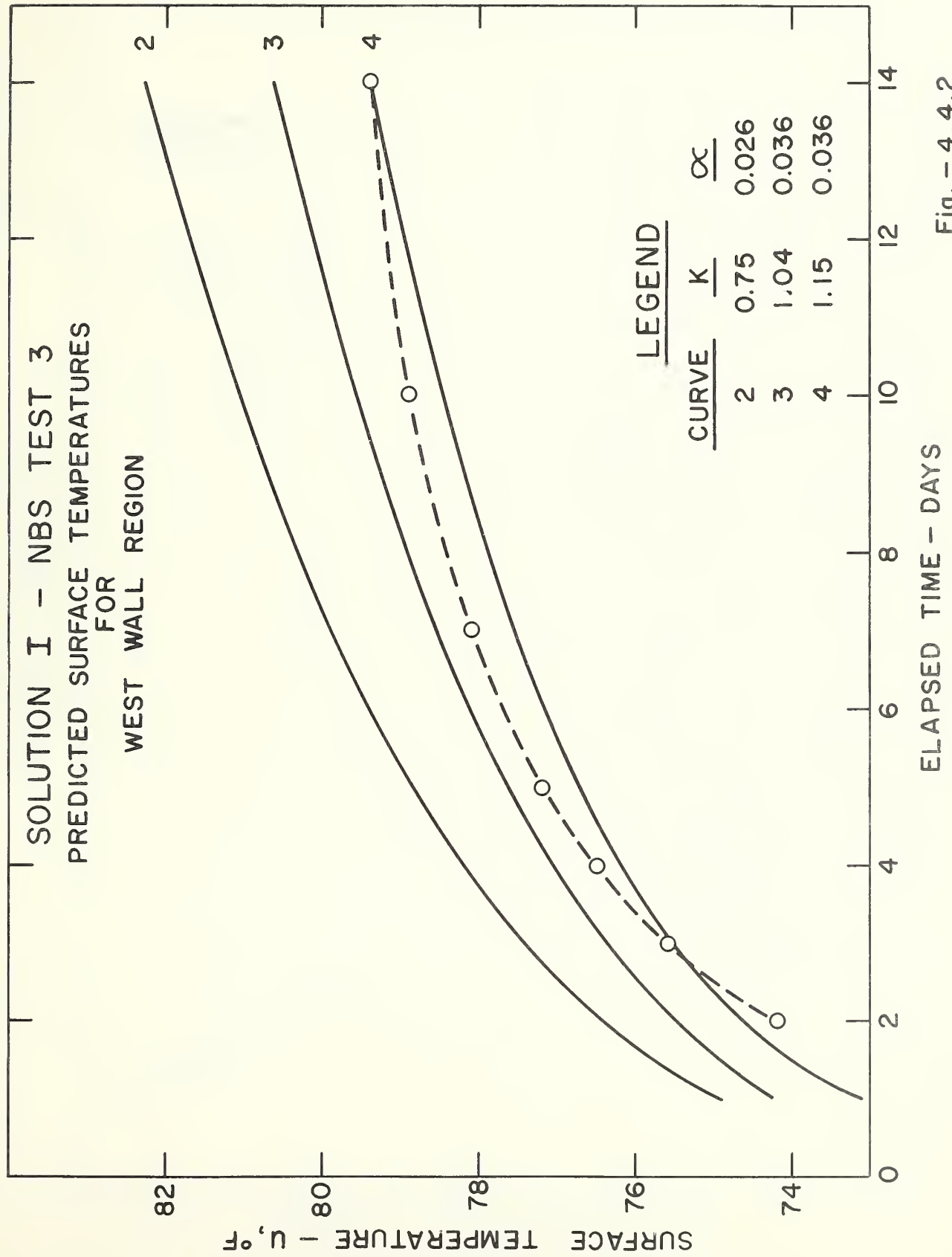


Fig. - 4.4.2

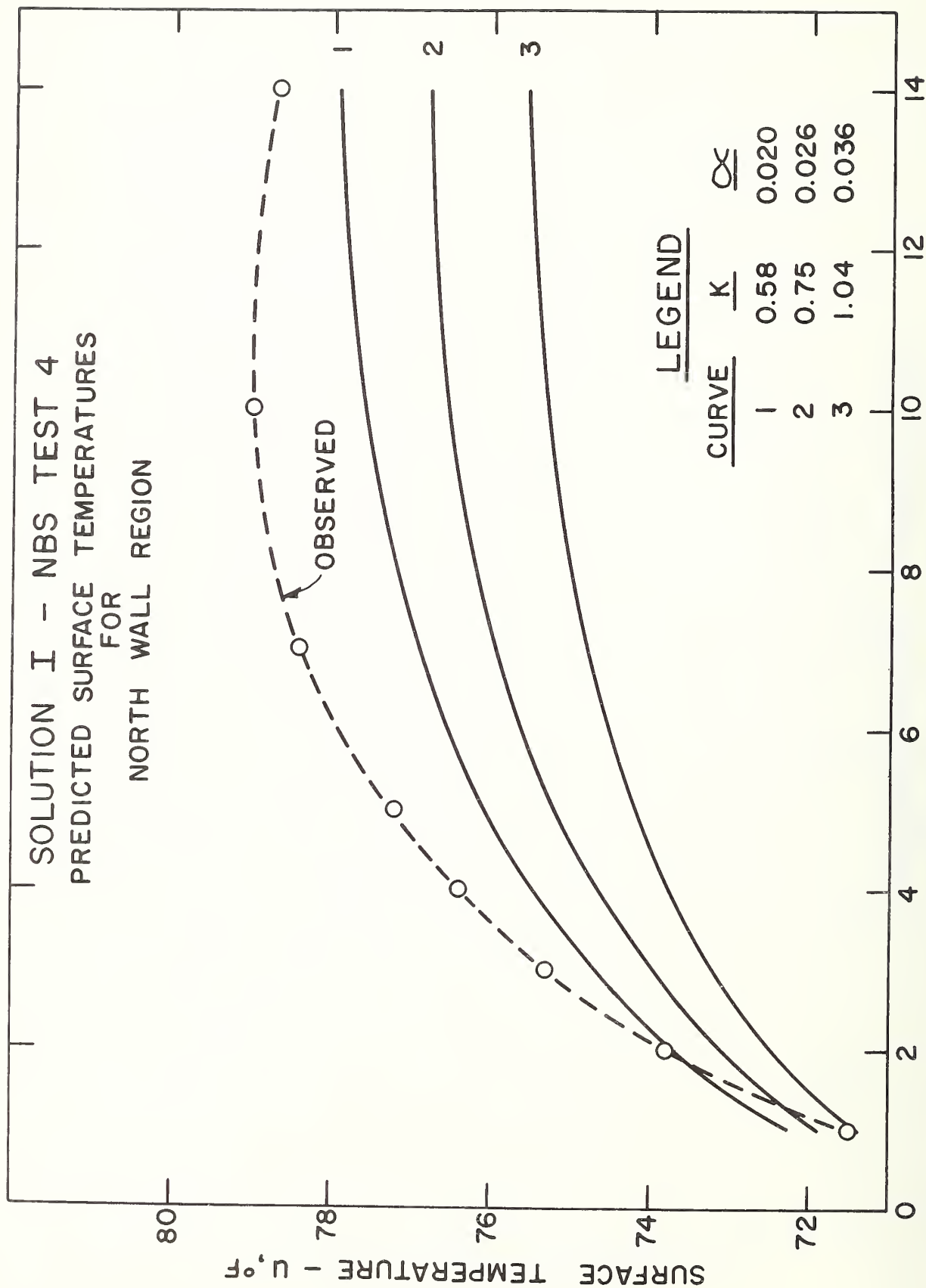
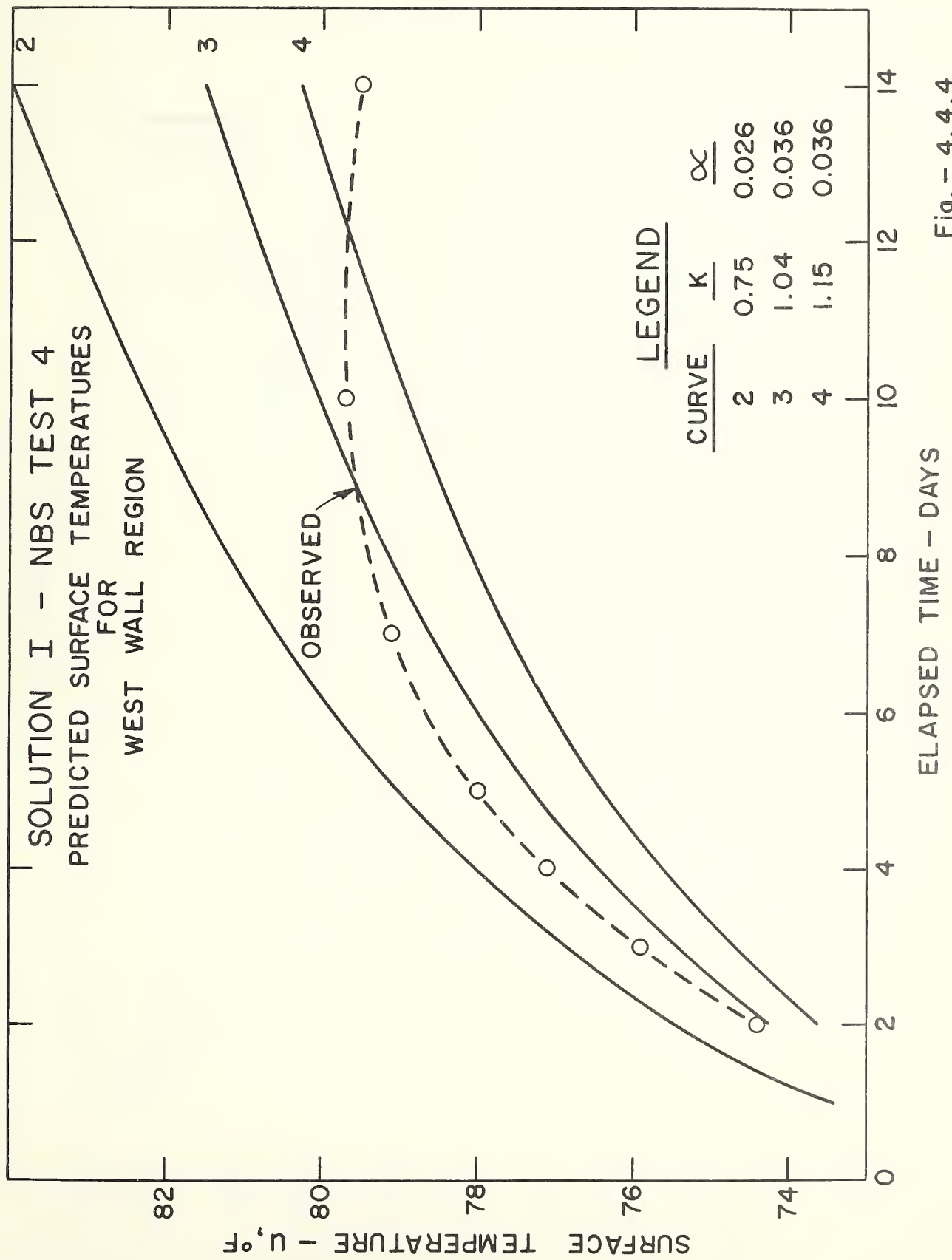


Fig. - 4.4.3



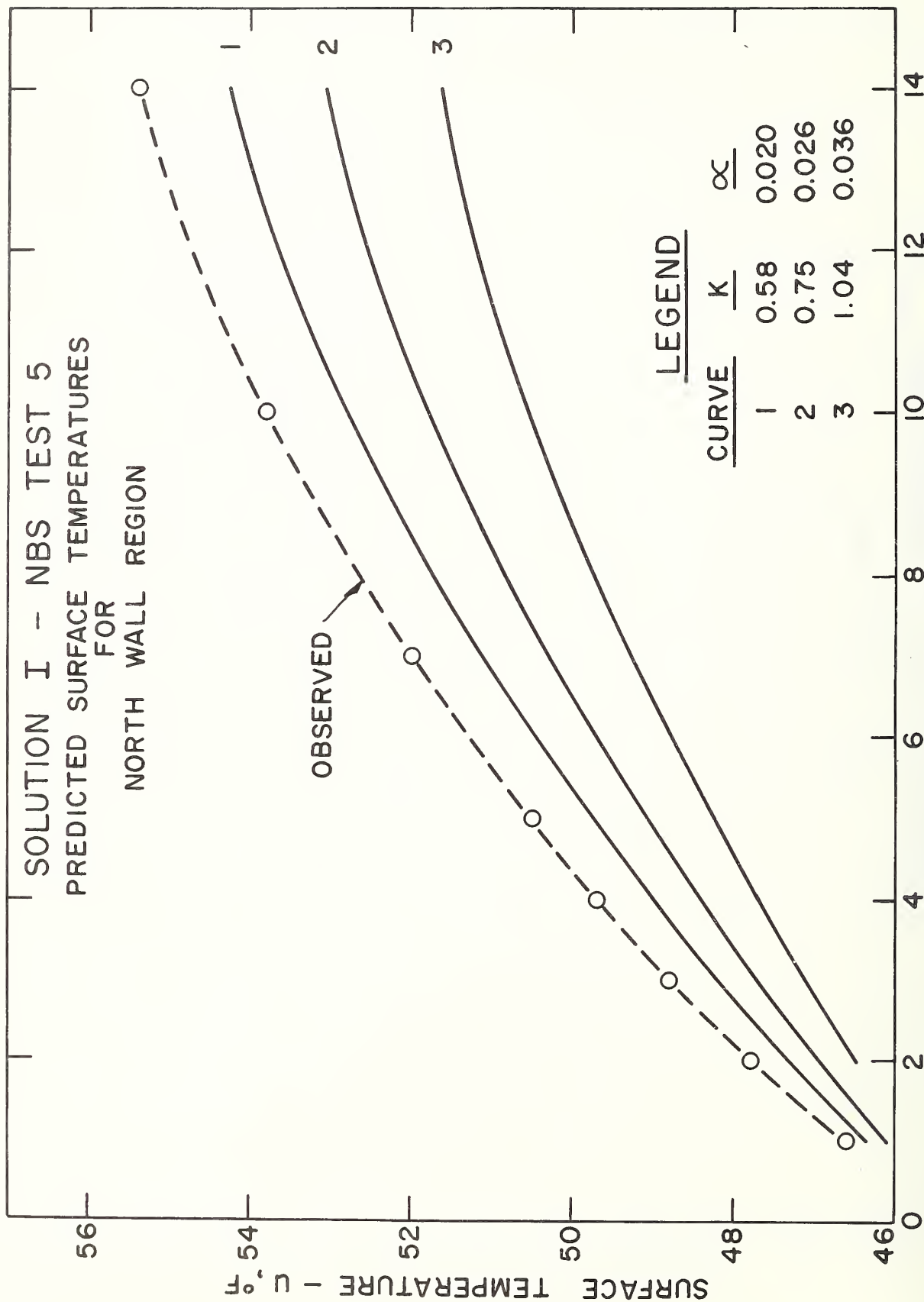


Fig. - 4.4.5

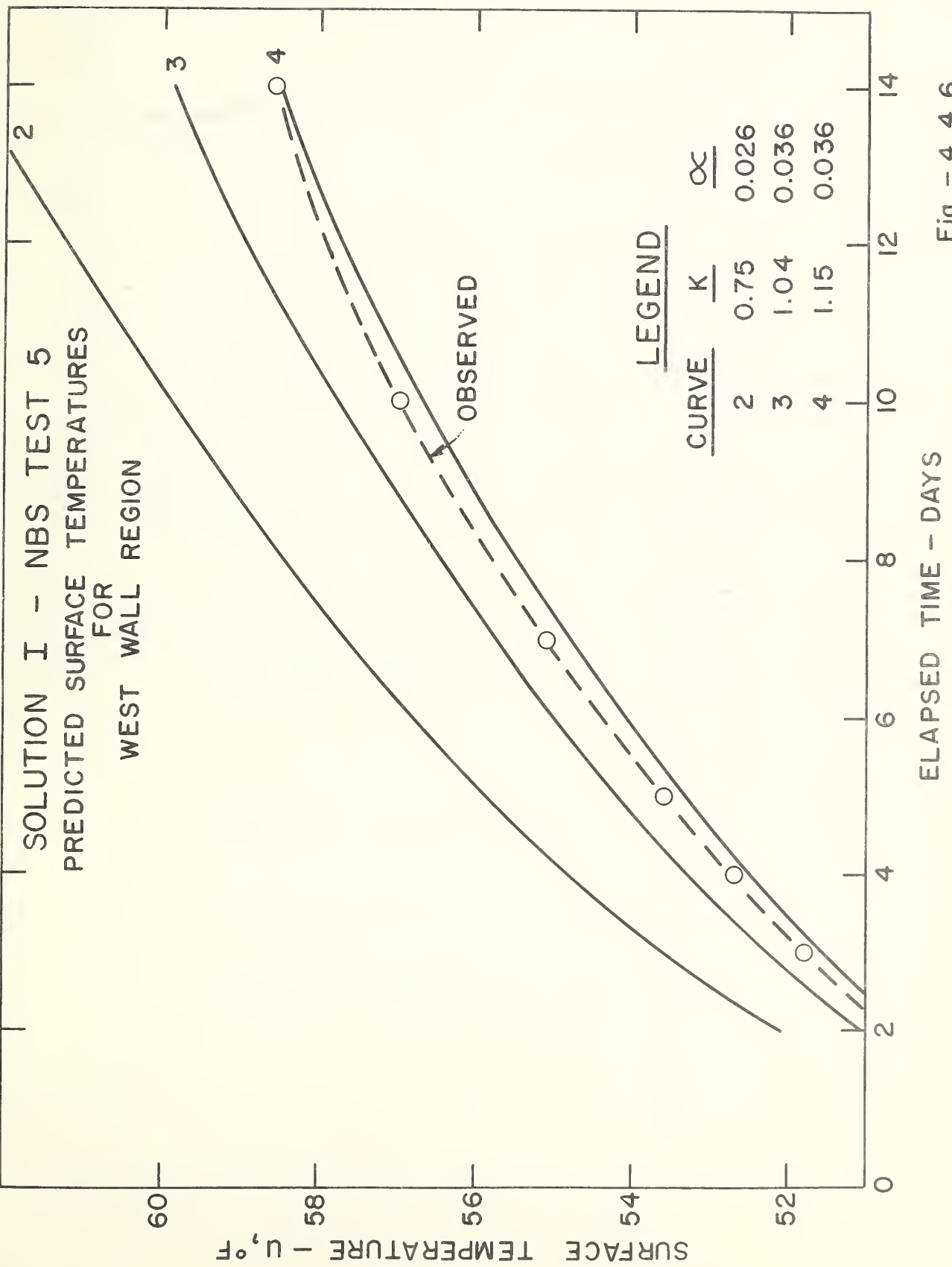


Fig. - 4.4.6

INTERIOR SURFACE TEMPERATURES PREDICTED BY SOLUTION I

Interior Surface Temperatures-°F

-24-

A comparison of analytical predictions with experimental data from NBS Test 4 is included in this section to show the effect on the observed curve of an adverse ambient temperature change which occurred about halfway through the test and continued for its duration. This can be seen in Figures 4.4.3 and 4.4.4 where the value of observed temperature at fourteen days is actually lower than the value at ten days, producing an observed performance impossible to duplicate with models of this kind. For this reason, it will be discarded for discussion purposes in the succeeding solutions.

Further inspection of the figures for NBS Tests 3 and 5 shows that the predicted curves have a basically different shape from the observed curve, which levels off more rapidly with increasing time. The continuing rise of the predicted curves is due to the one-dimensional nature of the solution in which the heat flow is confined to only one direction in space. The shelter itself could lose heat in three dimensions, with the additional heat sinks emanating from the corners becoming more important with increasing time. This resulted in an observed curve which leveled off rapidly, appearing to approach a constant temperature.

These observations suggest a spherical model, which conducts heat in three dimensions. This approximation should accordingly produce a temperature-time curve of more reasonable shape, since the solution is bounded in time.

5. SOLUTION II

5.1 Statement of Problem

Infinite homogeneous medium bounded internally by a sphere of radius a . The heat flux F_0 is constant across the surface $r = a$. The initial temperature is uniform.

5.2 Mathematical Summary

The differential equation to be satisfied by the temperature rise θ is

$$\frac{\partial \theta}{\partial t} = \alpha \left[\frac{1}{r^2} \frac{\partial}{\partial r} \left(r^2 \frac{\partial \theta}{\partial r} \right) \right], r \geq a, t > 0 \quad (1)$$

with the following initial and boundary conditions:

$$r \geq a, t = 0, \theta = 0 \quad (2)$$

$$r = a, t > 0, -K \frac{\partial \theta}{\partial r} = F_0 \quad (3)$$

$$r \rightarrow \infty, t > 0, \theta \rightarrow 0 \quad (4)$$

The solution for temperature rise is

$$\theta = \frac{a^2 F_0}{rK} \left[\operatorname{erfc} \frac{r-a}{2\sqrt{\alpha t}} - \exp \left(\frac{r-a}{a} + \frac{\alpha t}{a^2} \right) \operatorname{erfc} \left(\frac{r-a}{2\sqrt{\alpha t}} + \sqrt{\frac{\alpha t}{a^2}} \right) \right] \quad (5)$$

For an initial temperature u_0 , the temperature at any distance r in the region is given by

$$u = u_0 + \theta \quad (6)$$

At the interior surface $r = a$, 5.2(5) reduces to

$$\theta = \frac{aF_0}{K} \left\{ 1 - \exp(T) \operatorname{erfc}\left(T^{\frac{1}{2}}\right) \right\} \quad (7)$$

where $T = \frac{at}{a^2}$.

5.3 Assumptions

This solution is available on p. 248 [10] and was used as a second approximation for predicting overall shelter performance.

The assumptions used in this approximation are listed and discussed below.

1) geometry - spherical model

The NBS shelter deviated from the spherical model in that part of the system was actually finite, bounded externally by the ground surface. It also differed in the obvious matter of shape, which would alter the local heat flow pattern.

Since the solution depends only on radial distance and time, as discussed in Section 1.3, it can make no distinction among the six surfaces. Thus, it provides only a single temperature prediction at a given radius in all directions.

a) equivalent spherical radius

Since the assumed shape in this model is a sphere, it was necessary to choose a sphere of such radius as to have heat transfer characteristics similar to those of the actual shelter. This was done in two elementary ways, as follows:

- i) by requiring the sphere to have the same surface area as the actual shelter, thus maintaining the same total heat loss rate. On this basis, the equivalent radius is 5.7 feet.
- ii) by requiring the sphere to have the same volume to surface area ratio as the actual shelter, thus taking into account, to some extent, the difference in shape. On this basis, the equivalent radius is 4.0 feet.

2) homogeneous heat conduction region

This assumption was discussed in Section 4.3.

3) uniform initial temperature

Since this model is spherically symmetric in every respect, it follows that only one value of initial temperature can be used. Therefore, the six average region temperatures u_0 , listed in Table 3.1.1, were arithmetically averaged to obtain a single overall initial temperature.

5.4 Results

Figure 5.4.1 compares the observed interior surface temperatures with predicted values using Solution II, for the two values of equivalent spherical radius described in the preceding section and for two sets of earth thermal properties, including the preferred values. Figure 5.4.2 shows similar comparisons for NBS Test 5.

The observed temperatures shown in these figures are arithmetic averages of the smoothed experimental data for all surfaces, including the roof.

The values of heat flux F_o used in computing these results were arithmetic averages of the cumulative averages, including the roof, listed in Table B.1 of Appendix B.

5.5 Discussion

Inspection of Figures 5.4.1 and 5.4.2 shows that better agreement was achieved between observed and predicted values by using the estimated minimum values of earth properties rather than the preferred values. It can also be seen that the equivalent surface area radius of 5.7 feet gave closer agreement than the volume to surface area radius. For the minimum values, the 5.7 foot radius gave agreement to within 1°F or less at $t = 336$ hours for each test, whereas the 4.0 foot radius provided agreement to about 2°F .

Of the two choices for equivalent spherical radius described, the spherical cavity which provided an interior surface area ($a = 5.7$ feet) equal to that of the parallelepiped shelter would be expected to give better agreement between the predicted and observed surfaces temperatures because the test shelter had a low aspect ratio and thus the total amount of earth serving as a heat sink was more nearly comparable in the two cavities.

Further inspection of Figures 5.4.1 and 5.4.2 shows that the shapes of the predicted curves for the spherical model leveled off more rapidly than those for Solution I, as would be expected. The effect of the ground surface boundary can be interpreted as a reduction in the volume of earth available to the shelter for heat conduction, but may not, in all seasons of the year, represent a reduction in the total heat absorption capacity of the region.

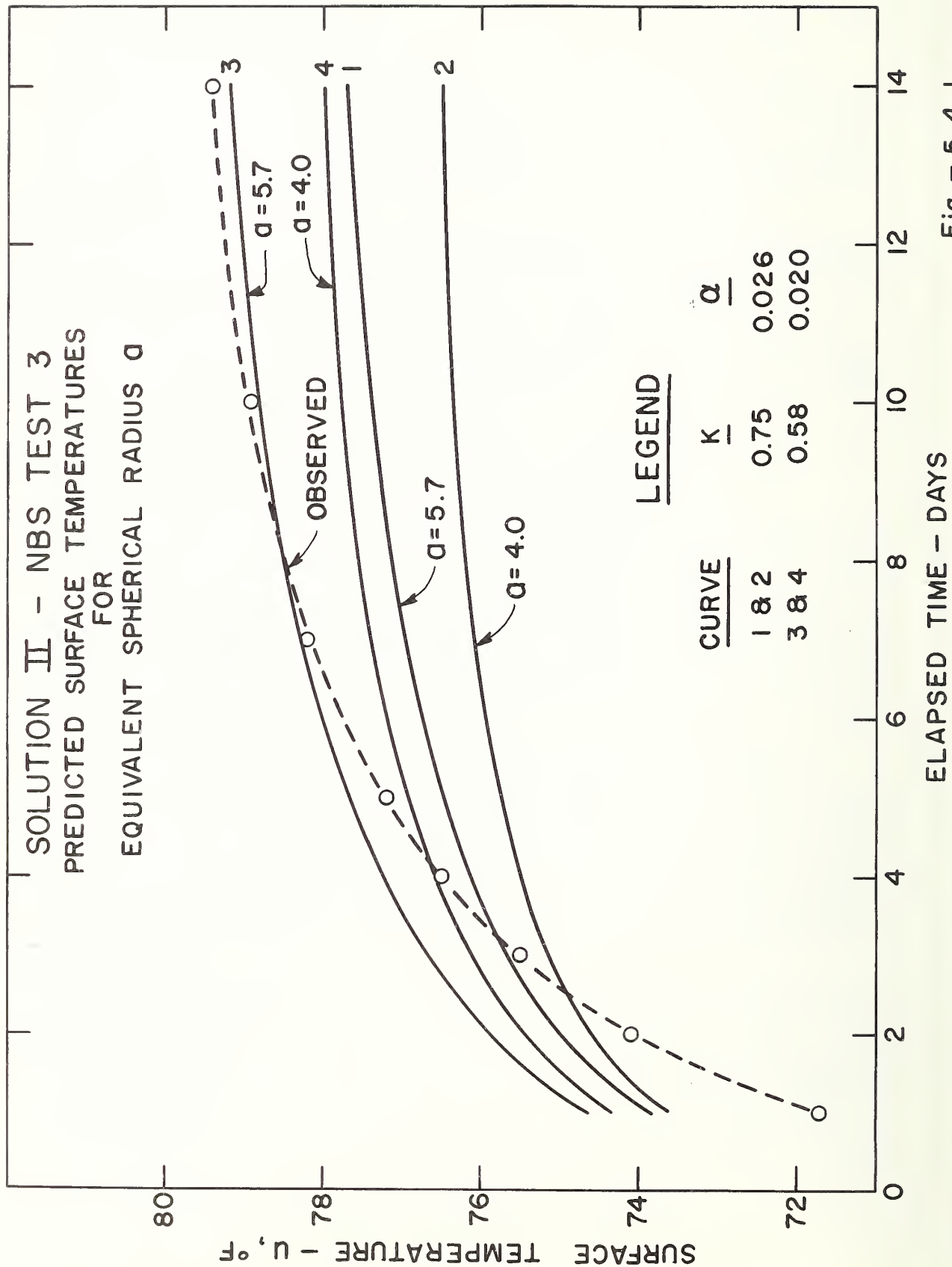


Fig. - 5.4.1

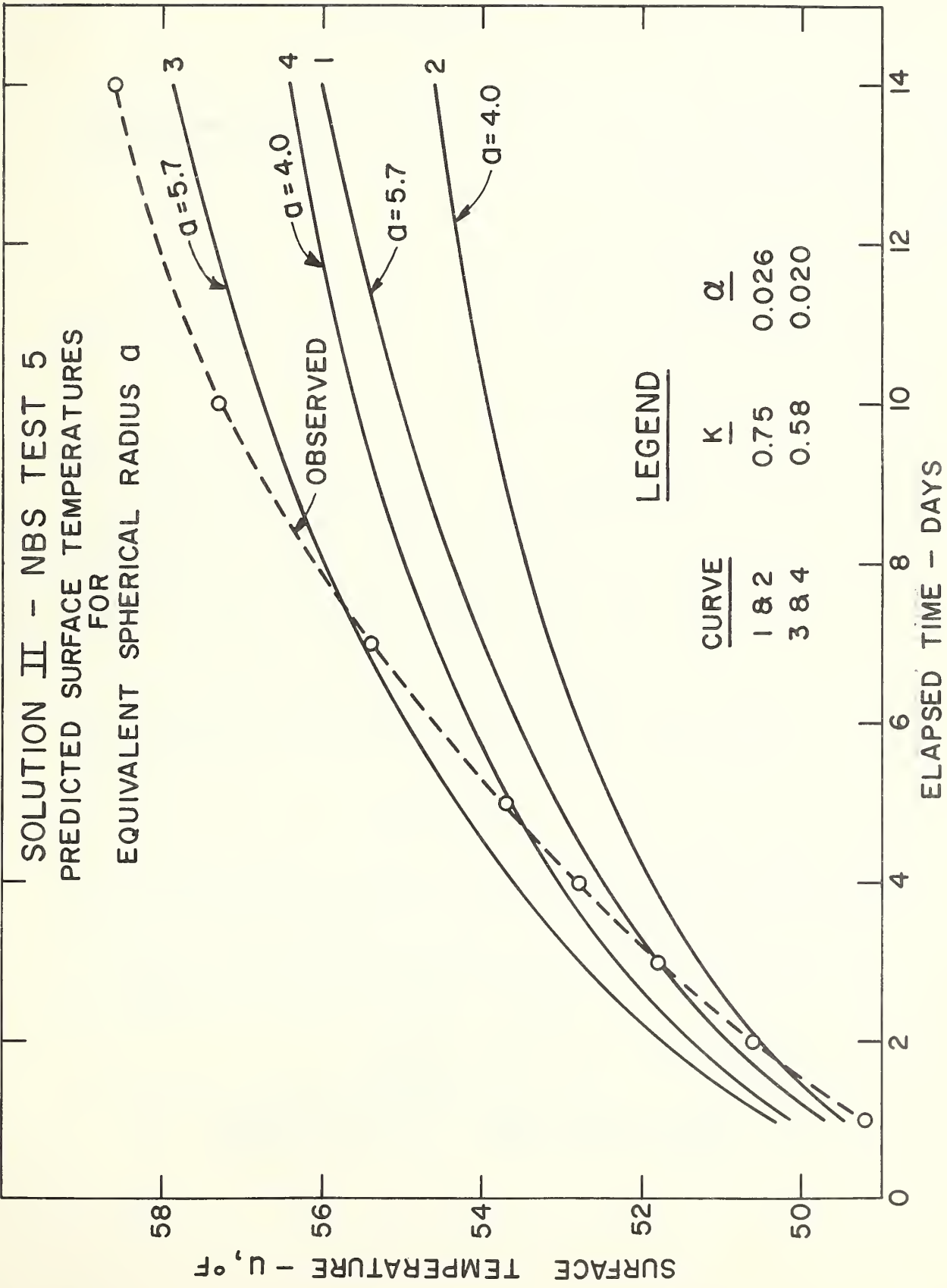


Fig. - 5.4.2

6. SOLUTION III

6.1 Statement of Problem

Infinite homogeneous region bounded internally by an infinitely long cylinder of radius a . The heat flux F_0 is constant across the surface $r = a$. The initial temperature is uniform.

6.2 Mathematical Summary

The differential equation to be satisfied by the temperature rise θ is

$$\frac{\partial \theta}{\partial t} = \alpha \left[\frac{\partial^2 \theta}{\partial r^2} + \frac{1}{r} \frac{\partial \theta}{\partial r} \right], \quad r \geq a, \quad t > 0 \quad (1)$$

with the following initial and boundary conditions:

$$r > a, \quad t = 0, \quad \theta = 0 \quad (2)$$

$$r = a, \quad t > 0, \quad -K \frac{\partial \theta}{\partial r} = F_0 \quad (3)$$

$$r \rightarrow \infty, \quad t > 0, \quad \theta \rightarrow 0 \quad (4)$$

The solution of the Laplace transformed equation is

$$\bar{\theta} = \frac{F_0 K_0(qr)}{q K_p K_1(qa)} \quad (5)$$

An asymptotic series expansion of Eq. 6.2(5) yields the solution for temperature rise for small values of time

$$\begin{aligned} \theta = & \frac{2F_0}{K} \left[\frac{\alpha a t}{r} \right]^{\frac{1}{2}} \left\{ i \operatorname{erfc} \frac{r-a}{2\sqrt{\alpha t}} - \frac{(3r+a)}{4ar} [\alpha t]^{\frac{1}{2}} i^2 \operatorname{erfc} \frac{r-a}{2\sqrt{\alpha t}} \right. \\ & + \frac{9a^2 + 6ar + 33r^2}{32a^2 r^2} [\alpha t] i^3 \operatorname{erfc} \frac{r-a}{2\sqrt{\alpha t}} \\ & \left. - \frac{75a^3 + 27a^2 r + 33ar^2 + 249r^3}{128a^3 r^3} [\alpha t]^{\frac{3}{2}} i^4 \operatorname{erfc} \frac{r-a}{2\sqrt{\alpha t}} + \dots \right\} \quad (6) \end{aligned}$$

For an initial temperature u_0 , the temperature at any distance r in the region is given by

$$u = u_0 + \theta \quad (7)$$

At the interior surface $r = a$, 6.2(6) reduces to

$$\theta = \frac{2aF_0}{K} T^{\frac{1}{2}} \left\{ \frac{1}{\sqrt{\pi}} - \frac{1}{4} T^{\frac{1}{2}} + \frac{1}{4\sqrt{\pi}} T - \frac{3}{32} T^{\frac{3}{2}} + \dots \right\} \quad (8)$$

where $T = \frac{\alpha t}{a^2}$.

6.3 Convergence

The first two terms of this series solution, Eq. 6.2(6), were available on p. 339 [10], and were tried as a third approximation for predicting overall shelter performance. However, the contribution from the second term was found to be considerable for moderate values of the Fourier number T , suggesting that one or more higher order terms might contribute significantly.

Two additional terms were obtained by expanding the modified Bessel functions of the second kind, which appear in Eq. 6.2(5), into asymptotic series, performing the indicated division, and taking the inverse transform of each term.

The expression in Eq. 6.2(8) converges for small values of T , but will diverge for large values. The change from convergence to divergence appears to occur at approximately $T = 1$. For values of T in the neighborhood of 1, convergence may be quite slow, so that many terms of the series would be needed to provide reasonable accuracy. In this case, four terms of the series were sufficient to produce accuracy of the order of hundredths of a degree Fahrenheit.

A large time solution p. 339 [10], would be required to produce convergence for values $T > 1$.

6.4 Assumptions

The assumptions used in this approximation are listed and discussed below.

1) geometry - cylindrical model

The NBS shelter deviated even more from this model than it did from the previous spherical model. In addition to the reasons given in paragraph (1) of Section 5.3, the cylinder is assumed to be infinite in length, as well as circular in shape. However, as stated in Section 5.5, this model was introduced for purely mathematical reasons.

Like the previous solution, this solution provides only a single temperature at a given radius, in all directions normal to the central axis of the cylinder.

a) equivalent cylindrical radius

The cylindrical radius chosen to approximate the shelter was obtained by assuming that the shelter was a cylindrical cavity whose length (l) was equal to the longest internal dimension of the shelter and whose radius was such that the curved area, $2\pi r l$, was equal to the total shelter surface area. This method yielded an equivalent radius of 6.0 feet. Only the curved area was used to represent the total surface area because no heat flows axially in the cylindrical model.

2) homogeneous heat conduction region

This assumption was discussed in Section 4.3.

3) uniform initial temperature

The same average initial temperature used in the previous solution was also used here, for the same reasons of symmetry.

6.5 Results

Figures 6.5.1 and 6.5.2 show interior surface temperatures versus time, predicted by Solution III, for an equivalent cylindrical radius, $a = 6.0$ ft. These curves together with the observed performance, were plotted for NBS Tests 3 and 5 for two sets of thermal properties, including the preferred earth values.

The observed temperatures shown on each figure are the same ones used in Section 5.4, and the values of heat flux F_0 used in the computations are the same as those used in the previous solution.

6.6 Discussion

Inspection of Figures 6.5.1 and 6.5.2 shows that the preferred earth thermal properties gave better agreement between predicted and observed temperatures for an equivalent cylindrical radius of 6.0 feet. This combination gave agreement to within less than 0.5°F for both tests, for elapsed times of both 168 and 336 hours. The shape and position of the predicted curves are an improvement over those produced by Solutions I and II.

At this point, further improvement dealing with models characterized by one space variable could probably be achieved by treating the composite case, or the nonuniform initial temperature case. These refinements would introduce considerable complexity into the mathematics; however, treating the one-dimensional model will avoid some of the complexity, and will give some indication of the magnitude of the effects. Since the composite nature of the heat conduction region is a fundamental property applicable to all concrete shelters, it will be treated in the following section.

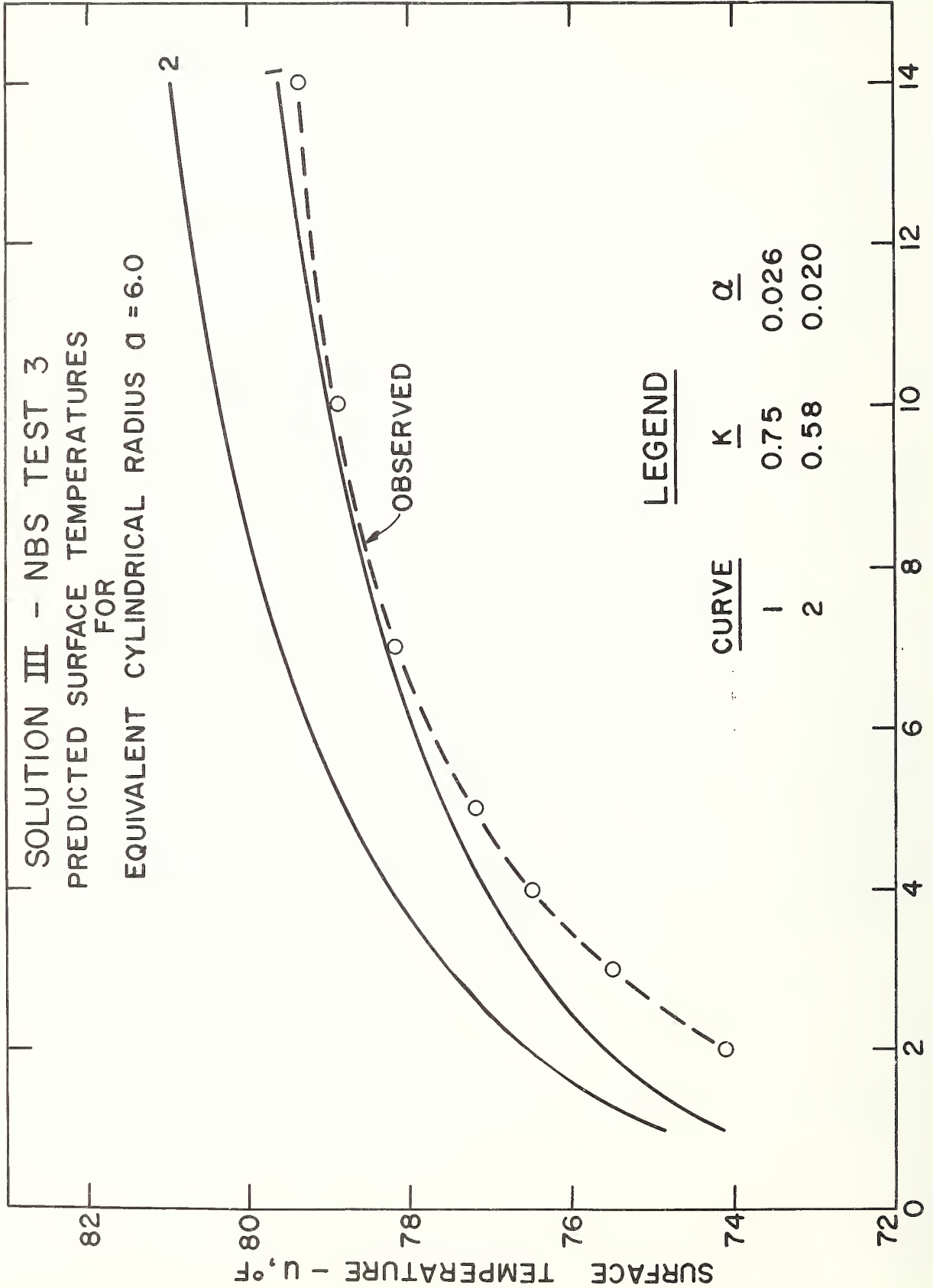


Fig. - 6.5.1

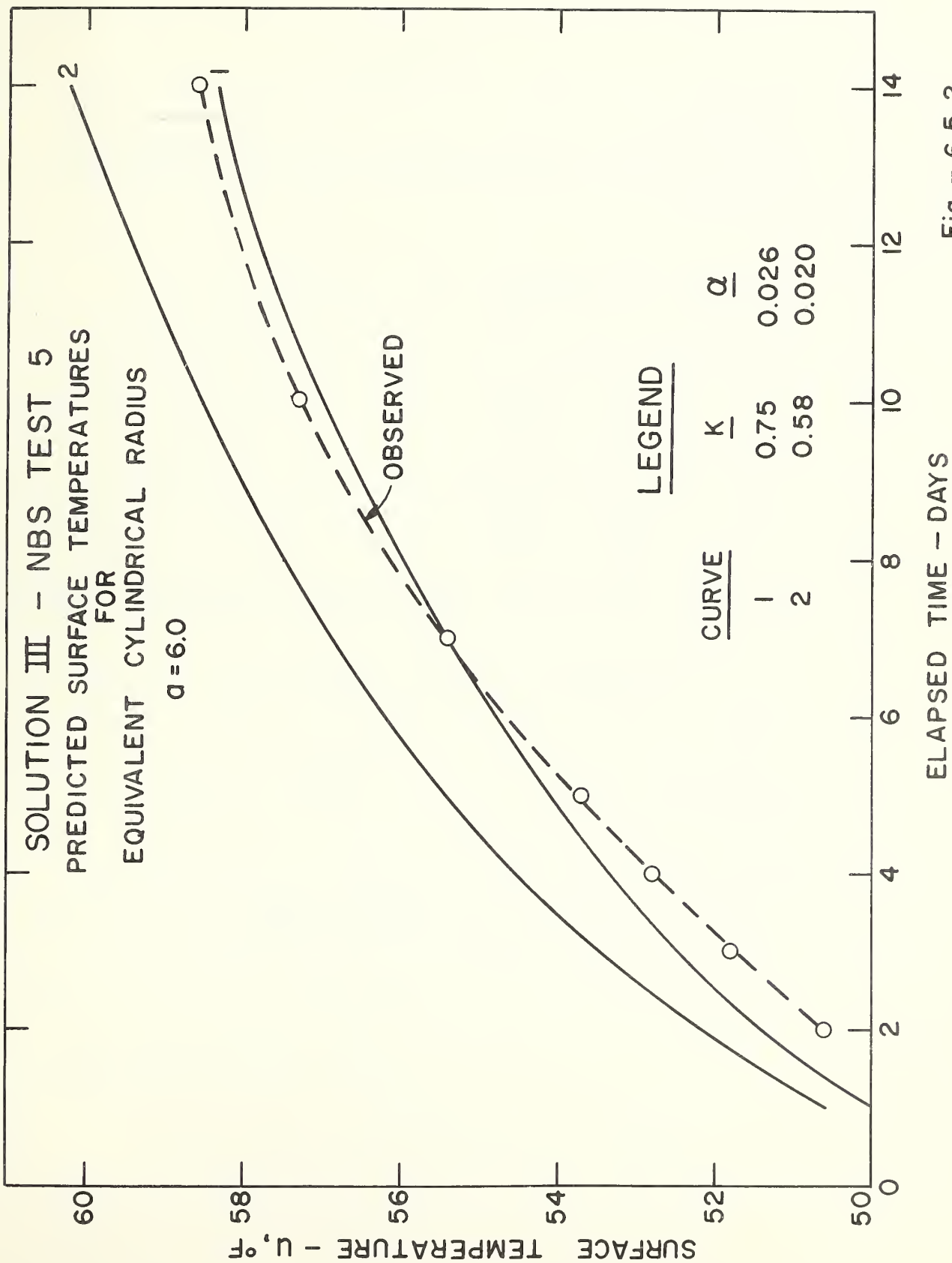


Fig. - 6.5.2

7. SOLUTION IV

7.1 Statement of Problem

Semi-infinite composite region. The heat flux F_0 is constant across the surface $x = -l$. The initial temperature is uniform.

7.2 Mathematical Summary

The differential equations to be satisfied by the temperature rise θ are

$$\frac{\partial \theta_1}{\partial t} = \alpha_1 \frac{\partial^2 \theta_1}{\partial x^2}, \quad -l < x < 0, \quad t > 0 \quad (1)$$

and

$$\frac{\partial \theta_2}{\partial t} = \alpha_2 \frac{\partial^2 \theta_2}{\partial x^2}, \quad 0 < x < \infty, \quad t > 0 \quad (2)$$

with the following initial and boundary conditions:

$$-l < x < 0, \quad t = 0, \quad \theta_1 = 0 \quad (3)$$

$$0 < x < \infty, \quad t = 0, \quad \theta_2 = 0 \quad (4)$$

$$x = -l, \quad t > 0, \quad -K_1 \frac{\partial \theta_1}{\partial x} = F_0 \quad (5)$$

$$x = 0, \quad t > 0, \quad \theta_1 = \theta_2 \quad (6)$$

$$x = 0, \quad t > 0, \quad K_1 \frac{\partial \theta_1}{\partial x} = K_2 \frac{\partial \theta_2}{\partial x} \quad (7)$$

$$x \rightarrow \infty, \quad t > 0, \quad \theta_2 \rightarrow 0 \quad (8)$$

The solutions of the Laplace transformed equations are

$$\bar{\theta}_1 = \frac{F_o}{q_1 K_{1p}} \left\{ \frac{\exp [-q_1(\ell + x)] - \beta \exp [-q_1(\ell - x)]}{1 + \beta \exp (-2q_1 \ell)} \right\} \quad (9)$$

and

$$\bar{\theta}_2 = \frac{2F_o}{q_1 K_{1p}(\sigma + 1)} \left\{ \frac{\exp [-q_1(\ell + xk)]}{1 + \beta \exp (-2q_1 \ell)} \right\} \quad (10)$$

The inverse transformations yield the solution for temperature at any point in the concrete medium

$$u_1 = u_o + \frac{2\ell}{K_1} F_o T^{\frac{1}{2}} \sum_{n=0}^{\infty} (-1)^n \beta^n \left\{ \text{ierfc} \frac{(2n+1)+x/\ell}{2T^{\frac{1}{2}}} - \beta \text{ierfc} \frac{(2n+1)-x/\ell}{2T^{\frac{1}{2}}} \right\} \quad (11)$$

and the solution for temperature at any point in the earth medium

$$u_2 = u_o + \frac{2\ell}{K_1} (1-\beta) F_o T^{\frac{1}{2}} \sum_{n=0}^{\infty} (-1)^n \beta^n \text{ierfc} \frac{(2n+1)+kx/\ell}{2T^{\frac{1}{2}}} \quad (12)$$

where $T = \frac{\alpha_1 t}{\ell^2}$.

At the interior surface $x = -\ell$, Eq. 7.2(11) becomes

$$u_1 = u_o + \frac{2\ell}{K_1} F_o T^{\frac{1}{2}} \sum_{n=0}^{\infty} (-1)^n \beta^n \left\{ \text{ierfc} \frac{n}{T^{\frac{1}{2}}} - \beta \text{ierfc} \frac{n+1}{T^{\frac{1}{2}}} \right\} \quad (13)$$

At the concrete-earth interface $x = 0$, either 7.2(11) or (12) may be used, giving

$$u = u_o + \frac{2\ell}{K_1} (1-\beta) F_o T^{\frac{1}{2}} \sum_{n=0}^{\infty} (-1)^n \beta^n \text{ierfc} \frac{(2n+1)}{2T^{\frac{1}{2}}} \quad (14)$$

7.3 Convergence

Since $0 < \operatorname{ierfc}(x) \leq 1/\sqrt{\pi}$ for all values of x , the convergence of $(-\beta)^n$ is sufficient to insure convergence of Eqs. 7.2(11) and (12). Therefore the series converges whenever $|\beta| < 1$. This condition is always satisfied, as can be seen from an examination of the definition:

$$\beta = \frac{\sigma - 1}{\sigma + 1} \quad \text{and} \quad \sigma = \frac{K_2}{K_1} \sqrt{\frac{\alpha_1}{\alpha_2}}$$

whence $-1 < \beta < 1$ for $0 < \sigma < \infty$.

7.4 Assumptions

Similar solutions were published in references [11] and [12], using a different origin for the coordinate system. This solution, Eqs. 7.2(11) and (12), was derived with the origin located at the interface for mathematical simplicity.

The assumptions used in this approximation are listed and discussed below.

1) geometry — one-dimensional model

This assumption is the same as for Solution I and was discussed in Section 4.3. It will be listed in the following solutions without further comment.

2) composite heat conduction region

The heat conduction region was a composite of 8 inches of concrete in perfect thermal contact with an infinite earth medium, so that the solution contains the thermal properties of both media. This assumption will be listed in the following solutions without further comment.

3) uniform initial temperature

This assumption is the same as for Solution I and was discussed in Section 4.3.

7.5 Results

Figures 7.5.1 through .4 show interior surface temperatures versus time, computed from Eq. 7.2(13), for the north and west wall conduction regions of NBS Tests 3 and 5, together with the observed performance.

Curves 1 and 3 show predicted performance based on the preferred concrete thermal properties and two sets of earth properties, including the preferred values. Curves 2 and 4 show performance based on estimated "maximum" concrete properties and two sets of earth properties, namely, estimated maximum and preferred values.

Table 7.5.1 shows predicted surface temperatures for the five semi-infinite regions of NBS Tests 3, 4, and 5, evaluated at elapsed times of one and two weeks, together with the observed temperatures and the resulting deviations. The computations were based on the preferred concrete and earth thermal properties.

Table 7.5.2 is similar to 7.5.1, except that the predicted surface temperatures were based on the maximum sets of thermal properties.

A numerical example for this solution is shown in Appendix C.

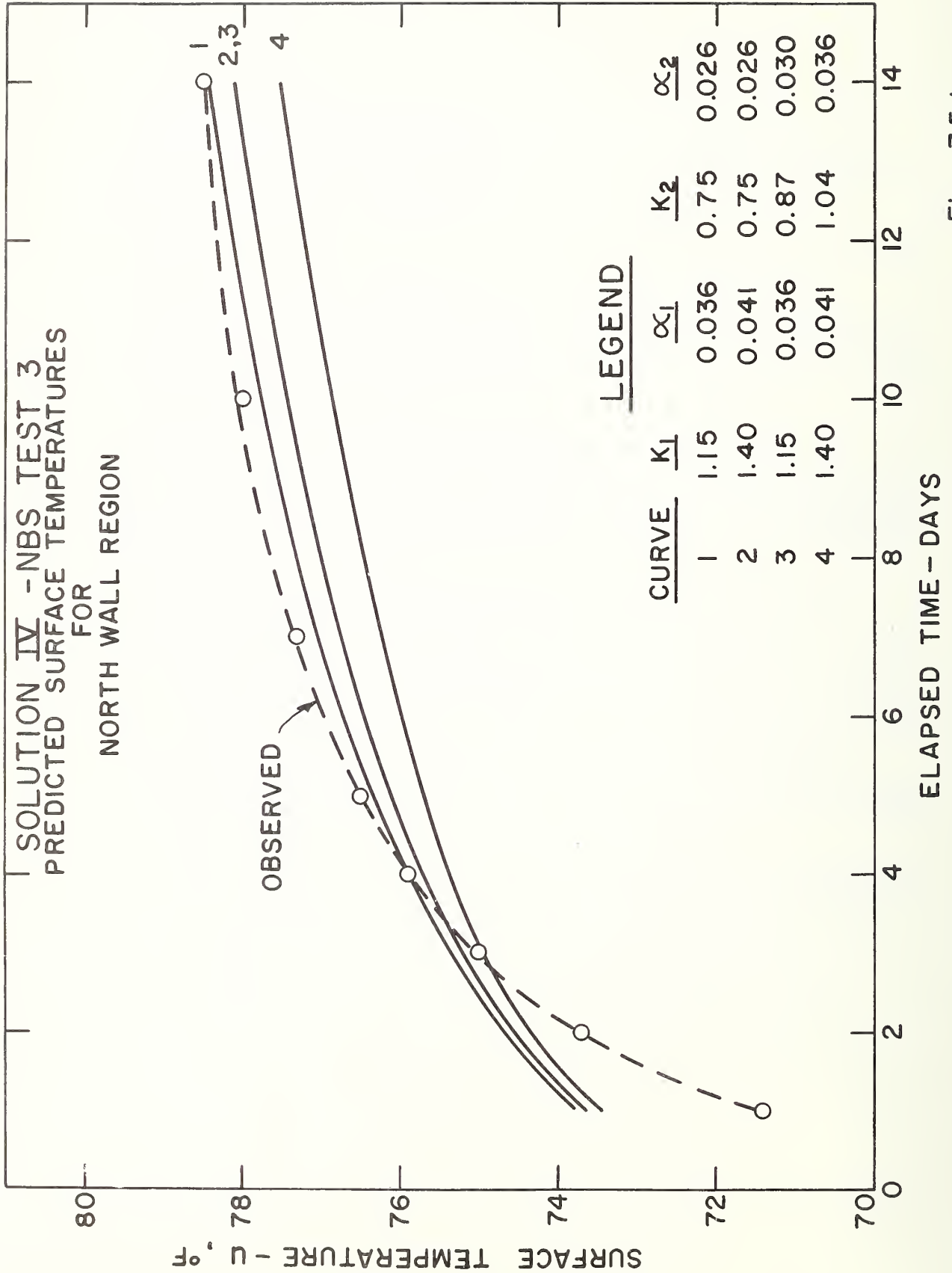


Fig.- 7.5.1

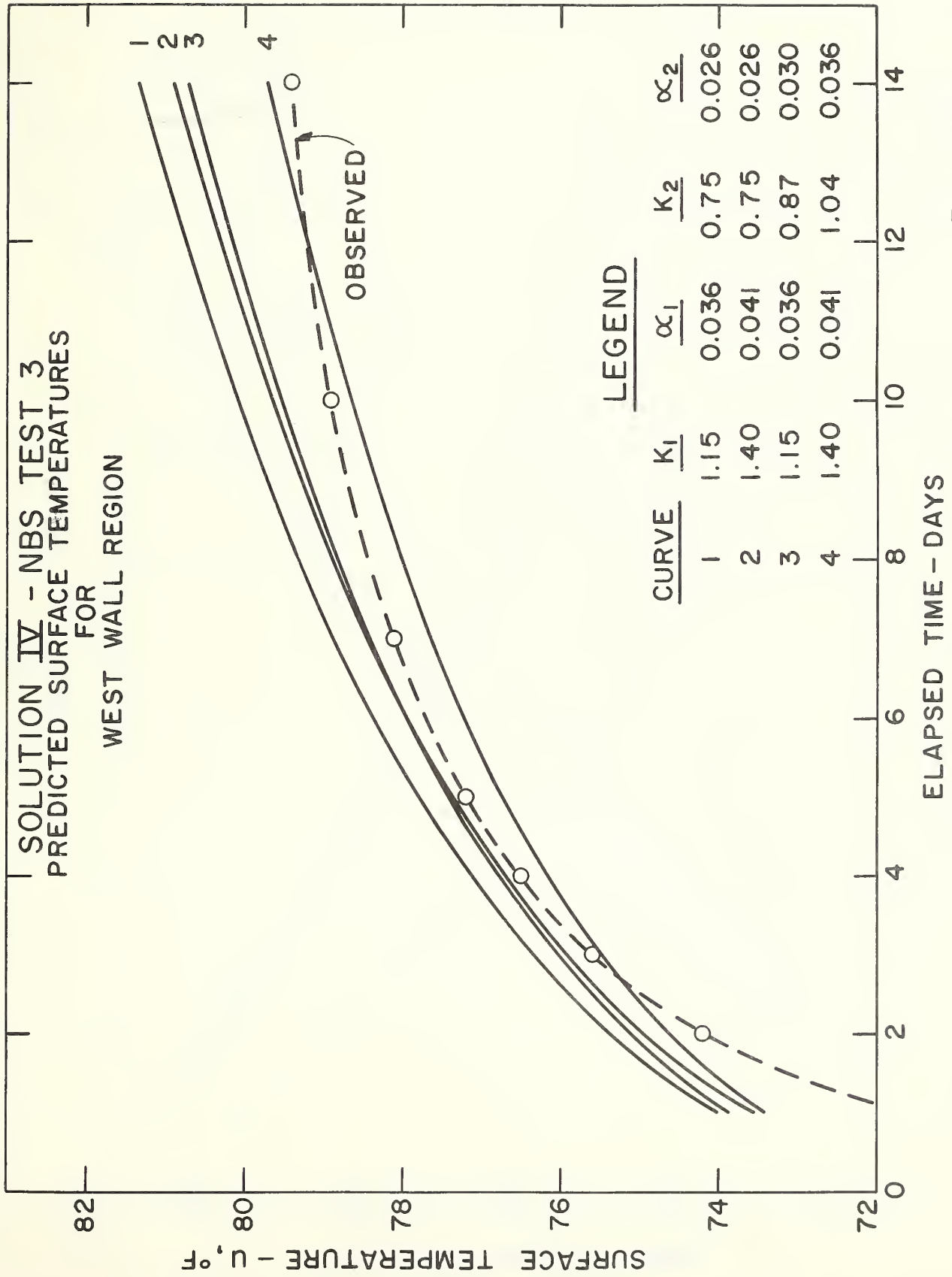


Fig.- 7.5.2

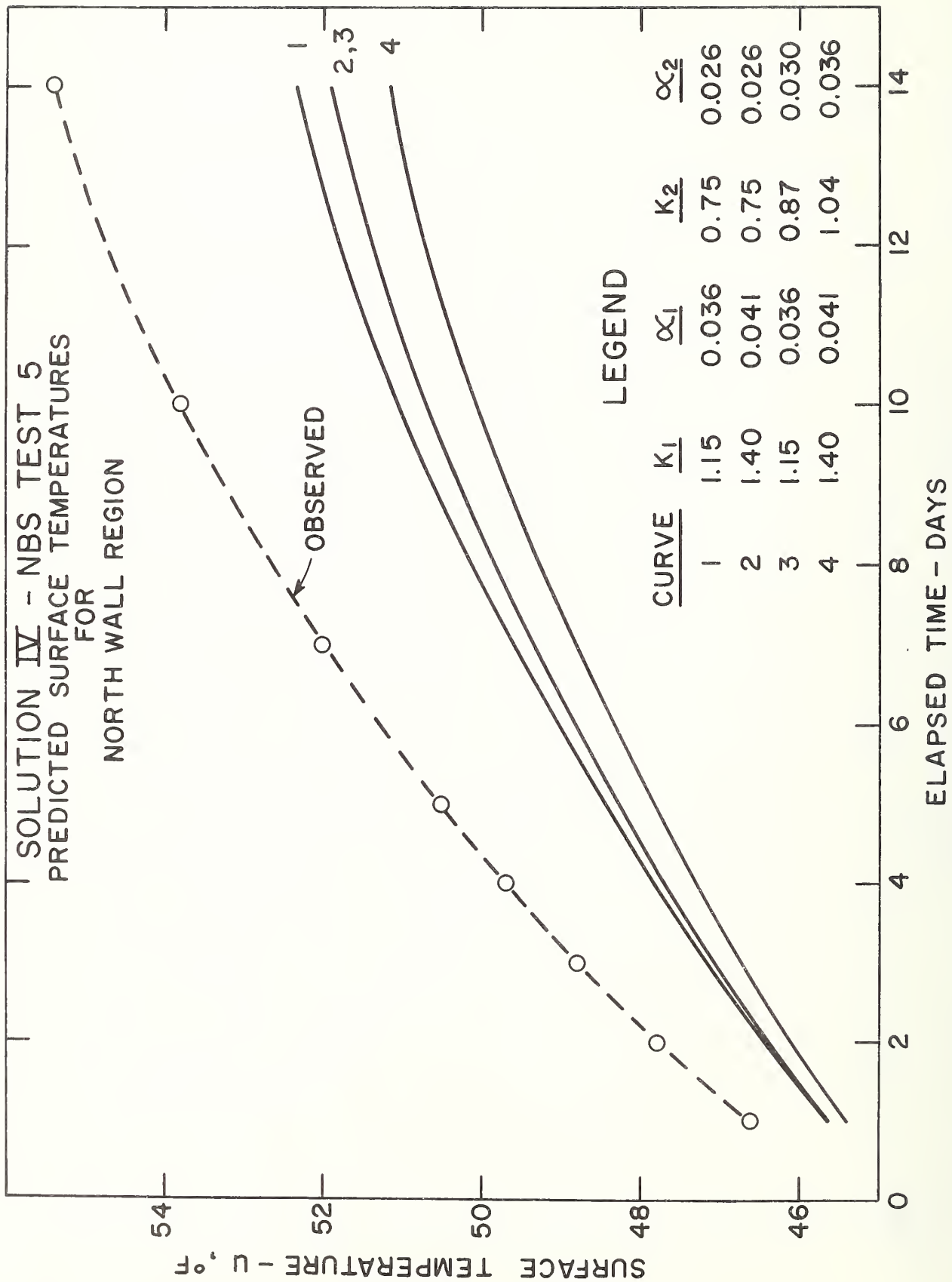


Fig.- 7.5.3

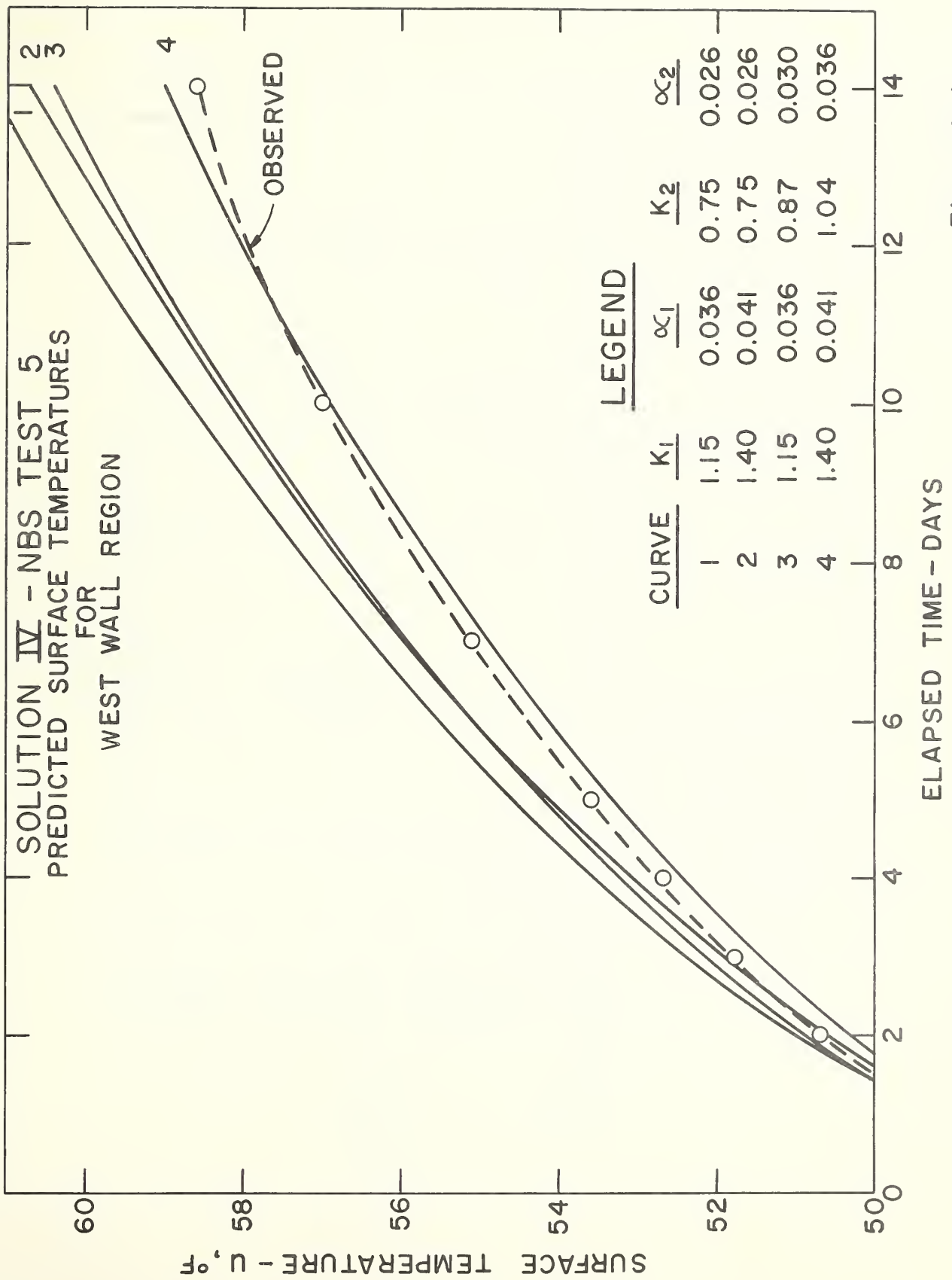


Fig. - 7.5.4

TABLE 7.5.1

INTERIOR SURFACE TEMPERATURES
PREDICTED BY SOLUTION IV

$$K_1 = 1.15 \quad \alpha_1 = 0.036$$

$$K_2 = 0.75 \quad \alpha_2 = 0.026$$

$$\sigma = 0.767$$

Elapsed Time Test Surface	Interior Surface Temperatures--°F					
	168 Hours			336 Hours		
	Predicted	Observed	Deviation	Predicted	Observed	Deviation
3	North	76.9	-0.4	78.5	78.5	0.0
	West	78.9	0.8	81.3	79.4	1.9
	South	81.0	1.2	8.28	81.0	1.8
	East	80.8	1.9	83.3	80.1	3.2
	Floor	78.3	2.5	82.5	77.3	5.2
4	North	75.2	-3.2	76.2	78.7	-2.5
	West	79.3	0.2	82.8	79.5	3.3
	South	79.1	-1.1	81.6	79.8	1.8
	East	78.5	-0.6	81.0	79.5	1.5
	Floor	76.9	1.5	81.0	76.7	4.3
5	North	49.6	-2.4	52.3	55.4	-3.1
	West	56.4	1.3	61.2	58.6	2.6
	South	61.3	4.4	68.2	60.2	8.0
	East	58.3	1.4	63.5	60.2	3.3
	Floor	56.1	1.3	59.6	57.5	2.1

TABLE 7.5.2

INTERIOR SURFACE TEMPERATURES
PREDICTED BY SOLUTION IV

$$K_1 = 1.40 \quad \alpha_1 = 0.041$$

$$K_2 = 1.04 \quad \alpha_2 = 0.036$$

$$\sigma = 0.793$$

Elapsed Time Test Surface	Interior Surface Temperatures-°F					
	168 Hours			336 Hours		
	Predicted	Observed	Deviation	Predicted	Observed	Deviation
3	North	76.2	-1.1	77.5	78.5	-1.0
	West	77.6	-0.5	79.7	79.4	0.3
	South	79.3	-0.5	80.8	81.0	-0.2
	East	79.4	0.5	81.6	80.1	1.5
	Floor	76.4	0.6	80.0	77.3	2.7
4	North	74.4	-4.0	75.2	78.7	-3.5
	West	77.7	-1.4	80.7	79.5	1.2
	South	77.6	-2.6	79.7	79.8	-0.1
	East	77.1	-2.0	79.2	79.5	-0.3
	Floor	75.2	-0.2	78.7	76.7	2.0
5	North	48.8	-3.2	51.2	55.4	-4.2
	West	54.9	-0.2	59.0	58.6	0.4
	South	59.1	2.2	64.9	60.2	4.7
	East	56.4	-0.5	60.8	60.2	0.6
	Floor	55.4	0.6	58.3	57.5	0.8

7.6 Discussion

Inspection of Figures 7.5.1 and .3 shows that the preferred thermal properties of concrete and earth (Curve 1) gave better agreement for the north wall region. This region, as previously pointed out, was selected as the least typical in the sense of conforming least to the one-dimensional model. The maximum values of thermal properties (Curve 4) gave better agreement for the west wall region, as well as for the other three regions, in most cases. These findings are similar to those pointed out by Solution I, and can be seen from Table 7.5.2 which shows that in 10 out of 15 cases, the maximum values produced agreement to within 1.5°F at the end of a two-week period. The preferred sets, on the other hand (Table 7.5.1), produced agreement to within the same amount in only 2 out of 15 cases. This lack of agreement for the preferred sets of values is due to the one-dimensional nature of the solution which has already been seen to cause high predictions. However, it should be recalled that the purpose of this solution is to examine the importance of the composite assumption.

Curves 2 and 3, based on approximately equal fractional increases in concrete values on one hand and earth values on the other, indicate, when compared with Curve 1, that the two media play about equal roles in conducting heat away from the shelter for two-week periods. However, since the earth is generally less conductive than the concrete, and becomes increasingly utilized for heat storage as time increases, it would ultimately be expected to control the heat flow.

This tendency can be seen from further examination of Curves 1, 2, and 3 in Figs. 7.5.2 and .4 which shows that increasing the concrete properties lowers the temperature more than increasing the earth properties in the first week, but less in the second week. However, the lower temperatures at the end of two weeks (Curve 3) are not significantly lower than Curve 2, and the reason that the greater mass of earth involved is not a dominant factor by this time will be discussed in Section 10.2.

This solution can be further improved, at the expense of some increase in mathematical complexity, by considering the non-uniform initial temperature distribution which actually existed. (See Appendix A).

8. SOLUTION V

8.1 Statement of Problem

Semi-infinite composite region. The heat flux F_0 is constant across the surface $x = -l$. Each medium has initial temperature $u = f(x)$.

8.2 Mathematical Summary

The differential equations to be satisfied by the temperature u are

$$\frac{\partial u_1}{\partial t} = \alpha_1 \frac{\partial^2 u_1}{\partial x^2}, \quad -l < x < 0, \quad t > 0 \quad (1)$$

and

$$\frac{\partial u_2}{\partial t} = \alpha_2 \frac{\partial^2 u_2}{\partial x^2}, \quad 0 < x < \infty, \quad t > 0 \quad (2)$$

with the following initial and boundary conditions:

$$-l < x < 0, \quad t = 0, \quad u_1 = ax + b \quad (3)$$

$$0 < x < \infty, \quad t = 0, \quad u_2 = c + (b-c) \exp(-mx) \quad (4)$$

$$x = -l, \quad t > 0, \quad -K_1 \frac{\partial u_1}{\partial x} = F_0 \quad (5)$$

$$x = 0, \quad t > 0, \quad u_1 = u_2 \quad (6)$$

$$x = 0, \quad t > 0, \quad K_1 \frac{\partial u_1}{\partial x} = K_2 \frac{\partial u_2}{\partial x} \quad (7)$$

$$x \rightarrow \infty, \quad t > 0, \quad u_2 \rightarrow c \quad (8)$$

The solutions of the Laplace transformed equations are

$$\begin{aligned} \bar{u}_1 = & \left\{ \frac{F_0 + aK_1}{q_1 K_1 p} \right\} \left\{ \frac{\exp [-q_1(\ell + x)] - \beta \exp [-q_1(\ell - x)]}{1 + \beta \exp (-2q_1 \ell)} \right\} \\ & + \left\{ \frac{(b - c) K_2 (q_2 - m)}{q_1 K_1 (\sigma + 1) (p - \alpha_2 m^2)} \right\} \left\{ \frac{\exp [-q_1(2\ell + x)] + \exp (q_1 x)}{1 + \beta \exp (-2q_1 \ell)} \right\} \\ & + \left\{ \frac{q_1 \sigma (c-b) - a}{q_1 p (\sigma + 1)} \right\} \left\{ \frac{\exp [-q_1(2\ell + x)] + \exp (q_1 x)}{1 + \beta \exp (-2q_1 \ell)} \right\} + \frac{ax + b}{p} \end{aligned} \quad (9)$$

and

$$\begin{aligned} \bar{u}_2 = & \left\{ \frac{F_0 + aK_1}{q_1 K_1 p} \right\} \left\{ \frac{\exp [-q_1(\ell + xk)] - \beta \exp [-q_1(\ell - xk)]}{1 + \beta \exp (-2q_1 \ell)} \right\} \\ & + \left\{ \frac{q_1 \sigma (c-b) - a}{q_1 p (\sigma + 1)} \right\} \left\{ \frac{\exp (-q_1 xk) + \exp [-q_1(2\ell + xk)]}{1 + \beta \exp (-2q_1 \ell)} \right\} \\ & + \left\{ \frac{(b - c)(q_1 K_1 \sigma - mK_2)}{q_1 K_1 (\sigma + 1) (p - \alpha_2 m^2)} \right\} \left\{ \frac{\exp (-q_1 xk) + \exp [-q_1(2\ell + xk)]}{1 + \beta \exp (-2q_1 \ell)} \right\} \\ & + \left\{ \frac{(b - c)}{p - \alpha_2 m^2} \right\} \left\{ \exp (-mx) - \exp (-q_1 xk) \right\} \\ & + \left\{ \frac{(b-c) \exp (-q_1 xk) + c}{p} \right\} \end{aligned} \quad (10)$$

The inverse transformations yield the solution for temperature at any point in the concrete medium

$$\begin{aligned}
 u_1 = & \frac{2\ell}{K_1} (F_0 + aK_1) T^{\frac{1}{2}} \sum_{n=0}^{\infty} (-\beta)^n \left[\text{ierfc} \frac{(2n+1) + x/\ell}{2T^{\frac{1}{2}}} - \beta \text{ierfc} \frac{(2n+1) - x/\ell}{2T^{\frac{1}{2}}} \right] \\
 & - a\ell(1-\beta) T^{\frac{1}{2}} \sum_{n=0}^{\infty} (-\beta)^n \left[\text{ierfc} \frac{2(n+1) + x/\ell}{2T^{\frac{1}{2}}} + \text{ierfc} \frac{2n - x/\ell}{2T^{\frac{1}{2}}} \right] \\
 & - (b-c) \frac{(1+\beta)}{2} \sum_{n=0}^{\infty} (-\beta)^n \left[\text{erfc} \frac{2(n+1) + x/\ell}{2T^{\frac{1}{2}}} + \text{erfc} \frac{2n - x/\ell}{2T^{\frac{1}{2}}} \right] \\
 & + (b-c) \frac{(1+\beta)}{2} \sum_{n=0}^{\infty} (-\beta)^n \left\{ \text{erfc} \left[\frac{2(n+1) + x/\ell}{2T^{\frac{1}{2}}} + \frac{\ell m}{k} T^{\frac{1}{2}} \right] \exp \left[\left(\frac{\ell m}{k} \right)^2 T \right. \right. \\
 & \left. \left. + 2(n+1) \frac{\ell m}{k} + \frac{mx}{k} \right] + \text{erfc} \left[\frac{2n - x/\ell}{2T^{\frac{1}{2}}} + \frac{\ell m}{k} T^{\frac{1}{2}} \right] \exp \left[\left(\frac{\ell m}{k} \right)^2 T \right. \right. \\
 & \left. \left. + 2n \frac{\ell m}{k} - \frac{mx}{k} \right] \right\} + ax + b
 \end{aligned} \tag{11}$$

and the solution for temperature at any point in the earth medium

$$\begin{aligned}
 u_2 = & \frac{2\ell}{K_1} (F_0 + aK_1) T^{\frac{1}{2}} \sum_{n=0}^{\infty} (-\beta)^n (1-\beta) \text{ierfc} \frac{(2n+1) + kx/\ell}{2T^{\frac{1}{2}}} \\
 & - a\ell(1-\beta) T^{\frac{1}{2}} \sum_{n=0}^{\infty} (-\beta)^n \left[\text{ierfc} \frac{2(n+1) + kx/\ell}{2T^{\frac{1}{2}}} + \text{ierfc} \frac{2n + kx/\ell}{2T^{\frac{1}{2}}} \right]
 \end{aligned}$$

$$\begin{aligned}
 & - (b-c) \frac{(1+\beta)}{2} \sum_{n=0}^{\infty} (-\beta)^n \left[\operatorname{erfc} \frac{2(n+1) + kx/\ell}{2T^{\frac{1}{2}}} + \operatorname{erfc} \frac{2n + kx/\ell}{2T^{\frac{1}{2}}} \right] \\
 & + (b-c) \frac{(1+\beta)}{2} \sum_{n=0}^{\infty} (-\beta)^n \left\{ \operatorname{erfc} \left[\frac{2(n+1) + kx/\ell}{2T^{\frac{1}{2}}} + \frac{\ell m}{k} T^{\frac{1}{2}} \right] \exp \left[\left(\frac{\ell m}{k} \right)^2 T \right. \right. \\
 & \left. \left. + 2(n+1) \frac{\ell m}{k} + mx \right] + \operatorname{erfc} \left[\frac{2n+kx/\ell}{2T^{\frac{1}{2}}} + \frac{\ell m}{k} T^{\frac{1}{2}} \right] \exp \left[\left(\frac{\ell m}{k} \right)^2 T \right. \right. \\
 & \left. \left. + 2n \frac{\ell m}{k} + mx \right] \right\} + \frac{b-c}{2} \left\{ \operatorname{erfc} \left[\frac{\ell m}{k} T^{\frac{1}{2}} - \frac{kx/\ell}{2T^{\frac{1}{2}}} \right] \exp \left[\left(\frac{\ell m}{k} \right)^2 T - mx \right] \right. \\
 & \left. - \operatorname{erfc} \left[\frac{\ell m}{k} T^{\frac{1}{2}} + \frac{kx/\ell}{2T^{\frac{1}{2}}} \right] \exp \left[\left(\frac{\ell m}{k} \right)^2 T + mx \right] \right\} + (b-c) \operatorname{erfc} \frac{kx/\ell}{2T^{\frac{1}{2}}} + c \quad (12)
 \end{aligned}$$

where $T = \frac{a_1 t}{\ell^2}$.

At the interior surface $x = -\ell$, Eq. 8.2(11) becomes

$$\begin{aligned}
 u_1 &= \frac{2\ell}{K_1} (F_0 + aK_1) T^{\frac{1}{2}} \sum_{n=0}^{\infty} (-\beta)^n \left[\operatorname{ierfc} \frac{n}{T^{\frac{1}{2}}} - \beta \operatorname{ierfc} \frac{n+1}{T^{\frac{1}{2}}} \right] \\
 & - 2a\ell(1-\beta)T^{\frac{1}{2}} \sum_{n=0}^{\infty} (-\beta)^n \operatorname{ierfc} \frac{2n+1}{2T^{\frac{1}{2}}} - (1+\beta)(b-c) \sum_{n=0}^{\infty} (-\beta)^n \operatorname{erfc} \frac{2n+1}{2T^{\frac{1}{2}}} \\
 & + (b-c)(1+\beta) \sum_{n=0}^{\infty} (-\beta)^n \operatorname{erfc} \left[\frac{2n+1}{2T^{\frac{1}{2}}} + \frac{\ell m}{k} T^{\frac{1}{2}} \right] \exp \left[\left(\frac{\ell m}{k} \right)^2 T \right. \\
 & \left. + (2n+1) \frac{\ell m}{k} \right] - a\ell + b \quad (13)
 \end{aligned}$$

At the concrete-earth interface $x = 0$, either 8.2(11) or (12) may be used, giving

$$\begin{aligned}
 u = & \frac{2\ell}{K_1} (F_0 + aK_1) T^{\frac{1}{2}} \sum_{n=0}^{\infty} (-\beta)^n (1-\beta) \operatorname{ierfc} \frac{2n+1}{2T^{\frac{1}{2}}} \\
 & - a\ell(1-\beta) T^{\frac{1}{2}} \sum_{n=0}^{\infty} (-\beta)^n \left[\operatorname{ierfc} \frac{n+1}{T^{\frac{1}{2}}} + \operatorname{ierfc} \frac{n}{T^{\frac{1}{2}}} \right] \\
 & - (b-c) \frac{(1+\beta)}{2} \sum_{n=0}^{\infty} (-\beta)^n \left[\operatorname{erfc} \frac{n+1}{T^{\frac{1}{2}}} + \operatorname{erfc} \frac{n}{T^{\frac{1}{2}}} \right] \\
 & + (b-c) \frac{(1+\beta)}{2} \sum_{n=0}^{\infty} (-\beta)^n \left\{ \operatorname{erfc} \left[\frac{n+1}{T^{\frac{1}{2}}} + \frac{\ell m}{k} T^{\frac{1}{2}} \right] \exp \left[\left(\frac{\ell m}{k} \right)^2 T + 2(n+1) \frac{\ell m}{k} \right] \right. \\
 & \left. + \operatorname{erfc} \left[\frac{n}{T^{\frac{1}{2}}} + \frac{\ell m}{k} T^{\frac{1}{2}} \right] \exp \left[\left(\frac{\ell m}{k} \right)^2 T + 2n \frac{\ell m}{k} \right] \right\} + b
 \end{aligned} \tag{14}$$

8.3 Convergence

The first two series in Eq. 8.2(11) are of the same form as that of Eq. 7.2(11), and converge for the reasons given in Section 7.3.

The third series contains complementary error functions which are also bounded

$$0 < \operatorname{erfc}(x) \leq 1$$

for all values of x . Therefore this series also converges whenever $|\beta| < 1$.

The remaining series converges for all values of T , whenever a certain condition among the parameters β , m , ℓ , α_1 , and α_2 is satisfied. This condition can be obtained by use of the ratio test for convergence. The absolute value of the ratio of the $(n+1)^{\text{th}}$ term to the n^{th} term of the series is

$$\frac{|\beta^{n+1}| \left\| \operatorname{erfc} \left[\frac{2(n+1)-x/\ell}{2T^{\frac{1}{2}}} + \frac{\ell m}{k} T^{\frac{1}{2}} \right] \right\| \exp \left[\left(\frac{\ell m}{k} \right)^2 T + 2(n+1) \frac{\ell m}{k} - \frac{mx}{k} \right]}{|\beta^n| \left\| \operatorname{erfc} \left[\frac{2n-x/\ell}{2T^{\frac{1}{2}}} + \frac{\ell m}{k} T^{\frac{1}{2}} \right] \right\| \exp \left[\left(\frac{\ell m}{k} \right)^2 T + 2n \frac{\ell m}{k} - \frac{mx}{k} \right]} \quad (1)$$

This reduces to

$$|\beta| \left\{ \frac{\operatorname{erfc} \left[\frac{2n-x/\ell}{2T^{\frac{1}{2}}} + \frac{\ell m}{k} T^{\frac{1}{2}} + \frac{1}{T^{\frac{1}{2}}} \right]}{\operatorname{erfc} \left[\frac{2n-x/\ell}{2T^{\frac{1}{2}}} + \frac{\ell m}{k} T^{\frac{1}{2}} \right]} \right\} \exp \left(2 \frac{\ell m}{k} \right) \quad (2)$$

The value of this expression must be less than one, in the limit of large n , for convergence. The bracketed term approaches one for large n , and thus the ratio of terms reduces to

$$|\beta| \exp \left(2 \frac{\ell m}{k} \right) \quad (3)$$

The condition for convergence, then, is that (3) be kept less than one. The smaller the value of T , the faster is the convergence, and for T corresponding to about 14 days, only a few terms are required.

Eq. 8.2(12) is similar to (11), with two additional terms which are not summed. These terms vanish for large T .

8.4 Assumptions

A solution of this type was not available in any of several apposite references examined, and was derived, as in the previous solution, with the origin of the coordinate system located at the interface.

The assumptions used in this approximation are listed and discussed below.

- 1) geometry — one-dimensional model
- 2) composite heat conduction region
- 3) non-uniform initial temperature

In the previous solutions, the initial temperature distribution throughout each region, e.g., $-l < x < \infty$, was assumed to be uniform, and an appropriate average value was used to represent the observed distribution shown in Appendix A. The figures in this appendix show that the initial temperature distribution was not uniform in most cases, especially at the beginning of NBS Test 3. Even though an initial condition such as that of Test 3 would not be likely to exist in an actual situation, especially one in which the shelter had been unoccupied for a long period of time, the kind of unusual distribution which did exist afforded an opportunity to observe its maximum effect and significance.

In this solution, the initial temperature was approximated in the concrete medium by a linearly increasing function, $u_1 = ax + b$, Eq. 8.2(3), and in the earth medium by the exponential function $u_2 = c + (b-c) \exp(-mx)$, Eq. 8.2(4). See Fig. 8.4.1 and Table 8.4.0.

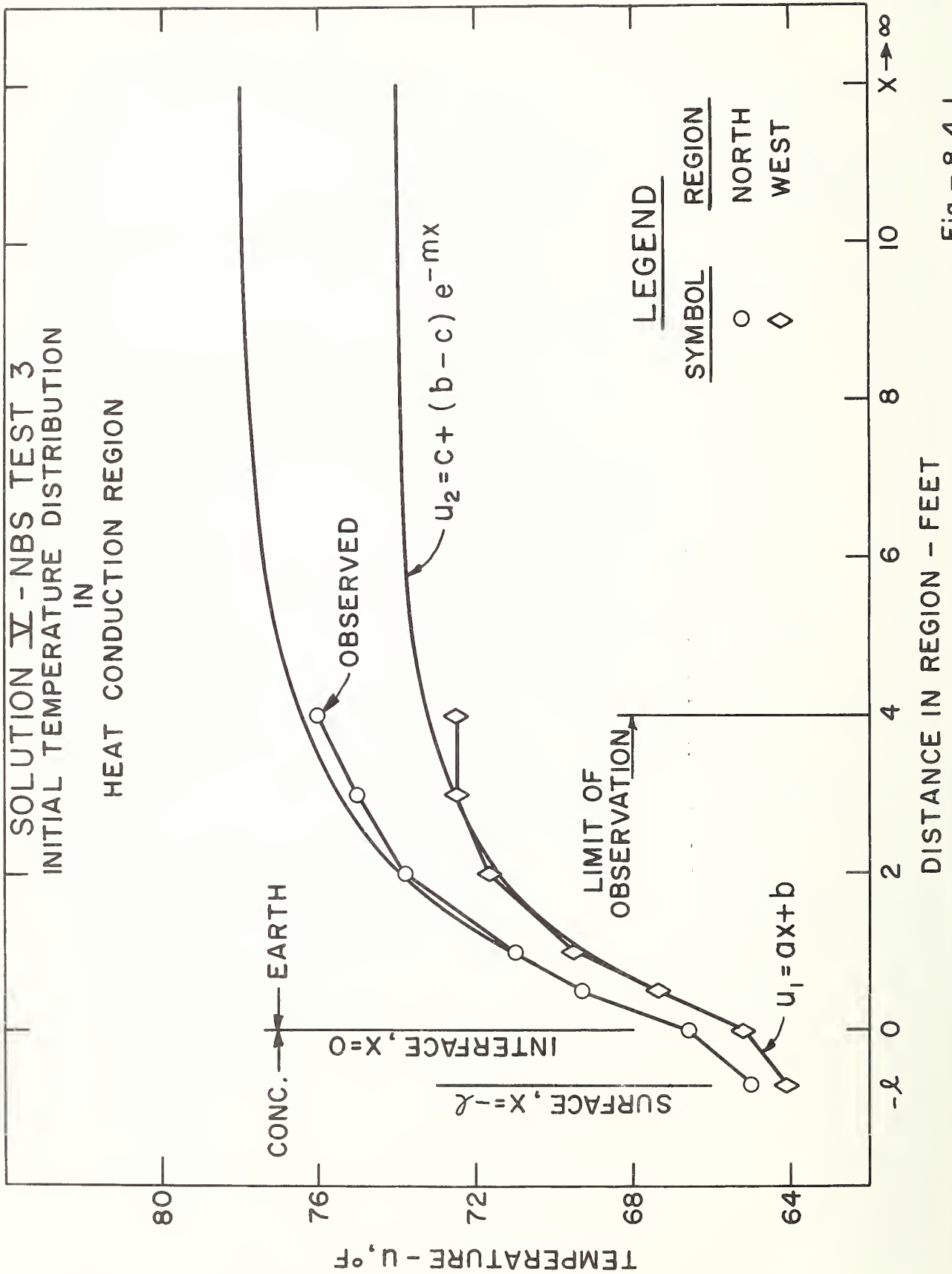


Fig. - 8.4.1

TABLE 8.4.0
VALUES OF CURVE-FITTING CONSTANTS
FOR SOLUTION V

Curve-Fitting Constants					
Test	Surface	a	b	c	m
3	North	2.40	66.6	78.0	0.50
	West	1.65	65.2	74.0	0.60
	South	1.00	61.7	76.0	0.50
	East	1.00	65.0	77.0	0.55
	Floor	1.40	63.8	66.0	0.60
4	North	0.30	66.1	73.0	0.40
	West	0.00	66.0	70.0	0.40
	South	0.00	66.0	71.0	0.40
	East	0.00	65.8	72.5	0.30
	Floor	-1.00	64.7	64.7	0.00
5	North	0.00	45.2	41.5	0.30
	West	0.00	46.0	43.5	0.30
	South	0.00	46.0	42.0	0.27
	East	0.00	45.6	40.5	0.30
	Floor	1.00	48.3	54.0	0.33

This figure partly reproduces Fig. 3 of Appendix A, showing the initial temperature distribution in the north and west wall heat conduction regions, selected as representative regions for detailed analysis in this report.

8.5 Results

Figure 8.5.1 shows interior surface temperatures versus time, predicted by Solution V, for the north wall conduction region of NBS Test 3, together with the observed performance.

Curves 1, 2 and 4 in Figure 8.5.1 were based on the preferred earth thermal properties while varying the concrete thermal properties to cover the range of values mentioned in Section 3.2.

Curves 1, 3 and 5 in Figure 8.5.1 were based on the preferred concrete thermal properties while varying the earth properties to cover an estimated range of values that might occur at the NBS test site.

Figure 8.5.2 shows similar temperature-time curves for the west wall conduction region of NBS Test 3.

Figure 8.5.3 shows a temperature-time curve for the west wall conduction region of NBS Test 5. The figure shows predicted performance, together with the observations, based on the preferred thermal properties only.

The values of the curve-fitting constants used in the computations are listed in Table 8.4.0.

The results of this solution were obtained on the IBM 7090 digital computer at the rate of 0.35 minutes per run. Each run consisted of computing temperatures at four positions in the concrete medium and eight positions in the earth medium, for the eight values of time shown in the figures, a total of 96 calculations.

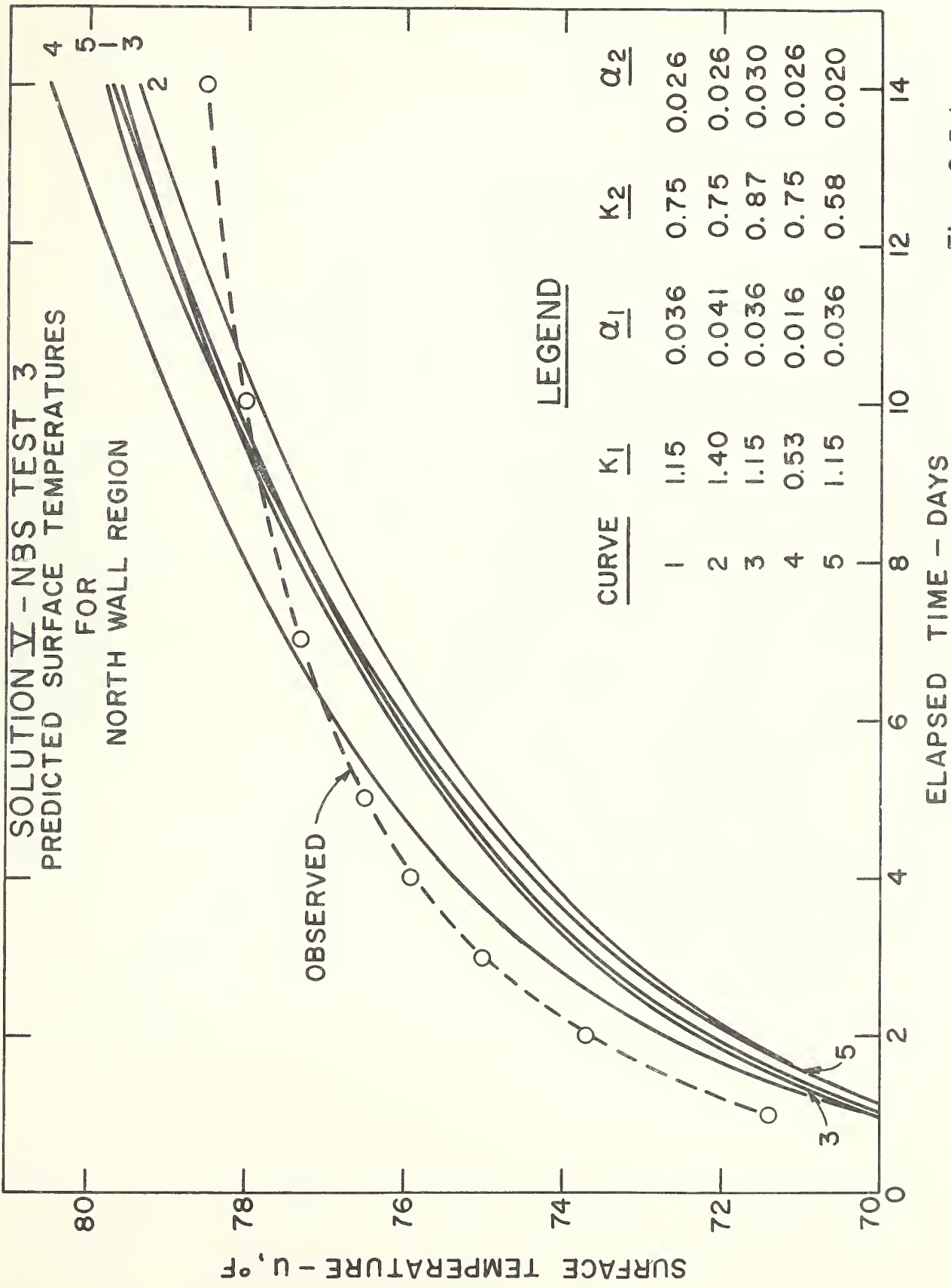


Fig. -8.5.1

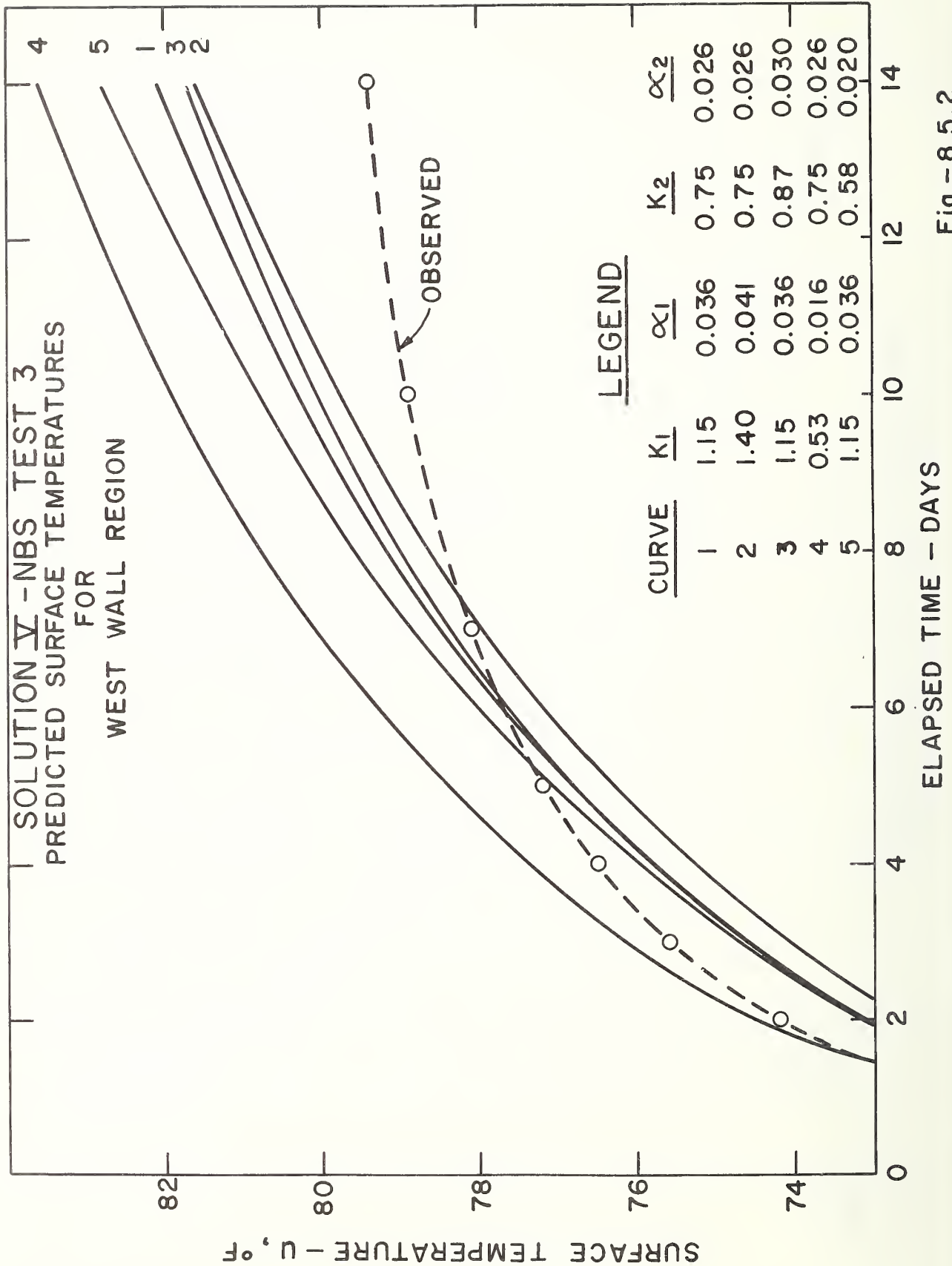


Fig.-8.5.2

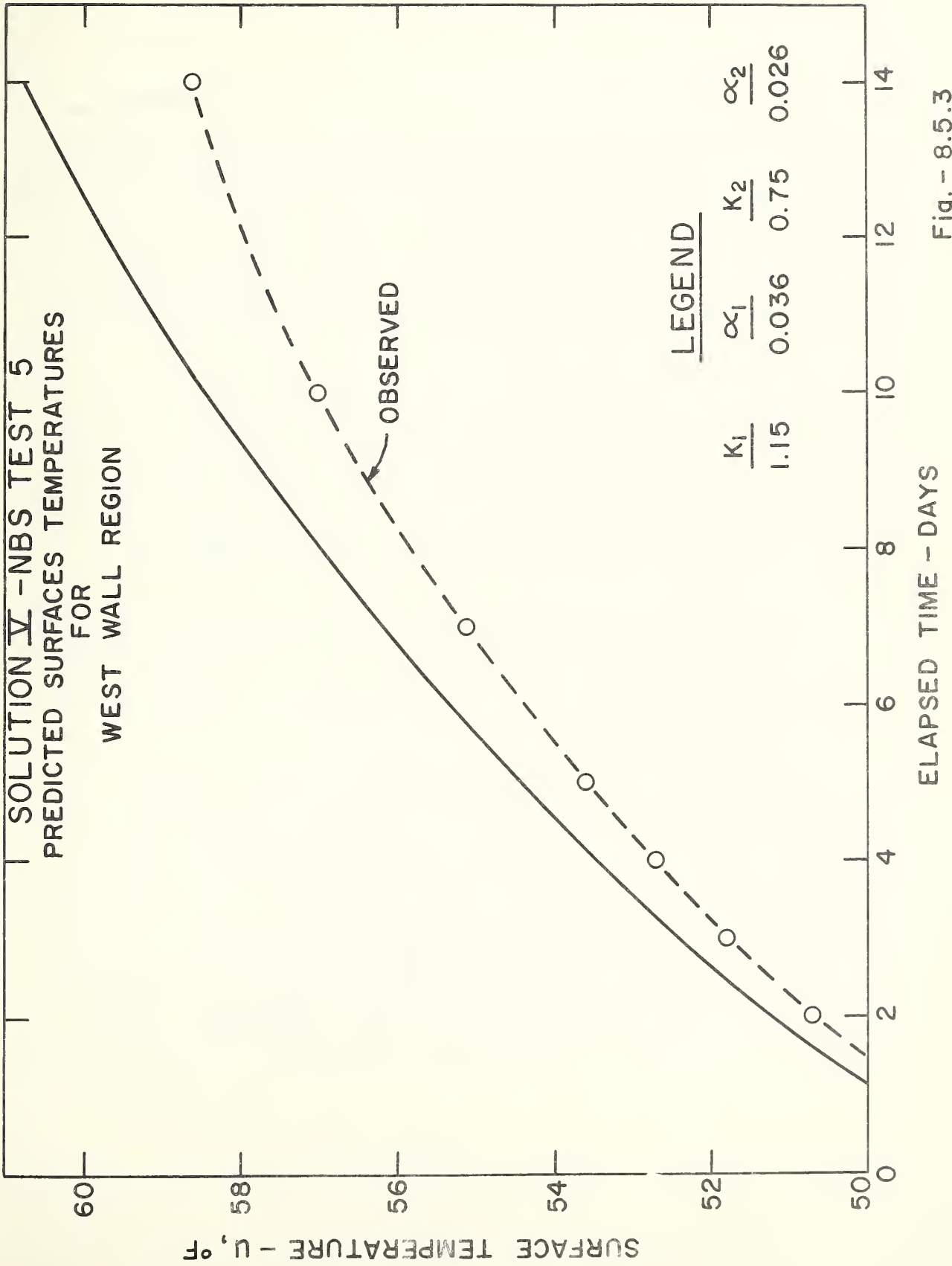


Fig. - 8.5.3

8.6 Discussion

Comparisons of Curves 1 and 2 in both Figures 8.5.1 and 8.5.2 show that an increase of 14 percent in the thermal diffusivity of the concrete decreased the inside surface temperature 0.5°F or less throughout the 14-day period. On the other hand, comparisons of curves 1 and 4 in Figures 8.5.1 and 8.5.2 show that a decrease of a little over 50 percent in the thermal diffusivity of the concrete from the preferred value increased the temperature about 1°F for the north wall surface and about 2°F for the west wall surface.

Comparisons of Curves 3 and 5 in Figures 8.5.1 and 8.5.2 show that an increase in thermal diffusivity of the earth from 0.02 to $0.03 \text{ ft}^2/\text{hr}$ caused a change of less than 0.5°F at any time in the surface temperature of the north wall and a maximum change of about 1°F in the surface temperature of the west wall after 14 days. Thus it appears that the thermal properties of the concrete in the composite model affects the surface temperature of the walls more significantly than the thermal properties of the earth.

Comparison of Figure 8.5.3 with Curve 1 of Figure 7.5.4 for Test 5 shows much similarity between the two, especially after the first week, indicating that when the initial temperature is reasonably uniform (See Fig. 5 of Appendix A), the predictions of Solution V approach those of Solution IV.

It was pointed out in Section 7.6 that Curves 2 and 3 of, e.g., Figure 7.5.2, cross at about 7 days, showing the tendency of the earth region to succeed the concrete as the dominant medium. In Solution V, however, Curves 2 and 3 of Figures 8.5.1 and 8.5.2 do not cross, even after 14 days, indicating that the concrete remained dominant throughout this period. The reason is that in Solution V the concrete was assumed to be initially colder than the earth, as shown in Figure 8.4.1, and therefore dominated the heat flow for a longer time than usual. This model serves to illustrate the fundamental interdependence of the composite nature of the region and the nonuniform initial temperature, which could only be seen in a solution containing both assumptions.

9. SOLUTION VI

9.1 Statement of Problem

Semi-infinite composite region. The heat flux F_0 is constant across the surface $x = -l$. Each medium has initial temperature $u = f(x)$.

9.2 Mathematical Summary

The differential equations to be satisfied by the temperature u are

$$\frac{\partial u_1}{\partial t} = \alpha_1 \frac{\partial^2 u_1}{\partial x^2}, \quad -l < x < 0, \quad t > 0 \quad (1)$$

$$\frac{\partial u_2}{\partial t} = \alpha_2 \frac{\partial^2 u_2}{\partial x^2}, \quad 0 < x < \infty, \quad t > 0 \quad (2)$$

with the following initial and boundary conditions:

$$-l < x < 0 \quad t = 0 \quad u_1 = ax + b \quad (3)$$

$$0 < x < \infty \quad t = 0 \quad u_2 = b + cx \exp(-mx) \quad (4)$$

$$x = -l \quad t > 0 \quad -K_1 \frac{\partial u_1}{\partial x} = F_0 \quad (5)$$

$$x = 0 \quad t > 0 \quad u_1 = u_2 \quad (6)$$

$$x = 0 \quad t > 0 \quad K_1 \frac{\partial u_1}{\partial x} = K_2 \frac{\partial u_2}{\partial x} \quad (7)$$

$$x \rightarrow \infty \quad t > 0 \quad u_2 \rightarrow b \quad (8)$$

The solutions of the Laplace transformed equations are

$$\begin{aligned} \bar{u}_1 = & \left\{ \frac{F_0 + aK_1}{q_1 K_1 p} \right\} \left\{ \frac{\exp[-q_1(l+x)] - \beta \exp[-q_1(l-x)]}{1 + \beta \exp(-2q_1 l)} \right\} \\ & - \left\{ \frac{a}{q_1 p (\sigma+1)} \right\} \left\{ \frac{\exp[-q_1(2l+x)] + \exp(q_1 x)}{1 + \beta \exp(-2q_1 l)} \right\} \\ & + \left\{ \frac{cK_2}{q_1 K_1 (\sigma+1) (p - \alpha_2 m^2)} \right\} \left\{ \frac{\exp[-q_1(2l+x)] + \exp(q_1 x)}{1 + \beta \exp(-2q_1 l)} \right\} \\ & - \left\{ \frac{2\alpha_2 cmK_2 (q_2 - m)}{q_1 K_1 (\sigma+1) (p - \alpha_2 m^2)^2} \right\} \left\{ \frac{\exp[-q_1(2l+x)] + \exp(q_1 x)}{1 + \beta \exp(-2q_1 l)} \right\} + \frac{ax + b}{p} \quad (9) \end{aligned}$$

and

$$\begin{aligned} \bar{u}_2 = & \left\{ \frac{F_0 + aK_1}{q_1 K_1 p} \right\} \left\{ \frac{[1-\beta] \exp[-q_1(l+xk)]}{1+\beta \exp(-2q_1 l)} \right\} \\ & - \left\{ \frac{a}{q_1 p (\sigma+1)} \right\} \left\{ \frac{\exp[-q_1(2l+xk)] + \exp(-q_1 xk)}{1+\beta \exp(-2q_1 l)} \right\} \\ & + \left\{ \frac{cK_2}{q_1 K_1 (\sigma+1) (p - \alpha_2 m^2)} \right\} \left\{ \frac{\exp[-q_1(2l+xk)] + \exp(-q_1 xk)}{1+\beta \exp(-2q_1 l)} \right\} \\ & - \left\{ \frac{2\alpha_2 cmK_2 (q_2 - m)}{q_1 K_1 (\sigma+1) (p - \alpha_2 m^2)^2} \right\} \left\{ \frac{\exp[-q_1(2l+xk)] + \exp(-q_1 xk)}{1+\beta \exp(-2q_1 l)} \right\} \\ & + \left\{ \frac{2\alpha_2 cm}{(p - \alpha_2 m^2)^2} \right\} \left\{ \exp(-q_1 xk) - \exp(-mx) \right\} + \frac{cx \exp(-mx)}{p - \alpha_2 m^2} + \frac{b}{p} \quad (10) \end{aligned}$$

The inverse transformations yield the solution for temperature at any point in the concrete medium

$$\begin{aligned}
 u_1 = & \frac{2\ell}{K_1} [F_0 + aK_1] T^{\frac{1}{2}} \sum_{n=0}^{\infty} (-\beta)^n \left[\text{ierfc} \frac{(2n+1)+x/\ell}{2T^{\frac{1}{2}}} - \beta \text{ierfc} \frac{(2n+1)-x/\ell}{2T^{\frac{1}{2}}} \right] \\
 & - a\ell(1-\beta) T^{\frac{1}{2}} \sum_{n=0}^{\infty} (-\beta)^n \left[\text{ierfc} \frac{2(n+1)+x/\ell}{2T^{\frac{1}{2}}} + \text{ierfc} \frac{2n-x/\ell}{2T^{\frac{1}{2}}} \right] \\
 & - \frac{c}{m} \frac{(1+\beta)}{2} \sum_{n=0}^{\infty} (-\beta)^n \left\{ \left[2 \left(\frac{\ell m}{k} \right)^2 T + 2(n+1) \frac{\ell m}{k} + \frac{mx}{k} \right] \text{erfc} \left[\frac{2(n+1)+x/\ell}{2T^{\frac{1}{2}}} + \frac{\ell m}{k} T^{\frac{1}{2}} \right] \right. \\
 & \left. \exp \left[\left(\frac{\ell m}{k} \right)^2 T + 2(n+1) \frac{\ell m}{k} + \frac{mx}{k} \right] \right\} \\
 & - \frac{c}{m} \frac{(1+\beta)}{2} \sum_{n=0}^{\infty} (-\beta)^n \left\{ \left[2 \left(\frac{\ell m}{k} \right)^2 T + 2n \frac{\ell m}{k} - \frac{mx}{k} \right] \text{erfc} \left[\frac{2n-x/\ell}{2T^{\frac{1}{2}}} + \frac{\ell m}{k} T^{\frac{1}{2}} \right] \right. \\
 & \left. \exp \left[\left(\frac{\ell m}{k} \right)^2 T + 2n \frac{\ell m}{k} - \frac{mx}{k} \right] \right\} \\
 & + \frac{c\ell}{k\sqrt{\pi}} (1+\beta) T^{\frac{1}{2}} \sum_{n=0}^{\infty} (-\beta)^n \left\{ \exp \left[- \left(\frac{2(n+1)+x/\ell}{2T^{\frac{1}{2}}} \right)^2 \right] + \exp \left[- \left(\frac{2n-x/\ell}{2T^{\frac{1}{2}}} \right)^2 \right] \right\}
 \end{aligned}$$

$$+ ax + b \quad (11)$$

and the solution for temperature at any point in the earth medium

$$\begin{aligned}
 u_2 = & \frac{2\ell}{K_1} [F_0 + aK_1] T^{\frac{1}{2}} \sum_{n=0}^{\infty} (-\beta)^n (1-\beta) \operatorname{ierfc} \frac{(2n+1) + kx/\ell}{2T^{\frac{1}{2}}} \\
 & - a\ell(1-\beta) T^{\frac{1}{2}} \sum_{n=0}^{\infty} (-\beta)^n \left[\operatorname{ierfc} \frac{2(n+1) + kx/\ell}{2T^{\frac{1}{2}}} + \operatorname{ierfc} \frac{2n + kx/\ell}{2T^{\frac{1}{2}}} \right] \\
 & - \frac{c}{m} \frac{(1+\beta)}{2} \sum_{n=0}^{\infty} (-\beta)^n \left\{ \left[2 \left(\frac{\ell m}{k} \right)^2 T + 2(n+1) \frac{\ell m}{k} + mx \right] \operatorname{erfc} \left[\frac{2(n+1) + kx/\ell}{2T^{\frac{1}{2}}} + \frac{\ell m}{k} T^{\frac{1}{2}} \right] \right. \\
 & \quad \left. \exp \left[\left(\frac{\ell m}{k} \right)^2 T + 2(n+1) \frac{\ell m}{k} + mx \right] \right\} \\
 & - \frac{c}{m} \frac{(1+\beta)}{2} \sum_{n=0}^{\infty} (-\beta)^n \left\{ \left[2 \left(\frac{\ell m}{k} \right)^2 T + 2n \frac{\ell m}{k} + mx \right] \operatorname{erfc} \left[\frac{2n + kx/\ell}{2T^{\frac{1}{2}}} + \frac{\ell m}{k} T^{\frac{1}{2}} \right] \right. \\
 & \quad \left. \exp \left[\left(\frac{\ell m}{k} \right)^2 T + 2n \frac{\ell m}{k} + mx \right] \right\} \\
 & + \frac{c\ell}{k\sqrt{\pi}} (1+\beta) T^{\frac{1}{2}} \sum_{n=0}^{\infty} (-\beta)^n \left\{ \exp \left[- \left(\frac{2(n+1) + kx/\ell}{2T^{\frac{1}{2}}} \right)^2 \right] + \exp \left[- \left(\frac{2n + kx/\ell}{2T^{\frac{1}{2}}} \right)^2 \right] \right\} \\
 & + \frac{c}{m} \left\{ \left[\left(\frac{\ell m}{k} \right)^2 T + \frac{mx}{2} \right] \operatorname{erfc} \left[\frac{\ell m}{k} T^{\frac{1}{2}} + \frac{kx/\ell}{2T^{\frac{1}{2}}} \right] \exp \left[\left(\frac{\ell m}{k} \right)^2 T + mx \right] \right. \\
 & \quad \left. - \left[\left(\frac{\ell m}{k} \right)^2 T - \frac{mx}{2} \right] \operatorname{erfc} \left[\frac{\ell m}{k} T^{\frac{1}{2}} - \frac{kx/\ell}{2T^{\frac{1}{2}}} \right] \exp \left[\left(\frac{\ell m}{k} \right)^2 T - mx \right] \right\} + b
 \end{aligned} \tag{12}$$

where $T = \frac{\alpha_1 t}{\ell^2}$.

At the interior surface $x = -\ell$, Eq. 9.2(11) becomes

$$\begin{aligned}
 u_1 = & \frac{2\ell}{K_1} [F_0 + aK_1] T^{\frac{1}{2}} \sum_{n=0}^{\infty} (-\beta)^n \left[\text{ierfc} \frac{n}{T^{\frac{1}{2}}} - \beta \text{ierfc} \frac{n+1}{T^{\frac{1}{2}}} \right] \\
 & - 2a\ell(1-\beta) T^{\frac{1}{2}} \sum_{n=0}^{\infty} (-\beta)^n \text{ierfc} \frac{2n+1}{2T^{\frac{1}{2}}} \\
 & - \frac{c}{m}(1+\beta) \sum_{n=0}^{\infty} (-\beta)^n \left\{ \left[2 \left(\frac{\ell m}{k} \right)^2 T + (2n+1) \frac{\ell m}{k} \right] \text{erfc} \left[\frac{2n+1}{2T^{\frac{1}{2}}} + \frac{\ell m}{k} T^{\frac{1}{2}} \right] \right. \\
 & \quad \left. \exp \left[\left(\frac{\ell m}{k} \right)^2 T + (2n+1) \frac{\ell m}{k} \right] \right\} \\
 & + \frac{2c\ell}{k\sqrt{\pi}} (1+\beta) T^{\frac{1}{2}} \sum_{n=0}^{\infty} (-\beta)^n \left\{ \exp \left[- \left(\frac{2n+1}{2T^{\frac{1}{2}}} \right)^2 \right] \right\} - a\ell + b
 \end{aligned} \tag{13}$$

At the concrete-earth interface $x = 0$, either 9.2(11) or (12) may be used, giving

$$\begin{aligned}
 u = & \frac{2\ell}{K_1} [F_0 + aK_1] T^{\frac{1}{2}} \sum_{n=0}^{\infty} (-\beta)^n (1-\beta) \operatorname{ierfc} \frac{2n+1}{2T^{\frac{1}{2}}} \\
 & - a\ell(1-\beta) T^{\frac{1}{2}} \sum_{n=0}^{\infty} (-\beta)^n \left[\operatorname{ierfc} \frac{n+1}{T^{\frac{1}{2}}} + \operatorname{ierfc} \frac{n}{T^{\frac{1}{2}}} \right] \\
 & - \frac{c}{m} \frac{(1+\beta)}{2} \sum_{n=0}^{\infty} (-\beta)^n \left\{ \left[2 \left(\frac{\ell m}{k} \right)^2 T + 2(n+1) \frac{\ell m}{k} \right] \operatorname{erfc} \left[\frac{n+1}{T^{\frac{1}{2}}} + \frac{\ell m}{k} T^{\frac{1}{2}} \right] \right. \\
 & \quad \left. \exp \left[\left(\frac{\ell m}{k} \right)^2 T + 2(n+1) \frac{\ell m}{k} \right] \right\} \\
 & - \frac{c}{m} \frac{(1+\beta)}{2} \sum_{n=0}^{\infty} (-\beta)^n \left\{ \left[2 \left(\frac{\ell m}{k} \right)^2 T + 2n \frac{\ell m}{k} \right] \operatorname{erfc} \left[\frac{n}{T^{\frac{1}{2}}} + \frac{\ell m}{k} T^{\frac{1}{2}} \right] \right. \\
 & \quad \left. \exp \left[\left(\frac{\ell m}{k} \right)^2 T + 2n \frac{\ell m}{k} \right] \right\} \\
 & + \frac{c\ell}{k\sqrt{\pi}} (1+\beta) T^{\frac{1}{2}} \sum_{n=0}^{\infty} (-\beta)^n \left\{ \exp \left[- \left(\frac{n+1}{T^{\frac{1}{2}}} \right)^2 \right] + \exp \left[- \left(\frac{n}{T^{\frac{1}{2}}} \right)^2 \right] \right\} + b
 \end{aligned} \tag{14}$$

9.3 Convergence

Equations 9.2(11) and (12) converge subject to the same condition discussed in Section 8.3, namely

$$|\beta| \exp\left(2\frac{\ell_m}{k}\right) < 1 \quad (1)$$

9.4 Assumptions

This solution was not available in the references examined, and was derived like the previous one. It differs from Solution V only in the form of the initial temperature.

The assumptions are:

- 1) geometry — one-dimensional model
- 2) composite heat conduction region
- 3) non-uniform initial temperature

As stated in Section 8.6, the region beyond 4 feet was expected to contribute to the surface temperatures, resulting in the need for a better approximation to the initial profile in this region. In this solution, the initial temperature was approximated in the concrete medium by a linear function $u_1 = ax + b$, Eq. 9.2(3), as in Solution V, and in the earth medium by the function $u_2 = b + cx \exp(-mx)$, Eq. 9.2(4), shown in Fig. 9.4.1 (See Table 9.4.0). This figure is completely analogous to Fig. 8.4.1. It can be seen that the function u_2 has a maximum corresponding to that suggested by the observed curve, and subsequently decays exponentially to the value b at infinite x . This is probably closer to the actual situation for a much greater distance into the earth, and should improve the solution for times greater than one week.

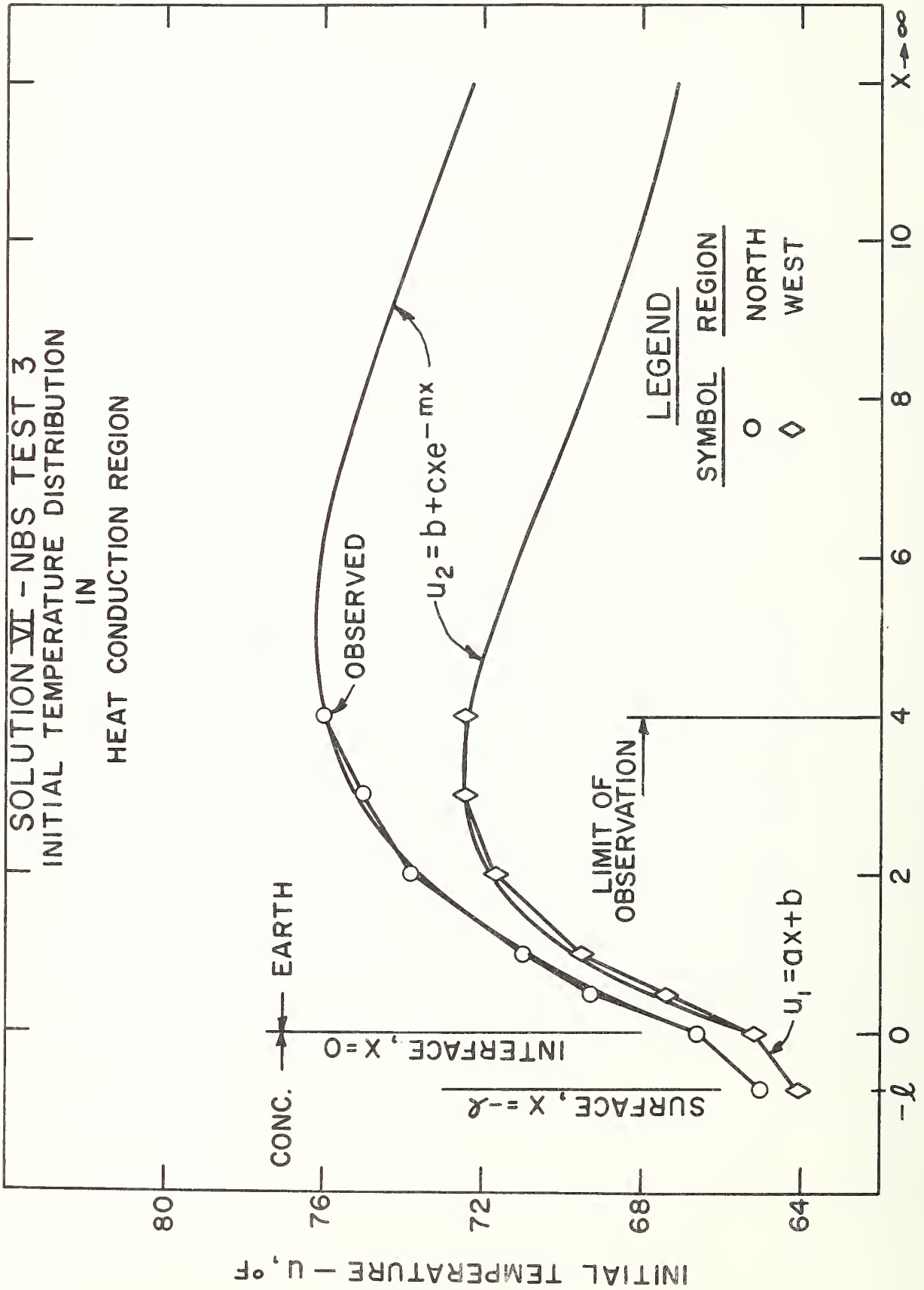


Fig. - 9.4.1

TABLE 9.4.0

VALUES OF CURVE-FITTING CONSTANTS
FOR SOLUTION VI

Curve-Fitting Constants					
Test	Surface	a	b	c	m
3	North	2.40	66.6	5.23	0.20
	West	1.65	65.2	5.96	0.30
	South	1.00	61.7	6.85	0.20
	East	1.00	65.0	5.79	0.20
	Floor	1.40	63.8	2.99	0.50
4	North	0.30	66.1	2.09	0.10
	West	0.00	66.0	1.46	0.15
	South	0.00	66.0	1.57	0.10
	East	0.00	65.8	1.83	0.10
	Floor	-1.00	64.7	0.00	0.00
5	North	0.00	45.2	-1.25	0.15
	West	0.00	46.0	-0.60	0.15
	South	0.00	46.0	-1.15	0.15
	East	0.00	45.6	-1.39	0.10
	Floor	1.00	48.3	-1.87	0.10

9.5 Results

Figures 9.5.1 and 9.5.2 are exactly analogous to the corresponding figures of Solution V. The curve for NBS Test 5 is omitted, since it is almost identical with that in Figure 8.5.3.

These results were also obtained with the aid of the digital computer, at approximately the same running time.

The values of the curve-fitting constants used in the computations are listed in Table 9.4.0.

9.6 Discussion

Inspection of Figures 9.5.1 and 9.5.2 shows the same general results concerning thermal properties found in Solution V, except that Curves 2 and 3 of Figure 9.5.2 do cross near the end of the test, indicating that the earth has begun to take over a little earlier than in Solution V. Since Solutions V and VI were derived on assumptions identical except for the initial temperature function u wide variations in results were not expected.

Solution VI represents the last investigation of one-dimensional, semi-infinite region, constant heat flux shelter models. A general discussion and comparison of all the solutions presented in this report follows in the next section.

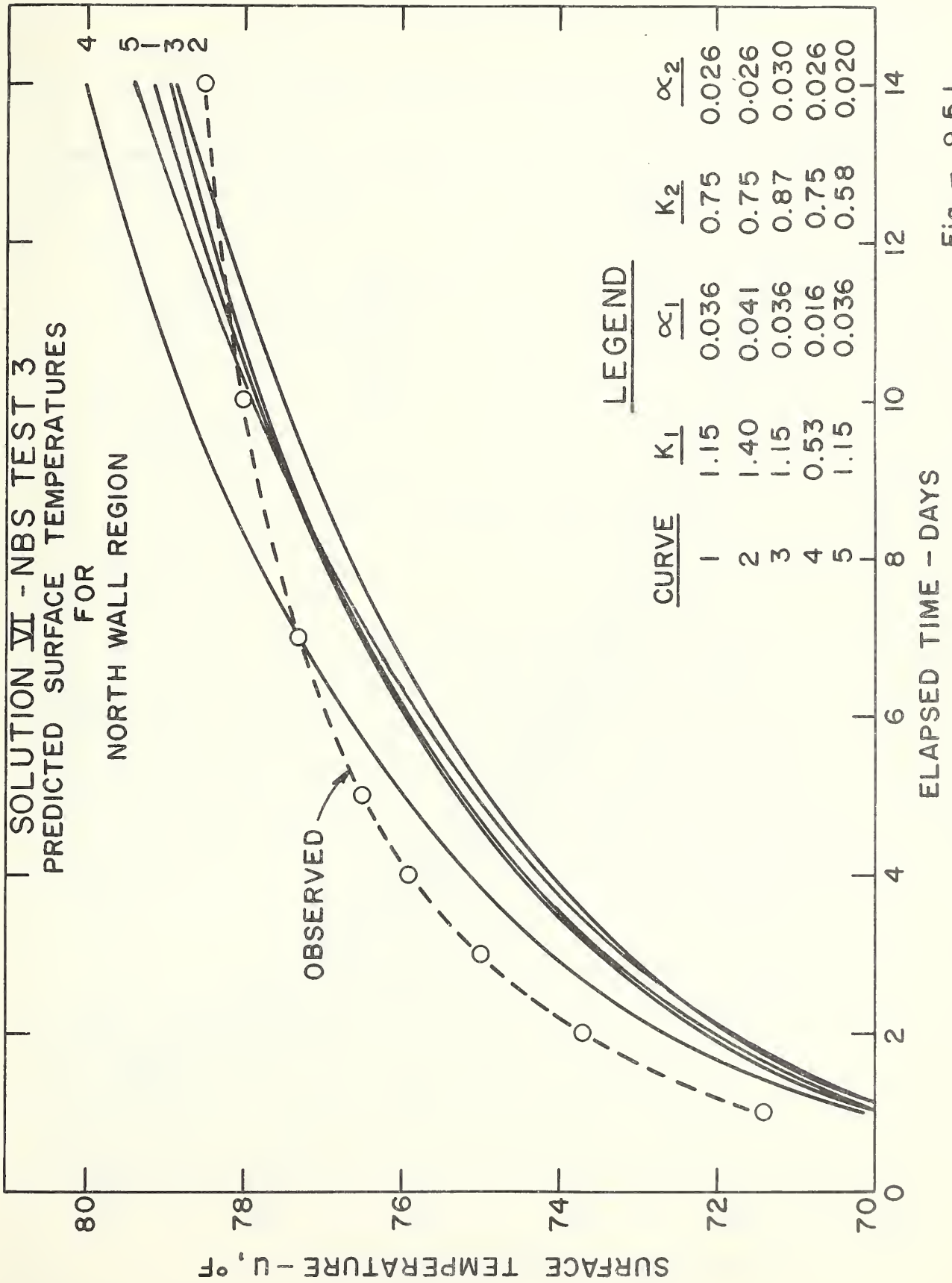


Fig. - 9.5.1

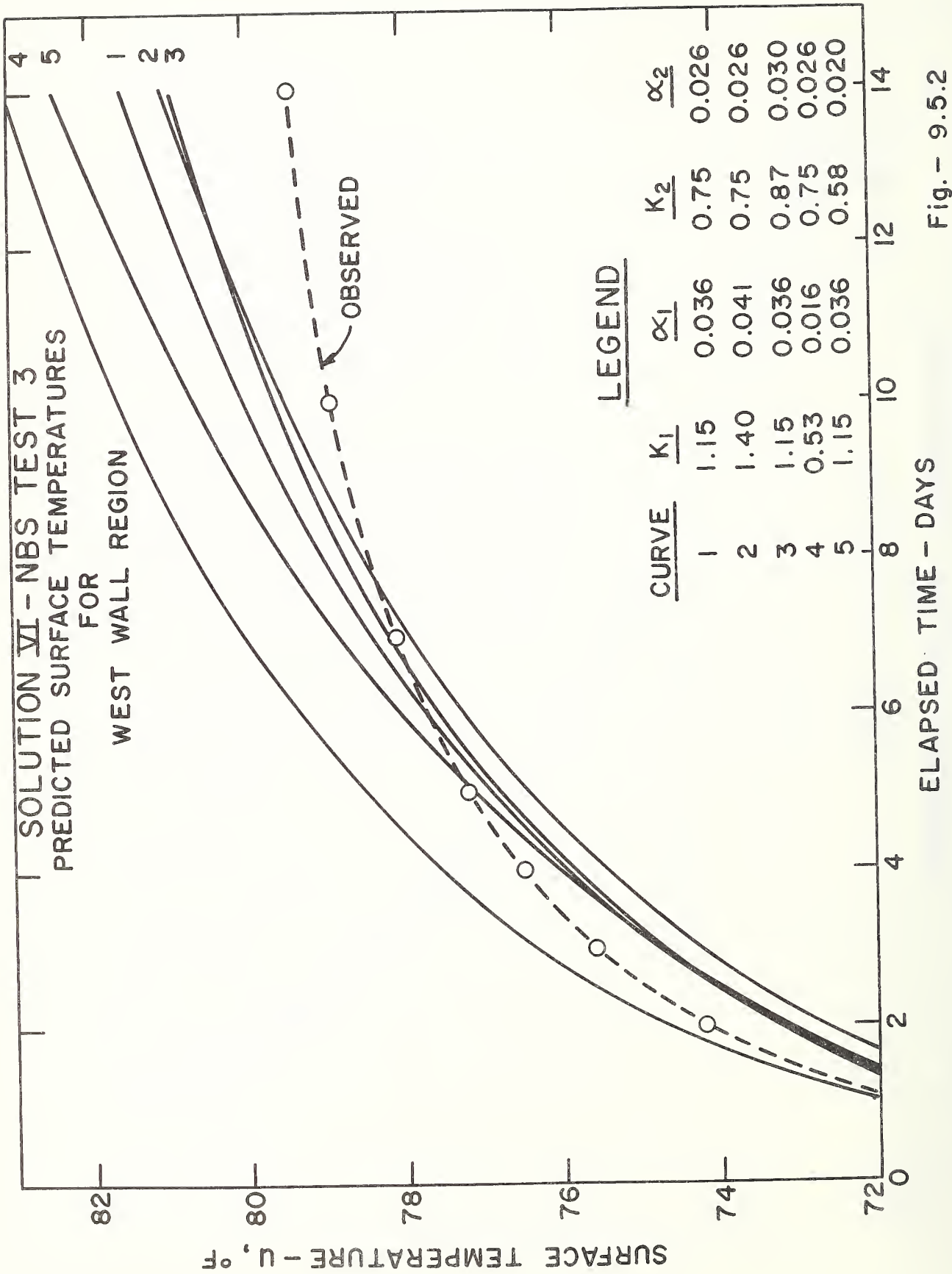


Fig. - 9.5.2

10. GENERAL DISCUSSION

The purpose of this section is to discuss the significance of the assumptions made in the individual solutions for four basic parameters, namely:

- 1) geometry
- 2) composition of region
- 3) initial temperature
- 4) thermal properties,

and also the questions of

- 5) shelter irregularities
- 6) treatment of the complete problem.

10.1 Geometry

The first three solutions provide a means of comparing the effects of the basic geometries considered, since they differ only in this respect. Figures 10.1.1, .2, and .3 show surface temperatures versus time predicted by Solutions I, II, and III for NBS Tests 3, 4, and 5, based on the preferred earth thermal properties. The equivalent radii used in Solutions II and III were determined on the basis of equal surface areas. Since Solution I, unlike the other two, represents a one-dimensional model and is applicable only to the individual surfaces, it could still be included in this comparison by assuming all six surfaces to be in one plane and using the same overall average values of heat flux and initial temperature.

It can be seen from these figures that Solution III, based on the cylindrical approximation, produces the most accurate predictions for two-week periods. As stated in Section 6.3, this solution might still be best for three-week periods and even longer with increasing size. In the case of large shelters, because of their shape and shallow depth, spherical approximations would not be applicable. With increasing size, the one-dimensional solutions become increasingly better.

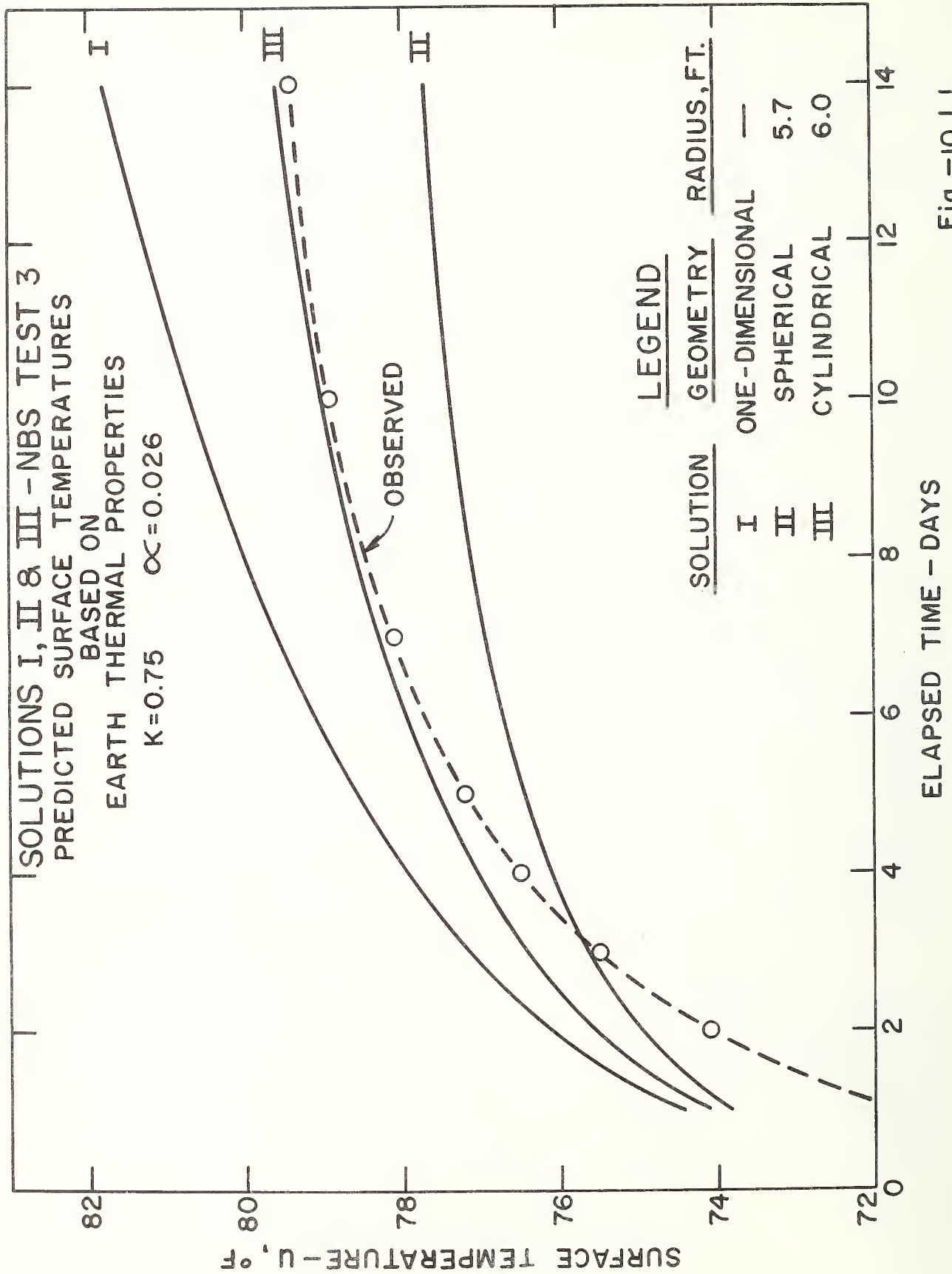


Fig.-10.1.1

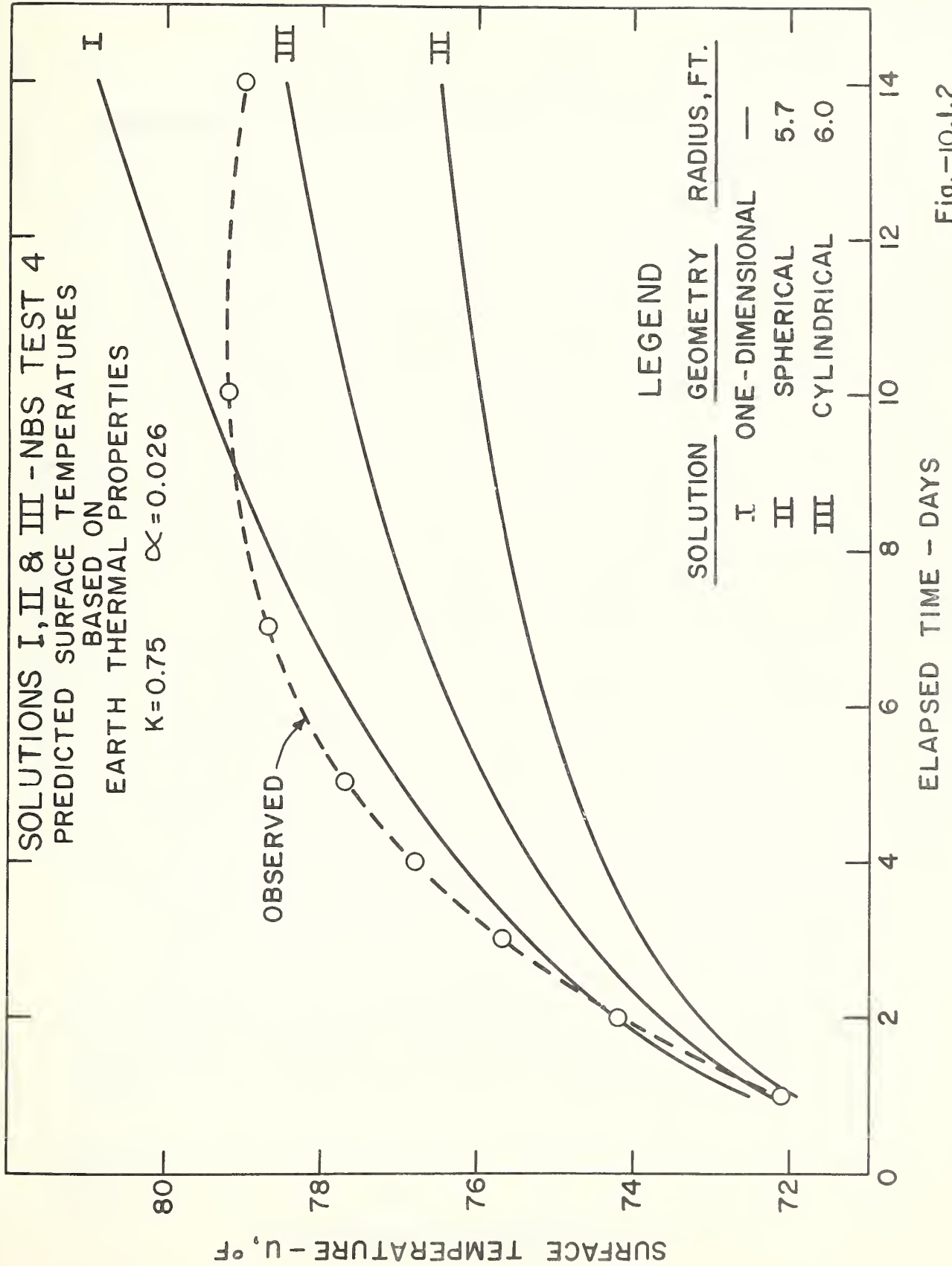


Fig.-10.1.2

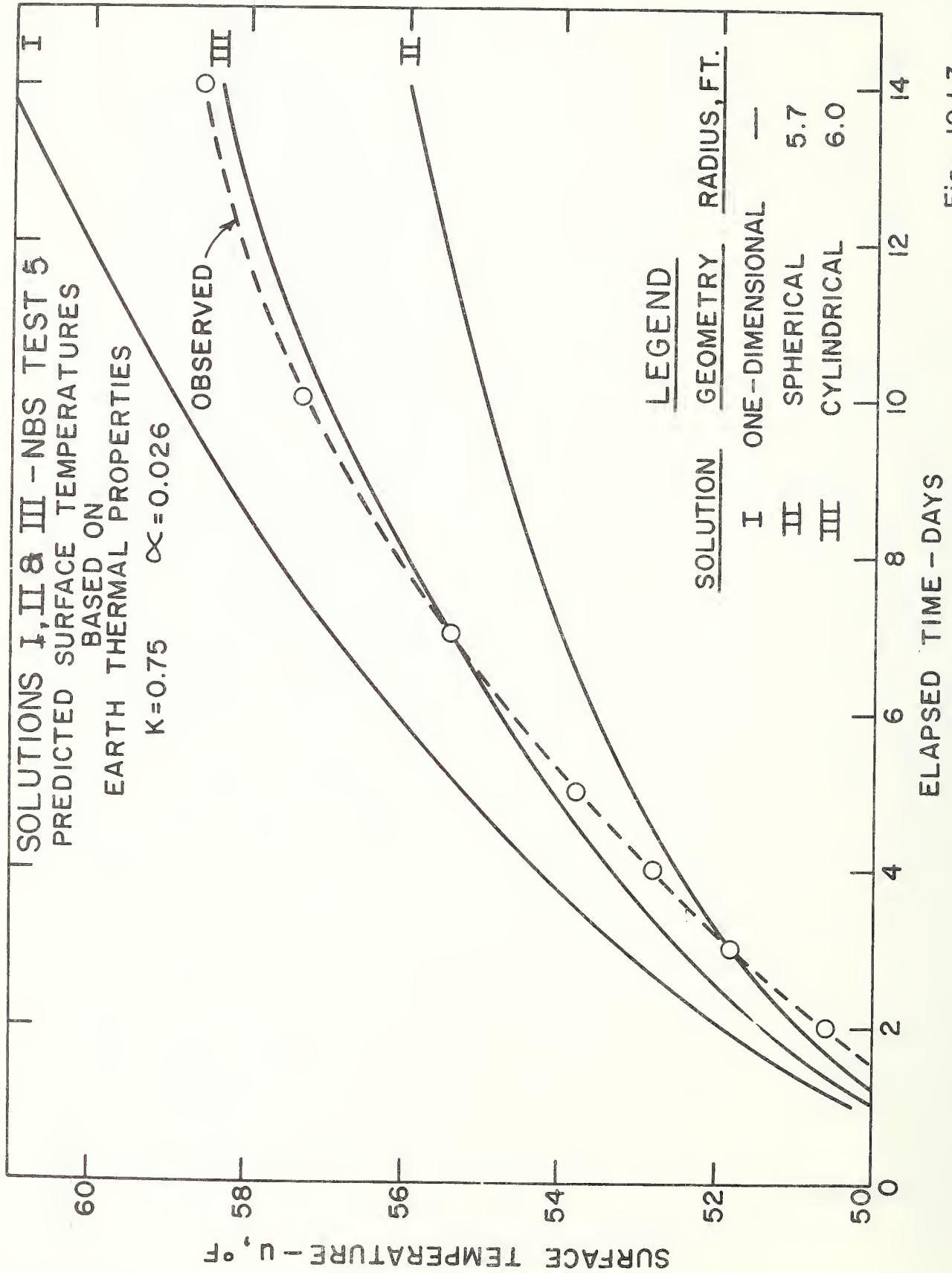


Fig.-10.1.3

10.2 Composite Region

In order to examine the significance of the composite assumption, it is necessary to compare Solutions I and IV. This comparison, however, is complicated by the question of which set of thermal properties in Solution I corresponds to which two sets in Solution IV. Figure 10.2.1 provides a comparison on the basis of the preferred concrete and earth thermal properties. The west wall region of NBS Test 3 was chosen as a typical case. This figure is a reproduction of Curves 2, 3, and 4 of Figure 4.4.2, and Curve 1 of Figure 7.5.2.

Inspection of Figure 10.2.1 shows Solution IV, Curve 1, lying between two cases of Solution I, Curves 2 and 4. The composite assumption lowers the predicted temperature toward Curve 4 for small values of time, when concrete dominates, and raises the prediction toward Curve 2 for large values of time, when the earth properties are of more significance. This effect is more clearly observed by comparing Solution IV with Solution I, Curve 3, which is based on an intermediate set of thermal properties.

It can be seen that some intermediate combination of thermal conductivity and diffusivity will translate Curve 3 into a position of optimum agreement with Curve 1, but never into complete agreement, since the times under consideration are neither small enough to approximate the whole region by concrete nor large enough to approximate it by earth. This result may or may not be true for the cylindrical and spherical models. While it seems likely that the effect of the concrete would be less in these models, because of the increasing mass of earth per unit surface area within a given distance from the surface, any differences could only be determined by solving the appropriate composite models.

It was first pointed out in Section 7.6 that in the one-dimensional geometry, the earth does not dominate the heat flow sufficiently, after two weeks, for the whole region to be treated as earth. This fact can be made plausible by calculating the relative amounts of heat stored in the concrete and earth, according to Solution IV. The heat stored in each medium is simply the integral of the temperature rise over the medium. Thus, the heat stored in the concrete is:

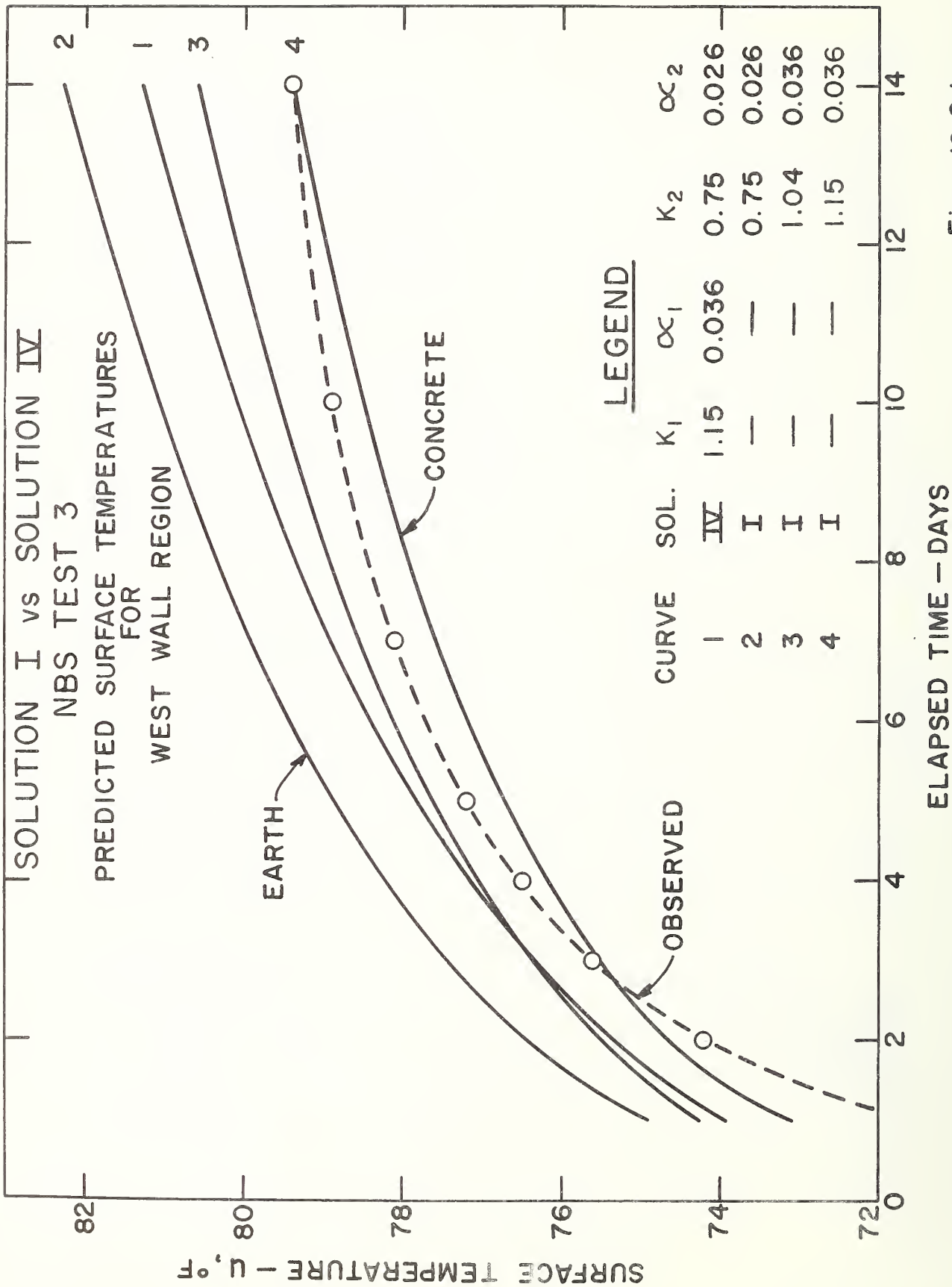


Fig. - 10.2.1

$$Q_1(t) = \int_{-\ell}^0 \rho_1 c_1 \theta_1(x,t) dx \quad (1)$$

and the heat stored in the earth

$$Q_2(t) = \int_0^{\infty} \rho_2 c_2 \theta_2(x,t) dx \quad (2)$$

The temperature rise, θ_1 and θ_2 , can be obtained from Eqs. 7.2(11) and (12), giving

$$Q_1(t) = F_0 t \sum_{n=0}^{\infty} (-\beta)^n \left\{ 4\beta i^2 \operatorname{erfc} \frac{n+1}{T^{\frac{1}{2}}} + 4i^2 \operatorname{erfc} \frac{n}{T^{\frac{1}{2}}} - 4(\beta+1)i^2 \operatorname{erfc} \frac{n+\frac{1}{2}}{T^{\frac{1}{2}}} \right\} \quad (3)$$

and

$$Q_2(t) = F_0 t (\beta+1) \sum_{n=0}^{\infty} (-\beta)^n 4i^2 \operatorname{erfc} \frac{n+\frac{1}{2}}{T^{\frac{1}{2}}} \quad (4)$$

Since $F_0 t$ is the total heat per unit area lost at time t , it follows that the fraction stored in the concrete is the coefficient of $F_0 t$ in Eq. (3), giving 24 percent when evaluated at $t = 336$ hours. It may be noted that this agrees fairly well with an estimate made in reference [1], based on measured temperatures in NBS Test 3. That estimate established the fraction of heat stored in all the concrete, including the shielding wall, at about 26 percent of the total heat stored within 4 feet of the shelter.

10.3 Initial Temperature

Figure 10.3.1 shows surface temperatures versus time predicted by Solutions IV, V, and VI for the north wall region of NBS Test 3, based on the preferred sets of thermal properties. Figure 10.3.2 shows similar curves for the west wall region. These figures facilitate a comparison between observed performance and three one-dimensional solutions which differ only in the form of the initial temperature.

Figures 10.3.1 and 10.3.2 show the effect of the particular temperature distribution which existed at the start of Test 3 on the predicted surface temperatures. The assumed temperature at the shelter surface for Solutions V and VI were as much as 5.6°F lower than the average value used in Solution IV, resulting in generally lower predictions from these latter solutions for the first 6 to 8 days of the test. However, the predicted surface temperature at the end of 14 days was higher from Solution VI than from Solution IV and still higher from Solution V.

Solution V was derived with the simplest exponential approximation to the initial temperature on the assumption that the region beyond 4 feet would have little effect on the surface temperature up to 14 days. The magnitude of the difference in the predicted temperatures at 14 days' time from Solutions IV and V, however, suggested that the effect of the earth temperature beyond 4 feet might be significant. It is probable that the initial temperature more than 4 feet from the shelter surface for Test 3 decreased as indicated in Figure 9.4.1.[1]. The effect of this latter assumption regarding the initial earth temperature beyond 4 feet is seen, from a comparison of Solutions V and VI, to be a decrease in shelter surface temperature of a little more than 0.5°F after 14 days.

Solutions V and VI represent successive refinements in the assumptions regarding the initial earth temperature. It appears that the effect of these refinements is not large after the first week of occupancy. Since a more nonuniform initial temperature distribution than that observed for Test 3 is not likely to occur in undisturbed earth, the initial temperature can be considered uniform for design purposes, unless the first week of occupancy is of comparable importance to the second week.

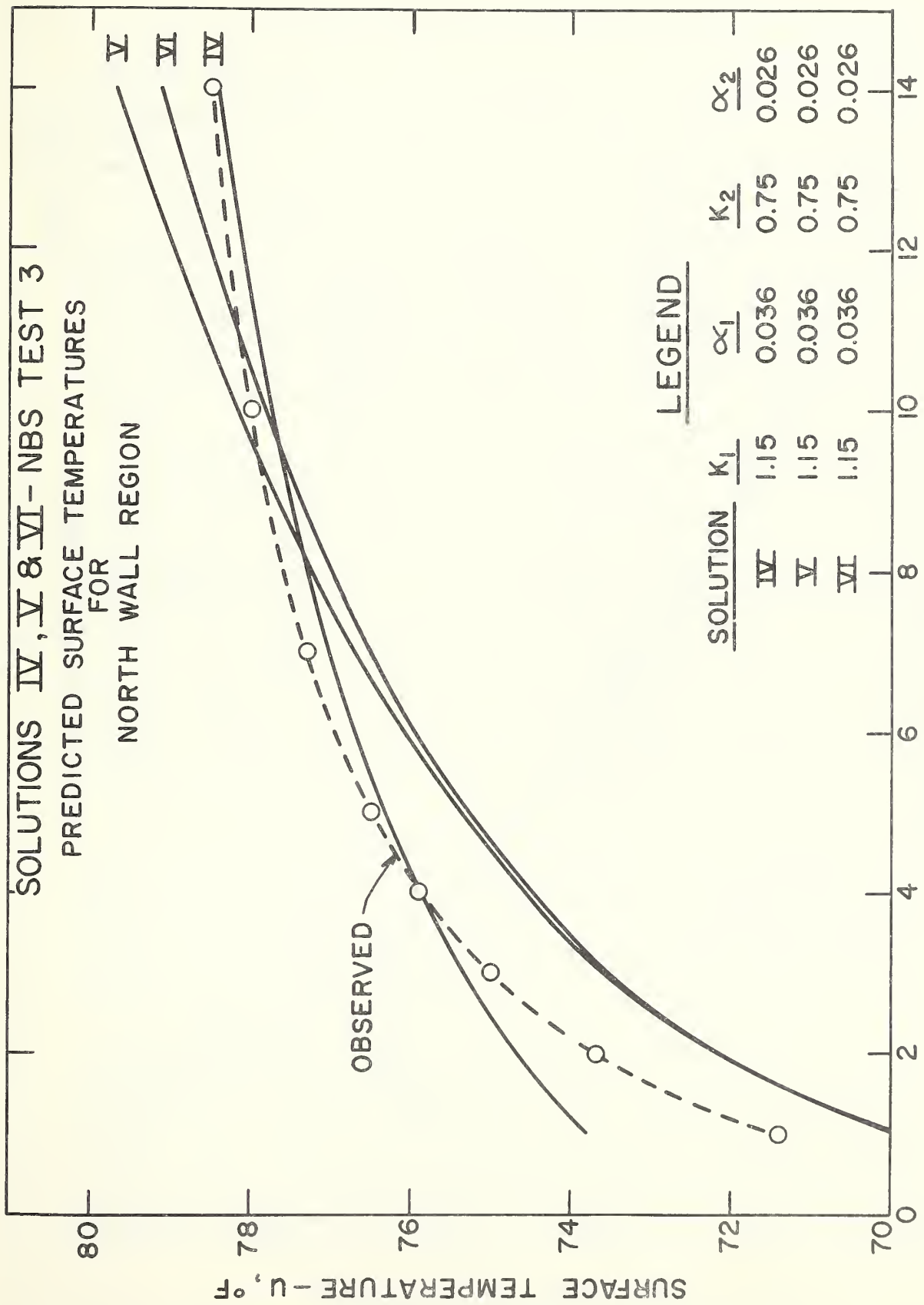
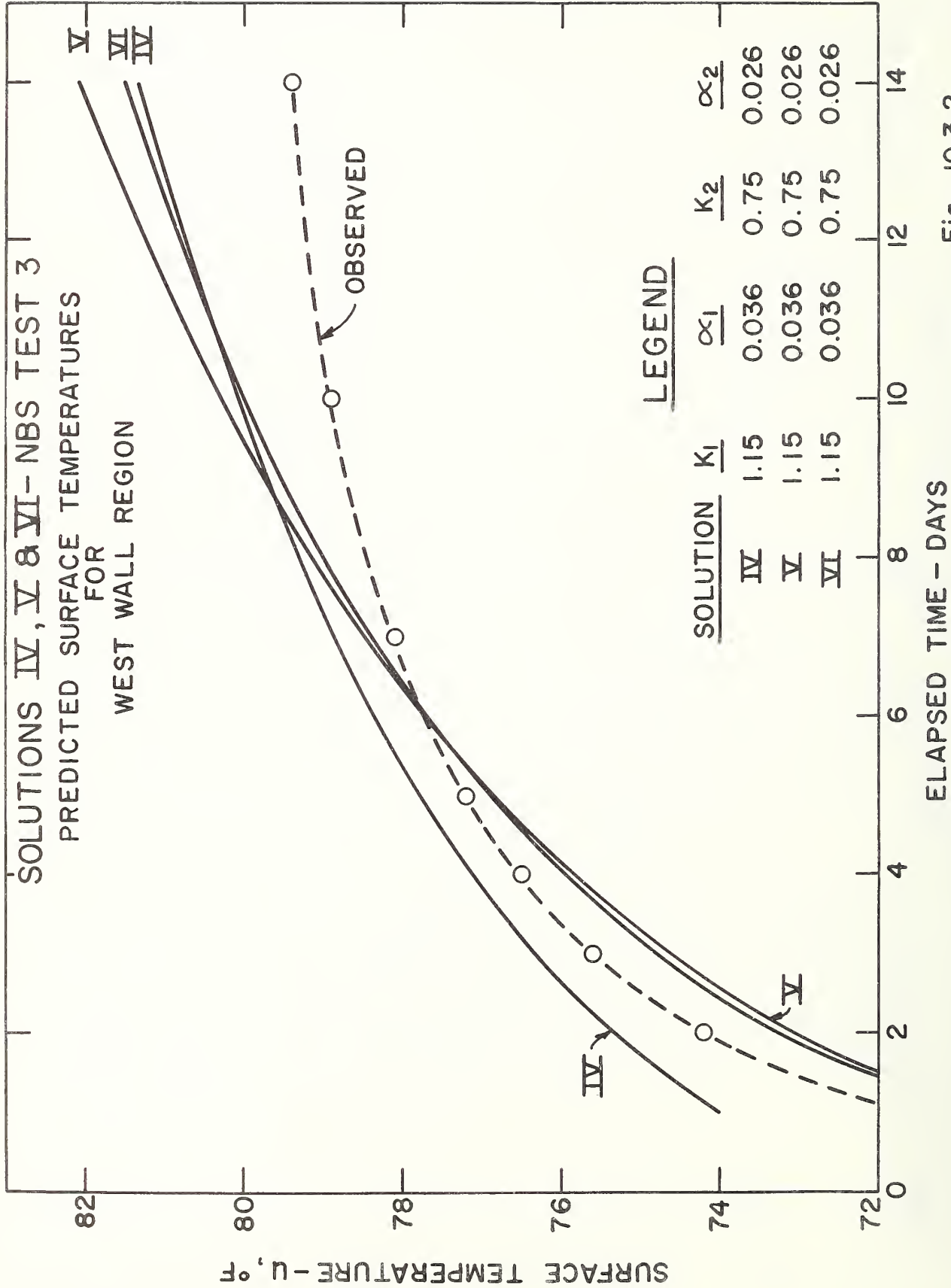


Fig.-10.3.1



Since the composite nature of the region and the non-uniform initial temperature have been taken into account in Solutions V and VI, the steepness of the curves in Figures 10.3.1 and 10.3.2 after the first week is due chiefly to the one-dimensional geometry.

10.4 Thermal Properties

It was observed in Sections 4.6 and 7.6, in discussing one-dimensional Solutions I and IV, that higher thermal properties for the conduction region produced better agreement between predicted and observed temperatures in most cases. The north wall region was an exception to this trend. Since heat flows in one direction only in a one-dimensional model, artificially high thermal properties were required to produce reasonable temperature predictions.

It seems probable that the NBS family shelter, without widely different width, length and height, would be best represented by a spherical cavity, especially if it were located deep in the earth. However, the comparison of observed and predicted surface temperatures by Solution II, (See. Fig. 5.4.1 and 5.4.2), indicate that the heat conduction region around the actual shelter was a less effective heat sink than that assumed for the spherical model during both the summer and winter tests. This was probably due to the effect of the relatively thin layer of earth over the shelter and the exposure to atmospheric conditions at the earth's surface and also to the difference in shape of the cavities. Thus, artificially low thermal properties were required for Solution II to best approximate the observed shelter surface temperatures.

Since the cylindrical model provided a larger heat sink per unit shelter surface area than the one-dimensional model, and a smaller heat sink per unit shelter surface area than the spherical model, it tended to produce the best agreement between predicted and observed surface temperature with the preferred, or most probable, thermal properties of the heat conduction medium.

In NBS Tests 3 and 4, significant absorption by the concrete walls of existing condensation would have raised the thermal properties; however, this possibility was minimized by the application of two coats of rubber-base paint. In NBS Test 5, due to the melted snow, the thermal properties of the earth could have been higher than the preferred set, but this was not indicated by the diffusivity determination discussed in Section 3.3.

The models used for this analysis implicitly assumed that the heat conduction in the concrete and earth was linear in nature, i.e., the thermal properties did not vary with temperature, so the classical linear heat flow theory was applicable. While it may be that the temperature dependence of the thermal properties could be neglected for the gradients encountered in these tests, these gradients nevertheless may have caused some moisture migration in the soil. This migration would have acted both to transfer sensible and latent heat directly, and to change the thermal properties, which are much more sensitive to moisture changes than to temperature changes [7]. The result is a problem of combined heat and moisture flow which involves coupled, non-linear, partial differential equations, amenable to solution by numerical analysis [13].

Although a few measurements of moisture content of the earth were made during the course of the five NBS tests, the data did not indicate whether significant moisture transfer occurred. It probably was not sufficient to cause significant changes in the thermal properties of the earth.

10.5 Shelter Irregularities

Throughout this analysis, both heat conduction media were assumed to be homogeneous, and in the case of the earth, infinite in extent. These conditions were not fully met by the NBS test shelter and site, due to certain irregularities in the walls and earth. The deviations for each region are listed as follows:

- 1) north wall region — a concrete road was located about ten feet from the wall, which might actually have acted as a heat source, storing heat from the sun. This additional heat source would tend to make the surface temperature rise faster, requiring lower thermal properties to make predictions agree with observations (cf. Sections 4.6 and 7.6). The hatchway exit, adjacent to this wall, might have affected the distribution of heat flux over the wall. The shielding wall might also have affected the heat flow distribution, by interfering with the radiation component of the internal heat exchange. This wall also contained the metal exhaust pipe, which would tend to conduct some heat directly to the air. It is for these reasons that this region was designated the least typical.
- 2) west wall region — the south half of this wall was probably exposed to more heat than the north half, due to the arrangement of simulated occupants and shielding wall, but since it faced uphill on a site of 12 percent grade, it was exposed to more earth than any other wall. This region was designated the most typical.
- 3) south wall region — the ventilating air supply system used during the NBS tests was located in the shielding wall and aimed at the south wall. Furthermore, three simulated occupants were located near this wall. This arrangement possibly affected the heat flux distribution. A spare ventilating air supply and exhaust system, installed in this wall, would tend again to conduct some heat directly to the air.

- 4) east wall region — this wall faced downhill and thus was exposed to less earth than any other wall. In fact, the original grade line was about one foot below the top edge of this wall. It was consequently the one most affected by weather conditions. Also, the hatchway portion of this wall received less heat than the rest.
- 5) floor region — this region had a truly infinite exposure of earth. However, the hatchway portion of the floor received less heat, and the arrangement of the simulated occupants and the supply air stream might have affected the heat flux distribution.

10.6 Shelter Environment

In this report, the conduction problem has been treated as separate from the rest of the shelter-environment system, using the known heat flux at the surfaces. While this procedure is not invalid, it is incomplete in the sense of omitting that part of the heat transfer process between the internal heat sources and the walls. A more complete treatment would take into account these sources, namely, ventilation and occupants. In such a problem, it would not be possible to treat each surface separately, as was done in the one-dimensional solutions, because the heat losses to all the surfaces are interrelated through the common sources. In that case, the simplest approach would be to use a single symmetrical model such as the cylinder or sphere, and according to Section 10.1, the cylinder is the better choice.

A cylindrical solution with heat source boundary conditions is available [14], and has been expanded and applied to the NBS shelter. However, the composite problem has not been found in a literature search, and the composite assumption may be important as seen in Section 10.2.

When the conduction problem is treated separately, the roof region can be accurately represented by a one-dimensional finite layer, with boundary conditions at both ceiling and ground surfaces. (Three such solutions have been developed, but are not included in this report.) Because of the proximity of the ground surface, the heat flow from the four walls is chiefly two-dimensional, except near the floor. The floor is exposed to the most earth of all the surfaces, and heat flow in that region is truly three-dimensional. These facts suggest that the overall effect might be two-dimensional, adding weight to the choice of cylindrical geometry as the best simple model.

It should be noted that none of the one-dimensional solutions in this report are really applicable to the floor region, because of its three-dimensional behavior. However, since the floor region was approximately semi-infinite, the predicted temperatures were included in the tables for the sake of completeness.

A variety of more elaborate models might be considered which would explicitly take into account the asymmetry caused by the ground surface. An example might be a closed hemispherical cavity convex downward located at a finite depth within a semi-infinite region. This model would probably exhibit a more desirable heat flow pattern, approximately one-dimensional in the roof region, two-dimensional at the sides, and three-dimensional at the bottom. Models of this type are, of course, mathematically complex.

11. CONCLUSIONS

On the basis of the analyses covered by this report, it is concluded that a cylindrical model provides the best predictions of the surface temperatures in a small underground shelter with limited earth cover, probably because it most nearly compensates for the effect of the finite region over the cavity. It is probable that a spherical model would be better if the small shelter were considerably deeper in the earth. The one-dimensional model was less effective in predicting temperatures in such a small shelter, but would probably be an adequate representation for larger shelters in which corner effects were relatively of less importance.

The composite nature of a concrete shelter surrounded by earth was shown to have a small effect on shelter surface temperatures. The higher thermal properties of concrete as compared to earth caused the shelter surface temperatures to be a little lower than if the entire conduction region was comprised of earth. This effect was slightly greater during the first week of occupancy than during the second. A heat conduction region comprised entirely of concrete might reduce surface temperatures as much as 3°F in a small shelter as compared to a shelter with only moist earth as a heat sink. This disparity would be even greater if the earth medium was essentially dry.

The initial distribution of temperature from the shelter surface to a distance of 4 feet into the surrounding medium was found to make an appreciable difference in the surface temperature during the first week of occupancy, but the effect was of little significance after two weeks.

The solutions described in this report do not take into account the effect of moisture migration on heat conduction, but these effects were believed to be small in the test shelter.

Further efforts toward fulfilling the overall objectives of this analytical study should begin with models that take into account heat generation and ventilation of the shelter, the finite roof cover, and the composite nature of the shelter surroundings.

APPENDIX A

INITIAL TEMPERATURE DISTRIBUTION

IN

SHELTER CONCRETE

AND

SURROUNDING EARTH MEDIUM

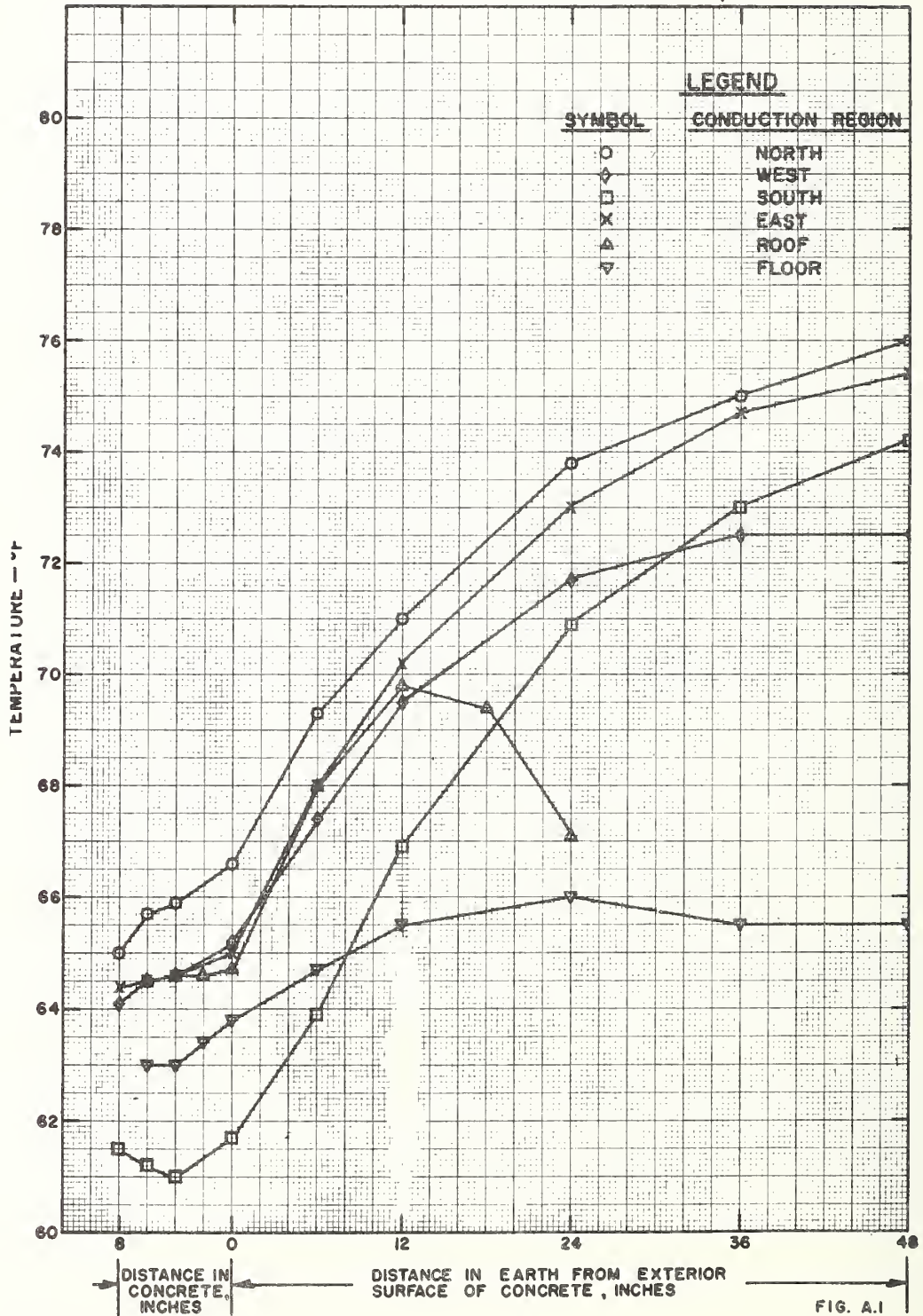
FOR

FIVE NBS SHELTER TESTS

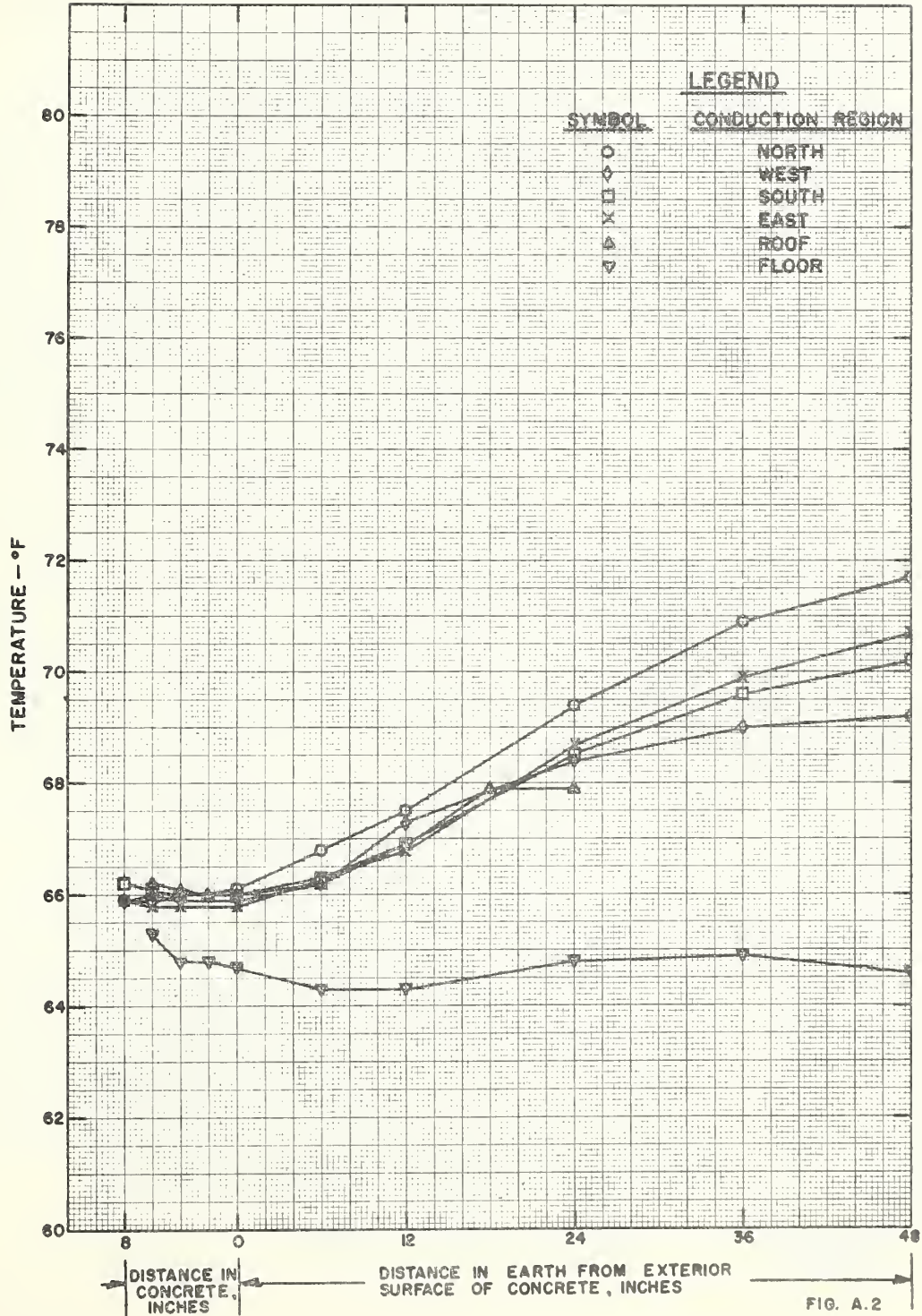
CONDUCTED BETWEEN

August 13, 1959 and April 8, 1960

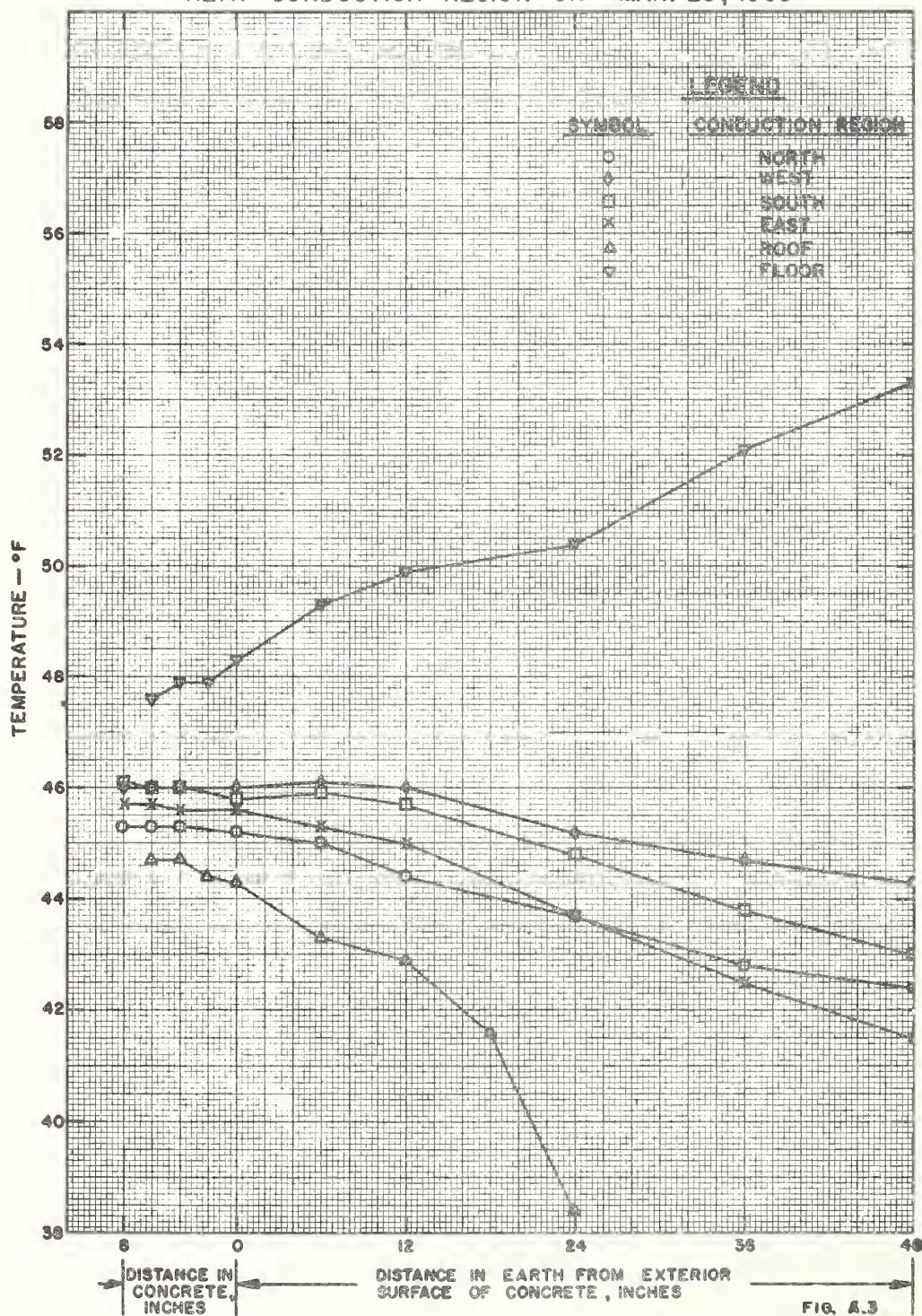
NBS TEST 3
INITIAL TEMPERATURE DISTRIBUTION IN
HEAT CONDUCTION REGION ON SEPT. 13, 1959



NBS TEST 4
INITIAL TEMPERATURE DISTRIBUTION IN
HEAT CONDUCTION REGION ON OCT. 6, 1959



NBS TEST '5
INITIAL TEMPERATURE DISTRIBUTION IN
HEAT CONDUCTION REGION ON MAR. 25, 1960



APPENDIX B

Heat Flux

The mathematical solutions in this report are based on a constant (time-independent) heat flux, applied uniformly over the entire bounded surfaces of each mathematical model. These are conditions which would appear more readily applicable to a sealed-up shelter, and which would fail to describe the case of ventilated shelters, whose heat flux would not be expected to be either constant or uniformly applied. Thus, in order to deal properly with the constant flux parameter appearing in each solution, it was necessary to extract numerical values from the experimental data based on methods considered to be compatible with the constant flux assumption. Three methods were considered and each is discussed below, one of which required the derivation of a new solution.

Method 1 Constant Heat Flux

Each solution based on this assumption required that a single value of heat flux be used for all values of time. This value could reasonably be selected as the overall average value, shown in Table B.1 at 336 hours, and which is close to the experimental value observed during approximately the seventh day of each test, for any surface. However, the observed performance diverges from this value for other times.

Method 2 Cumulative Average Heat Flux

This is the method used throughout the report. The values of heat flux were cumulative averages, values which are essentially time-dependent, averaged over the interval from 0 to t , and considered to be constant in that interval. The smaller intervals gave a better overall approximation than Method 1 because the values thus obtained were distributed such as to incorporate the observed exponential decay feature. Even though this method was obviously a deviation from the models, it was nevertheless considered to be a reasonable compromise

between the mathematical assumption and the experimental observations. The predicted curve determined on this basis is then actually a curve drawn through points obtained by solving each solution eight separate times, each time varying the heat flux in accordance with the cumulative average values listed in Table B.1.

Method 3 Prescribed Heat Flux

This method would have required the derivation of each solution on the basis of an actual time-dependent heat flux boundary condition, but, as previously mentioned, this was considered to be beyond the scope of this report. However, in order to determine the effects of the mathematical simplifications involved in Method 1, and of the "compromise" made in Method 2, Solution I was reworked by replacing Eq. 4.2(3), the constant flux condition, by

$$-K \frac{\partial \theta}{\partial x} = a + be^{-mt} \quad (1)$$

a prescribed flux condition approximating the experimental situation of exponentially decaying heat flux. This solution is identified as Solution IA.

The temperature rise θ at the interior surface $x = 0$ is then

$$\theta = \frac{2a}{K} \left[\frac{\alpha t}{\pi} \right]^{\frac{1}{2}} + \frac{2b}{K} \left[\frac{a}{m\pi} \right]^{\frac{1}{2}} D(\sqrt{mt}) \quad (2)$$

where $D(\sqrt{mt})$ represents Dawson's integral, equal in this case to the imaginary part of the complex error function. Both functions are tabulated in [15].

Figures B.1 and B.2 illustrate predicted surface temperatures obtained from Methods 1, 2, and 3, together with the observed data, for the north and west wall regions of NBS Test 3. In both cases, the prescribed flux solution, Solution IA, yielded results in closer agreement with the observed temperatures at fourteen days. Method 1 is generally better for the first seven days because the constant flux value used was lower than or about equal to the observed values for those times. At the end of fourteen days, the deviations in temperature between Methods 2 and 3 were less than 1°F for the west wall and practically negligible for the north wall. For times larger than 336 hours, results from Methods 2 and 3 will tend to merge, that trend being already visible in Figure B.1, so that the greatest deviation is probably encountered at times in the neighborhood of fourteen days or less.

A similar improvement using Eq.(1) could be made to the other solutions in this report, but the likelihood of uncovering deviations much wider than those illustrated by this solution appears doubtful.

TABLE B.1
CUMULATIVE AVERAGE VALUES OF
HEAT FLUX F_o

Test 3

Time	North	West	South	East	Roof	Floor
24	2.06	4.41	8.32	4.78	3.60	5.24
48	2.16	4.02	7.09	4.44	3.34	5.17
72	2.15	3.70	6.21	4.13	3.18	5.12
96	2.02	3.56	5.57	3.90	2.97	5.02
120	1.93	3.41	5.10	3.71	2.86	4.90
168	1.85	3.25	4.50	3.46	2.80	4.66
240	1.76	3.04	3.99	3.22	2.70	4.50
336	1.65	2.84	3.53	3.01	2.36	4.24

Test 4

Time	North	West	South	East	Roof	Floor
24	2.65	4.78	5.49	4.71	3.96	4.70
48	2.63	4.61	4.97	4.42	3.45	4.51
72	2.53	4.42	4.64	4.18	3.15	4.40
96	2.48	4.34	4.40	4.02	2.93	4.35
120	2.45	4.28	4.26	3.90	2.77	4.32
168	2.31	4.10	3.98	3.74	2.41	4.23
240	2.07	3.87	3.63	3.42	2.27	4.04
336	1.83	3.69	3.35	3.18	2.36	3.90

Test 5

Time	North	West	South	East	Roof	Floor
24	1.81	4.19	6.38	5.74	4.57	1.73
48	1.82	3.99	6.08	5.35	4.27	1.74
72	1.85	3.93	5.96	5.26	4.16	1.76
96	1.89	3.89	5.88	5.18	4.01	1.78
120	1.90	3.84	5.79	5.10	3.80	1.81
168	2.02	3.91	5.80	5.09	3.44	1.95
240	2.09	3.90	5.74	4.97	2.99	2.08
336	2.06	3.86	5.65	4.76	2.80	2.19

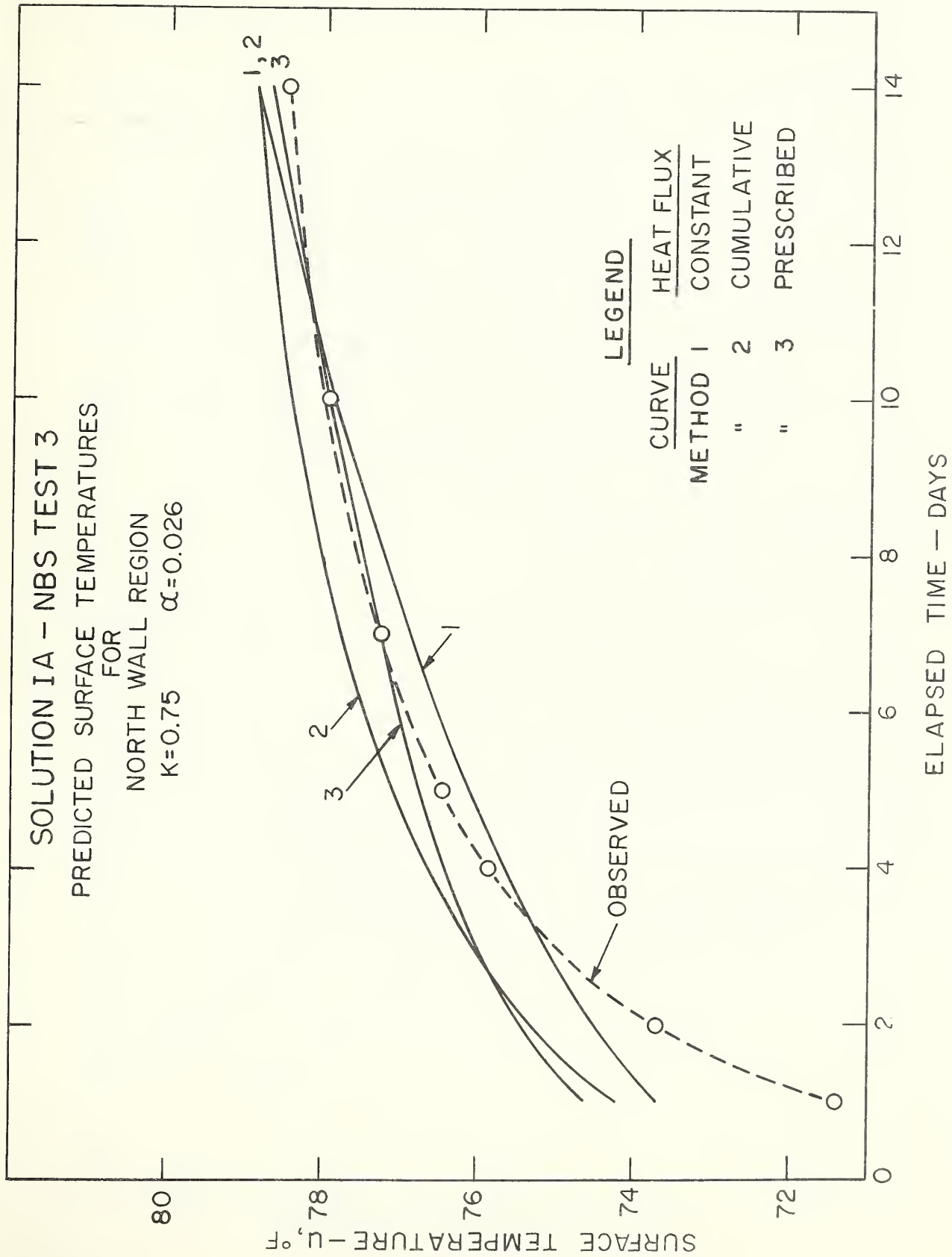


FIG. - B.1

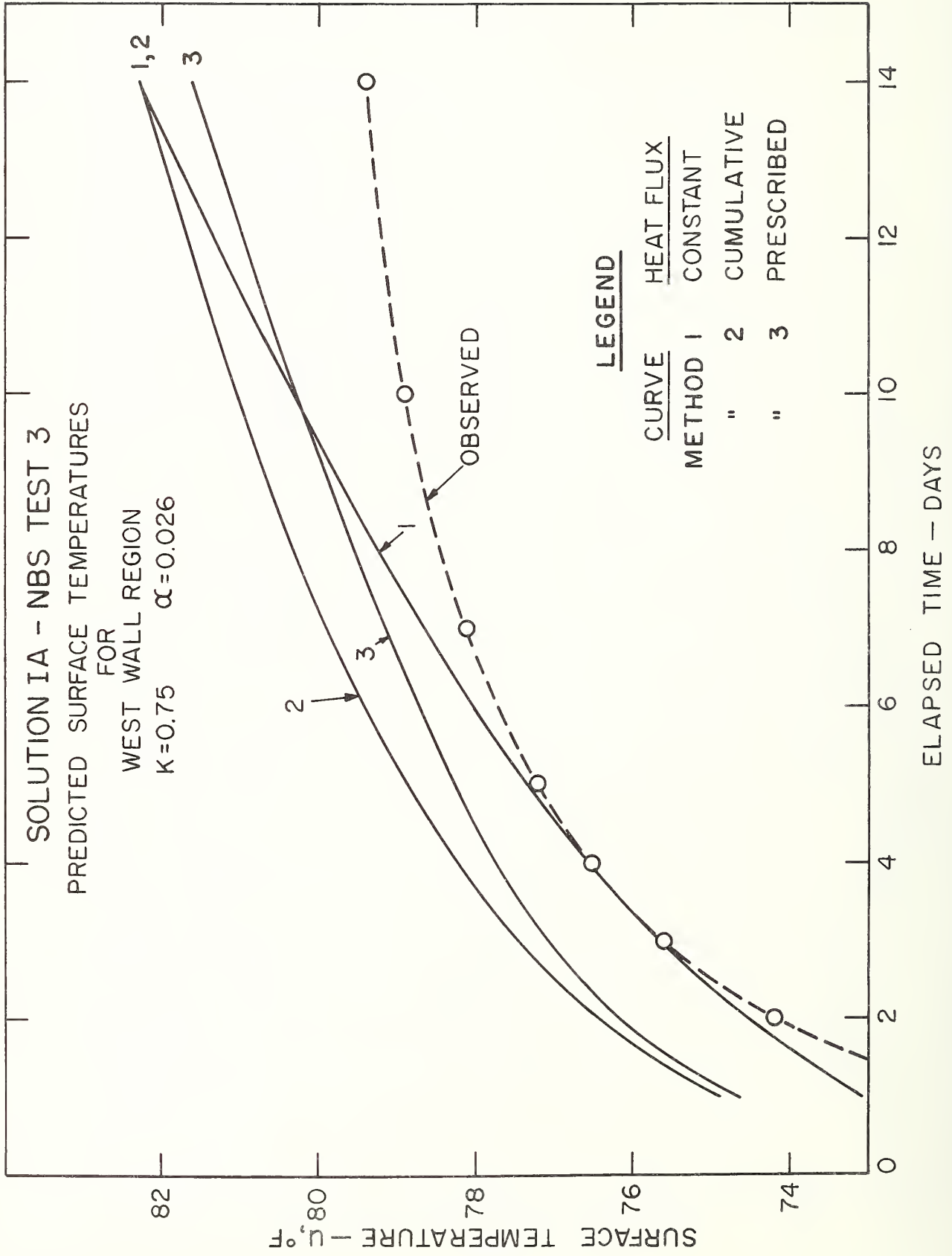


FIG. - B.2

APPENDIX C

Numerical Example

The example worked out below for Solution IV is the type of computation necessary to obtain numerical results from any of the first four solutions contained in this report.

To compute the interior surface temperature u_1 , at $x = -l$, for the north wall of NBS Test 3 at 336 hours, Eq. 7.2(13) is manipulated as follows.

Rewriting the summation portion of the equation in a slightly more convenient form yields

$$\sum_{n=0}^{\infty} (-1)^n \beta^n \left\{ 2 \operatorname{ierfc} \frac{n}{T^{\frac{1}{2}}} - 2\beta \operatorname{ierfc} \frac{n+1}{T^{\frac{1}{2}}} \right\} \quad (1)$$

The factor of 2 was brought inside the summation sign because the integral error function of the first order is usually tabulated in this form. Numerical values for this function, as well as for those of higher order appearing in Solution III, are tabulated in [15] and in Appendix II of [10].

Expanding summation (1) to produce sufficient convergence for the desired accuracy for the particular values of time, wall thickness, and thermal properties involved will require, in this example, the first four terms, and a convenient arrangement for listing these terms is shown below. At $n=0, 1, 2, 3\dots$, the summation reduces to the following:

$$n = 0, \quad 2 \operatorname{ierfc} (0) - 2\beta \operatorname{ierfc} \left[\frac{1}{T^{\frac{1}{2}}} \right]$$

$$n = 1, \quad -2\beta \operatorname{ierfc} \left[\frac{1}{T^{\frac{1}{2}}} \right] + 2\beta^2 \operatorname{ierfc} \left[\frac{2}{T^{\frac{1}{2}}} \right]$$

$$n = 2, \quad 2\beta^2 \operatorname{ierfc} \left[\frac{2}{T^{\frac{1}{2}}} \right] - 2\beta^3 \operatorname{ierfc} \left[\frac{3}{T^{\frac{1}{2}}} \right]$$

$$n = 3, \quad -2\beta^3 \operatorname{ierfc} \left[\frac{3}{T^{\frac{1}{2}}} \right] + \text{negligible term}$$

Eq. 7.2(13) can be rewritten, combining the above terms, to read

$$u_1 = u_0 + \frac{F_0 \ell}{K_1} T^{\frac{1}{2}} \left\{ 2 \operatorname{ierfc} (0) - 2\beta \left[2 \operatorname{ierfc} \left(\frac{1}{T^{\frac{1}{2}}} \right) \right] + 2\beta^2 \left[2 \operatorname{ierfc} \left(\frac{2}{T^{\frac{1}{2}}} \right) \right] - 2\beta^3 \left[2 \operatorname{ierfc} \left(\frac{3}{T^{\frac{1}{2}}} \right) \right] + \dots \right\} \quad (2)$$

The following substitutions can now be made in the above expression to obtain the required numerical result:

$$\text{From Table 3.1.1,} \quad u_0 = 71.7$$

$$\text{From Table B.1,} \quad F_0 = 1.65$$

$$\begin{aligned} \text{From Table 7.5.1,} \quad K_1 &= 1.15 \\ \alpha_1 &= 0.036 \\ \sigma &= 0.767 \end{aligned}$$

$$\text{Thickness of concrete,} \quad \ell = 0.667$$

$$\text{Therefore,} \quad T = \frac{\alpha_1 t}{\ell^2} = 27.216$$

$$\text{and} \quad \beta = \frac{\sigma-1}{\sigma+1} = -0.1316$$

Substituting in (2), we get

$$u_1 = 71.7 + \frac{(1.65)(0.667)}{1.15} (5.2169) \left\{ 1.1284 + 0.2632(0.7862) \right. \\ \left. + 0.0346(0.5235) + 0.0046(0.3321) + \dots \right\}$$

$$u_1 = 71.7 + 6.76 = 78.46 \text{ or } 78.5^\circ\text{F},$$

the predicted value shown in Table 7.5.1.

It should be noted that Solutions V and VI are too cumbersome for the type of manipulation shown in the above example, especially when many computations are required. Even when convergence is fairly rapid, the use of a digital computer is almost a necessity. As indicated in Sections 8.5 and 9.5, these two solutions were programmed in Fortran language for use on the IBM 7090 computer, and these programs are available from the Mechanical Systems Section of NBS.

APPENDIX D

References

- [1] Achenbach, P.R., Drapeau, F.J.J., and Phillips, C.W., Studies of Environmental Factors in a Family-Size Underground Shelter, Mechanical Systems Section, Building Research Division, National Bureau of Standards, Washington, D. C., March 1961.
- [2] Proceedings of the American Concrete Institute, Volume 34, May-June 1938.
- [3] American Society of Heating, Refrigerating, and Air-Conditioning Engineers, Guide and Data Book, 1961.
- [4] Marks, L.S., Mechanical Engineers' Handbook, Fifth Edition, 1951.
- [5] Thermal Properties of Concrete, American Society of Heating and Ventilating Engineers, Research Bulletin No. 2, Volume 53, September 1947.
- [6] Ingersoll, L.R., Zobel, O.J., and Ingersoll, A.C., Heat Conduction, University of Wisconsin Press, Revised Edition, 1954.
- [7] Kersten, M.S., Thermal Properties of Soils, University of Minnesota, Engineering Experiment Station Bulletin No. 28, June 1949.
- [8] Chang, Jen-Hu, Ground Temperature, Volume I, Harvard University, Blue Hill Meteorological Observatory, Milton, Massachusetts, June 1958.
- [9] Carson, J.E., Analysis of Soil and Air Temperatures by Fourier Techniques, Journal of Geophysical Research, Volume 68, No. 8, April 15, 1963.

- [10] Carslaw, H.S., and Jaeger, J.C., Conduction of Heat in Solids, Oxford University Press, Second Edition, 1959.
- [11] Matricon, M., Étude de la Répartition de la Chaleur dans L'Anticathode d'un Tube à Rayons X, Le Journal de Physique et le Radium, Tome 12, janvier 1951.
- [12] Griffith, M.V., and Horton, G.K., The Transient Flow of Heat Through a Two-Layer Wall, Proc. Phys. Soc., Volume 58, 1946.
- [13] De Vries, D.A., Simultaneous Transfer of Heat and Moisture in Porous Media, Transactions, American Geophysical Union, Volume 39, No. 5, October 1958.
- [14] Heat Transfer in Deep Underground Tunnels, National Building Studies Research Paper No. 26, Her Majesty's Stationery Office, London, 1958.
- [15] National Bureau of Standards, Applied Mathematics Series 55, Handbook of Mathematical Functions, June 1964.

